METABOLIC REGULATION OF THE METHYLERYTHRITOL 4-PHOSPHATE (MEP) PATHWAY: SPECIFIC ROLE OF DEOXY-D-XYLULOSE 5-PHOSPHATE SYNTHASE (DXS)

By

Aparajita Banerjee

A DISSERTATION

Submitted to
Michigan State University
in partial fulfillment of the requirements
for the degree of

Biochemistry and Molecular Biology—Doctor of Philosophy

2015

ABSTRACT

METABOLIC REGULATION OF THE METHYLERYTHRITOL 4-PHOSPHATE (MEP) PATHWAY: SPECIFIC ROLE OF DEOXY-D-XYLULOSE 5-PHOSPHATE SYNTHASE (DXS)

By

Aparajita Banerjee

The 2-*C*-methyl-D-erythritol 4-phosphate (MEP) pathway is an important pathway for the biosynthesis of isopentenyl diphosphate (IDP) and dimethylallyl diphosphate (DMADP), the precursors of isoprenoids. Isoprenoids are ubiquitous natural products present in all different forms of life and have a wide variety of structures and functions. Some isoprenoids are involved in primary metabolic processes like photosynthesis, respiration, regulation of growth and development whereas many others have important roles in secondary metabolism. In addition, isoprenoids have numerous commercial applications as flavor and fragrance molecules, drugs, pigments, natural polymers, agrichemicals, cosmetics, biofuels, etc. Isoprene, the smallest member of the isoprenoid family, has different adverse effects on atmospheric chemistry. Despite having diverse functions, all isoprenoids are structurally based on C5 isoprenoid units. It was believed for a long time that the mevalonate (MVA) pathway is the only route for the biosynthesis of IDP. In early 1990s, it was discovered that an alternative (MEP) pathway exists for the biosynthesis of both IDP and DMADP. Soon after its discovery, the various enzymes and metabolites involved in this pathway were elucidated. However, not much was known about the metabolic regulation of this pathway.

Considering the numerous applications of isoprenoids, it was important to understand the metabolic regulation of the MEP pathway. Earlier studies suggested that DXS might play an important role in the regulation of the MEP pathway. The research work presented in this

dissertation mainly involves the study of the metabolic regulation of this pathway by focusing on the kinetic behavior of 1-deoxy-D-xylulose-5-phosphate synthase (DXS). A liquid chromatography-tandem mass spectrometry (LC-MS/MS) based assay was developed for DXS to study its kinetics in presence of different metabolites of the MEP pathway. It was observed that recombinant DXS from *Populus trichocarpa* (*Pt*DXS) is feedback-inhibited by IDP and DMADP, the two end products of this pathway. Mechanistic studies of this inhibition showed that both IDP and DMADP compete with thiamin diphosphate (ThDP) for binding at the active site of the enzyme. Feedback regulation of DXS plays an important role in controlling the carbon flux through this pathway and thus constitutes a significant regulatory mechanism of this pathway. A modified *Pt*DXS, which would exhibit reduced binding affinity for IDP/DMADP and thereby relieving the feedback inhibition partially or completely, would be important for biotechnological uses. Site-directed mutagenesis was used to engineer an improved *Pt*DXS that has reduced affinity for IDP and DMADP. This engineered *Pt*DXS was also shown to have higher K_m for ThDP than the WT enzyme. Therefore, this mutant of *Pt*DXS would be important for biotechnological applications if high concentration of ThDP is maintained.

To my mom

ACKNOWLEDGEMENTS

I am fortunate to have tremendous amount of support and encouragement from a number of individuals throughout my entire graduate life. First and foremost, I would like to thank my advisor, Dr. Thomas D. Sharkey. I would not have been able to accomplish this work without his guidance and valuable advices. His patience and thoughtful suggestions always helped me to find directions when things did not work quite as expected. He always gave me the freedom to learn new things and pursue my own ideas. His faith in my potential has certainly made me more confident in all my endeavors. His insightful guidance has made this journey of my graduate life truly memorable, enriched, and rewarding. I simply cannot express in words my gratitude for him. In my experience, he has been an outstanding mentor (which is also reflected by the innumerable honors and awards that he has received so far). I genuinely consider myself to be fortunate to get this opportunity to pursue my graduate study with him.

I would like to thank my collaborator and one of my committee members, Dr. Honggao Yan for his contribution in cloning the poplar DXS gene and also doing the computational modeling studies. The modeling studies definitely added greatly to my experimental work and made it a convincing and complete story. I would also like to thank my other committee members, Dr. Kevin Walker, Dr. Yair Shachar-Hill, and Dr. Christoph Benning for their valuable suggestions and advice. I would like to give special thanks to Dr. Dan Jones for all his advice and support for the mass spec work. I probably had countless questions for him when I first started doing mass spec. He always answered them with patience and a smile, which definitely made me feel better and less-hesitant. It would not have been possible for me to establish the mass spec assay, which was instrumental in studying DXS kinetics, without his great help.

I am extremely thankful to Dr. Sean Weise for his incredible support. He always helped and guided me both in and outside the lab whenever I needed them. As a great lab manager, he always maintained an extremely organized, safe, and pleasurable work atmosphere in the lab. Also, I would like to appreciate his great talent to keep us entertained in his own humorous way. Far away from home, he has truly been a friend, philosopher and guide. I am also thankful to Dr. Ziru (James) Li for his great help in the lab and strong encouragement throughout these years. I got the initial training from him when I first joined the lab. Since then I had the luxury of asking him innumerable questions which he always answered with great patience. I would also like to thank numerous undergraduate students, who helped me in several of my experiments. I am thankful to all the current and former lab members with whom I have shared the bench with. Thank you Chris Harvey, Alexandra Lantz, Dr. Sarathi Wijetilleke, Dr. Dennis Gray and a countless undergraduate students for making the lab a wonderful and enjoyable work place for me.

I would like to express my sincere acknowledgement to the amazing supporting staffs in the department and the facilities. Thank you Jessica Lawrence, Kaillathe (Pappan) Padmanabhan, Teresa Vollmer, Laurie Secord, Mary Villarreal, Jim Stewart, Pat Ungren, Joyce Robinson, Lijun Chen, Scott Smith, and Chao Li for your remarkable help and support throughout these years.

Finally, I would like to thank my family and friends for being there for me through all these long years. A special thank should go to my loving and caring husband, Mr. Ayan Bhattacharya. He stood by me through thick and thin and helped me navigate through the various stresses of graduate life. I simply would not have been able to sustain through this long journey without his outstanding support and immense encouragement. I would also like to express my heartfelt gratitude to my mother, Dr. Shyamali Banerjee. Without her strong will power, unconditional

support, and enormous motivation, I would not have reached here today. I am also very thankful to the family of my loving sister and the family of my in laws for their continuous encouragement throughout these years. Last but not the least; I would like to thank all my friends in and outside MSU for making this journey lively and enjoyable.

TABLE OF CONTENTS

LIST OF TABLES

LIST OF FIGURES

KEY TO ABBREVIATIONS

ADH	alcohol dehydrogenase
ANOVA	analysis of variance
AThDP	adenosine thiamin diphosphate
AThTP	adenosine thiamin triphosphate
ATP	adenosine triphosphate
Bis-tris	2-[bis(2-hydroxyethyl)amino]-2-(hydroxymethyl)propane-1,3-diol
CDPME	4-(cytidine 5'-diphospho)-2-*C*-methyl-D-erythritol
CDPMEP	4-(cytidine 5'-diphospho)-2-*C*-methyl-D-erythritol 2-phosphate
CMK	4-(cytidine 5'-diphospho)-2-*C*-methyl-D-erythritol kinase
CMS	4-(cytidine 5'-diphospho)-2-*C*-methyl-D-erythritol synthase
CTP	cytidine triphosphate
DHAP	dihydroxyacetone phosphate
DMADP	dimethylallyl diphosphate
DOX-d_2	dideuterated deoxyxylulose
DTT	dithiothreitol
DXP	1-deoxy-D-xylulose 5-phosphate
DXR	1-deoxy-D-xylulose-5-phosphate reductoisomerase
DXS	1-deoxy-D-xylulose-5-phosphate synthase
E4P	erythrose 4-phosphate
EDTA	ethylenediaminetetraacetic acid
ESI	electrospray ionization
F6P	fructose 6-phosphate
FBP	fructose 1,6-bisphosphate

Fd	ferredoxin
FDP	farnesyl diphosphate
Fsr	fosmidomycin resistance
GAP	D-glyceraldehyde 3-phosphate
GDP	geranyl diphosphate
GPDH	α-glycerophosphate dehydrogenase
H	hill coefficient
HCl	hydrochloric acid
HDR	4-hydroxy-3-methylbut-2-enyl diphosphate reductase
HDS	4-hydroxy-3-methylbut-2-enyl diphosphate synthase
HEThDP	hydroxyethyl thiamin diphosphate
HILIC	hydrophilic interaction chromatography
HMBDP	4-hydroxy-3-methylbut-2-enyl diphosphate
HPL	hydroperoxide lyase
HPLC	high-performance liquid chromatography
IC_{50}	half maximal inhibitory concentration
IDI	isopentenyl diphosphate isomerase
IDP	isopentenyl diphosphate
IMP	isopentenyl monophosphate
IPTG	isopropyl β-D-1-thiogalactopyranoside
IS	internal standard
IspS	isoprene synthase
k_{cat}	turnover number
K_i	inhibition constant
K_m	Michaelis constant

LC	liquid chromatography
LThDP	C2α-lactylthiamin diphosphate
MBO	methylbutenol
MCS	2-*C*-methyl-D-erythritol 2,4-cyclodiphosphate synthase
MEcDP	2-*C*-methyl-D-erythritol 2,4-cyclodiphosphate
MEP	2-*C*-methyl-D-erythritol 4-phosphate
Mg^{2+}	magnesium ion
$MgCl_2$	magnesium chloride
MRM	multiple reaction monitoring
MS/MS	tandem mass spectrometry
MVA	mevalonic acid
Na^+	sodium ion
NaCl	sodium chloride
NADH	reduced nicotinamide adenine dinucleotide
NADPH	reduced nicotinamide adenine dinucleotide phosphate
NH_2	amino group
Ni-NTA	nickel-nitrilotriacetic acid
NMR	nuclear magnetic resonance
NO	nitric oxide
OD	optical density
PCR	polymerase chain reaction
PDC	pyruvate decarboxylase
PDH	pyruvate dehydrogenase
PEP	phospho*enol*pyruvate
PGA	phosphoglyceric acid

P_i	inorganic phosphate
PK_p	plastidic pyruvate kinase
ppGpp	guanosine 3',5'-bispyrophosphate
PPT	phospho*enol*pyruvate/phosphate translocator
*Pt*DXS	*Populus trichocarpa* 1-deoxy-D-xylulose-5-phosphate synthase
PTFE	polytetrafluoroethylene
R 5-P	D-ribose 5-phosphate
RMSF	root-mean-squares fluctuation
ROS	reactive oxygen species
Ru 5-P	D-ribulose 5-phosphate
Rubisco	ribulose-1,5-bisphosphate carboxylase/oxygenase
RuBP	ribulose 1,5-bisphosphate
SDS-PAGE	sodium dodecyl sulfate-polyacrylamide gel electrophoresis
TEV	tobacco etch virus
ThDP	thiamin diphosphate
ThMP	thiamin monophosphate
ThTP	thiamin triphosphate
TIP3P	transferable intermolecular potential with three point charges
TK	transketolase
TPI	triose phosphate isomerase
TPP	thiamin pyrophosphate
TPT	triose phosphate/phosphate transporter
Tris	2-amino-2-hydroxymethyl-propane-1,3-diol
WT	wild type
Xu 5-P	xylulose 5-phosphate

CHAPTER 1

Insights into the MEP pathway regulation

Part of this chapter was adapted from the following manuscript.
[Banerjee, A., and Sharkey, T. D. (2014) Methylerythritol 4-phosphate (MEP) pathway metabolic regulation. *Natural Product Reports* **31**, 1043-1055] - Reproduced by permission of The Royal Society of Chemistry

1.1 INTRODUCTION

Isoprenoids, also known as terpenoids or terpenes, are ubiquitously found in all living organisms including both prokaryotes and eukaryotes (Wanke *et al.* 2001). They are considered the most diverse group of metabolites and have a broad variety of functions ranging from important biological roles to various commercial and biotechnological applications. Many isoprenoids play roles in primary biological processes like photosynthesis (carotenoids, chlorophylls, plastoquinone), respiration (ubiquinone), regulation of growth and development (gibberellic acid, abscisic acid, brassinosteroids, cytokinins, prenylated proteins), metabolism (sterols). They also play roles in various secondary biological processes like intracellular signal transduction (Ras proteins) and vesicular transport (Rab proteins), reproduction of plants by attracting pollinators and seed dispersers, defense mechanisms of plants against different biotic and abiotic stresses, and assembly of various cellular and organelle membranes (sterols, dolichols, carotenoids etc.) (Hemmerlin *et al.* 2003; Hunter 2007; Phillips *et al.* 2008; Rodríguez-Concepción 2006; Sacchettini & Poulter 1997; Wanke *et al.* 2001).

Isoprenoids also have important industrial applications as flavor and fragrance molecules, drugs, pigments, natural polymers, agrichemicals, cosmetics, biofuels etc. (Klein-Marcuschamer *et al.* 2007; Misawa 2011; Phillips *et al.* 2008; Roberts 2007; Rodríguez-Concepción 2006; Rude & Schirmer 2009). A wide variety of therapeutic properties of this group of natural products include anticancer, antiparasitic, antimicrobial, antiallergenic, antispasmodic, antihyperglycemic, anti-inflammatory, and immunomodulatory properties (Ajikumar *et al.* 2008). A well-known anticancer drug, paclitaxel, is a complex diterpenoid obtained from the bark of Pacific yew (Ajikumar *et al.* 2008). A wide variety of monoterpenes and sesquiterpenes contribute to various

odors ranging from fruity and flowery smell to woody and balsamic smell (Caputi & Aprea 2011). Different terpenoids like menthol (minty odor), D-carvone (spicy odor), D-limonene (orange peel odor), citral (lemon peel odor), and 1,8-cineole (Eucalyptus odor) are extensively used in flavor and fragrance industries (Caputi & Aprea 2011). Different terpenoids like β-carotene, lutein, zeaxanthin, lycopene, phytoene are widely used as pigments in food industries (Cserháti & Forgács 2001). Rubber, the most abundant polymer used in various industries, is chemically composed of linearly arranged polyterpenoids (McGarvey & Croteau 1995). Another important isoprenoid is isoprene (C_5H_8), the smallest member of isoprenoid family. It helps some plants contend with short term environmental changes such as temperature, ozone, and reactive oxygen species (ROS) (Sharkey *et al.* 2008). Isoprene also influences atmospheric chemistry in various ways (Sharkey *et al.* 2008).

In spite of the structural and functional diversities, all isoprenoids are based on branched five-carbon (C_5) skeleton units (also known as isoprenoid units), which can be further fused to form more complex structures. Except isoprene, two metabolic precursors, isopentenyl diphosphate (IDP) and its isomer dimethylallyl diphosphate (DMADP) constitute these isoprenoid units and lead to the formation of all the isoprenoids (Cordoba *et al.* 2009). Isoprene itself is synthesized from DMADP by the enzymatic action of isoprene synthase (Silver & Fall 1991; Silver & Fall 1995).

1.2 OVERVIEW OF THE MEP PATHWAY

1.2.1 Discovery

For many years, it was believed that IDP was synthesized exclusively through the acetate/mevalonate (MVA) pathway followed by its isomerization to DMADP by one of two different isopentenyl diphosphate isomerases (IDI1 and IDI2) (Eisenreich *et al.* 2004; Eisenreich *et al.* 1998; Nakamura *et al.* 2001). Studies involving labeling of polyprenoids by feeding ^{13}C-labeled precursors indicated that an alternative pathway exists for the biosynthesis of isoprenoids (Eisenreich *et al.* 1998). In the early 1990s, an alternative pathway, now known as the 2-*C*-methyl-D-erythritol 4-phosphate (MEP) pathway, was discovered in bacteria. The MEP pathway results in the synthesis of both IDP and DMADP (Eisenreich *et al.* 1998; Rohmer *et al.* 1993; Rohmer *et al.* 1996). Because the last step in the pathway makes both IDP and DMADP, bacteria do not require IDI and some do not have IDI. Subsequent studies have demonstrated the presence of the MEP pathway in plastids of green algae and higher plants (Arigoni *et al.* 1997; Eisenreich *et al.* 1996; Lichtenthaler *et al.* 1997a; Lichtenthaler *et al.* 1997b; Schwender *et al.* 1996; Schwender *et al.* 1997; Zeidler *et al.* 1997). Both the MEP and the MVA pathway are present in higher plants and are localized in the chloroplast and cytoplasm respectively (Hemmerlin *et al.* 2003). However, the MEP pathway is absent in humans.

1.2.2 Enzymatic steps

The MEP pathway is comprised of seven enzymatic steps (Figure 1.1) (Sharkey *et al.* 2008). It starts with the biosynthesis of 1-deoxy-D-xylulose 5-phosphate (DXP) from pyruvate and D-glyceraldehyde 3-phosphate (GAP) catalyzed by the enzyme 1-deoxy-D-xylulose-5-phosphate synthase (DXS) (Rodríguez-Concepción & Boronat 2002; Rohmer *et al.* 1996). DXS requires thiamin diphosphate (ThDP) and the divalent ion Mg^{2+}/Mn^{2+} for its activity. In the next step, DXP is converted to MEP by the enzyme 1-deoxy-D-xylulose-5-phosphate reductoisomerase (DXR). MEP is then converted to the cyclic intermediate methylerythritol 2,4-cyclodiphosphate (MEcDP) through three consecutive enzymatic steps involving cytidylation (CTP-dependent), phosphorylation (ATP-dependent), and cyclization. In the sixth step, MEcDP is converted into 4-hydroxy-3-methylbut-2-enyl diphosphate (HMBDP) catalyzed by HMBDP synthase (HDS). In the last step, HMDBP is reduced to IDP and DMADP by HMBDP reductase (HDR). IDP and DMADP are also isomerized by isopentenyl diphosphate isomerase (IDI).

DMADP serves as the precursor for isoprene. In isoprene emitting plants, isoprene synthase (IspS) catalyzes the formation of isoprene from DMADP (Figure 1.1). Higher ordered isoprenoids are synthesized from both IDP and DMADP through downstream enzymatic reactions (Figure 1.1).

1.2.3 Importance of studying MEP pathway

The absence of the MEP pathway in humans and its presence in eubacteria, apicomplexa parasites, and photosynthetic eukaryotes make it a target for development of new antibiotics, antiparasitic drugs, and herbicides (Cordoba *et al.* 2009; Rodríguez-Concepción 2004). Some isoprenoids have commercial applications as pigments, fragrance and flavors, drugs, and polymers (Rodríguez-Concepción 2006). A large number of natural products used as therapeutic agents are terpenoids. Various terpenoids with potential therapeutic activities are available in limited quantity from natural sources (Ajikumar *et al.* 2008). Metabolic engineering leading to improved biosynthetic production of these important terpenoids has commercial potential. A sesquiterpene antimalarial drug, artemisinin, comes from *Artemisina annua* but now has been engineered in yeast (Westfall *et al.* 2012). Some isoprenoids including carotenoids, tocopherols, and antimicrobial drugs are important targets for biotechnological manipulation (Cordoba *et al.* 2009; DellaPenna & Posgon 2006). Detailed knowledge about the regulation of the MEP pathway is critical for better use of this pathway in biotechnological applications.

Isoprene, another important isoprenoid, is emitted by many organisms including bacteria, plants, and humans. The global annual production of isoprene from plants is 600 Tg (teragrams), which is about one third of the global non-methane hydrocarbon emission (Guenther *et al.* 2006). Atmospheric chemistry is strongly affected by this large amount of isoprene from the biosphere. In the presence of nitric oxide, isoprene catalyzes the formation of ozone, which can cause atmospheric pollution and is detrimental to both humans and plants (Sharkey *et al.* 2008). There have been many attempts to build mechanistic models of isoprene emission from leaves, which should help identify gaps in its understanding and may better predict isoprene emission under

future conditions (Monson *et al.* 2012), but it has been difficult to determine the correct molecular basis for these models. A major limitation is understanding the metabolic regulation of the MEP pathway in isoprene-emitting leaves.

1.3 OVERVIEW OF DXS

1.3.1 Catalytic reaction

DXS catalyzes the condensation of pyruvate and D-glyceraldehyde-3-phosphate (D-GAP) in presence of ThDP and a divalent cation, Mg^{2+} or Mn^{2+}. In the catalytic reaction, pyruvate and D-GAP act as the donor and the acceptor molecules respectively. In addition to the physiological substrate D-GAP, recombinant DXS also accepts the non-phosphorylated D-glyceraldehyde (D-GA) as the acceptor molecule (Eubanks & Poulter 2003; Lois *et al.* 1998; Takahashi *et al.* 1998). DXS has also been shown to exhibit the ability to use non-polar aliphatic aldehydes, which are structurally different from the natural substrate D-GAP, as the acceptor molecule (Brammer & Meyers 2009).

DXS-catalyzed formation of DXP from pyruvate and D-GAP combines the chemistry of both decarboxylase and carboligase enzymes. Its catalytic reaction resembles that of other ThDP-dependent enzymes like acetolactate synthase, glyoxylate carboligase and transketolase (TK) (Brammer *et al.* 2011; Eubanks & Poulter 2003; Nemeria *et al.* 2012). Similar decarboxylase and carboligase chemistry is used to generate acetohydroxyacid and tartronate semialdehyde by acetolactate synthase and glyoxylate carboligase respectively (Brammer *et al.* 2011; Nemeria *et*

al. 2012). TK catalyzes the condensation between a variety of physiological substrates where a keto sugar acts as the donor substrate and an aldo sugar acts as the acceptor substrate (Eubanks & Poulter 2003). TK carries out the ThDP-mediated transfer of a 2-carbon fragment from the donor substrate to the acceptor substrate through the carboligation reaction, which is similar to the fundamental chemistry of DXS-catalyzed reaction (Wikner *et al.* 1997).

The catalytic reaction of DXS is initiated by the formation of the highly reactive ylide from the C2 atom of the thiazolium ring of ThDP followed by the nucleophilic attack of the ylide on the donor substrate pyruvate to form C2α-lactylthiamin diphosphate (LThDP), the predecarboxylation intermediate (Figure 1.2). It has been shown that a ternary complex is required to form between LThDP and GAP for the catalytic reaction of DXS (Brammer Basta *et al.* 2014; Brammer *et al.* 2011; Patel *et al.* 2012). It has also been observed that LThDP is stabilized by DXS in absence of GAP and the decarboxylation is facilitated by approximately 600-fold in presence of D-GAP (Patel *et al.* 2012). The decarboxylation of LThDP generates an enzyme-bound enamine, which carries out nucleophilic attack on the acceptor substrate D-GAP to synthesize DXP (Figure 1.2). The elimination of DXP from the enzyme regenerates ThDP-bound enzyme and completes the catalytic cycle.

Traditionally, all the ThDP-dependent enzymes are believed to operate by a classical ping-pong mechanism, which involves the binding of the donor substrate to the enzyme followed by the release of the first product leaving a modified enzyme and then the binding of the acceptor substrate to the modified enzyme followed by the release of the second product recycling back the unmodified enzyme (Frank *et al.* 2007). DXS seems to be mechanistically unique in this class of ThDP-dependent enzyme. The actual mechanism followed by DXS is not absolutely known and the collective reports in this regard are conflicting. Mechanistic studies on

Rhodobacter capsulatus DXS presented compelling evidence for the requirement of the ternary complex in its catalytic reaction (Eubanks & Poulter 2003). This work suggested an ordered mechanism for DXS with pyruvate binding first (Figure 1.3 A). Later studies by Matsue and coworkers proposed the classical ping-pong mechanism for DXS (Matsue *et al.* 2010) (Figure 1.3 B). In 2011, Brammer and coworkers reported that both D-GAP and pyruvate bind reversibly and independently to DXS. They suggested from this observation that the enzyme follows a novel rapid equilibrium random sequential mechanism (Brammer *et al.* 2011) (Figure 1.3 C). The stability of LThDP intermediate in absence of D-GAP and the requirement of ternary complex for decarboxylation does not support a ping-pong mechanism. The ordered mechanism with pyruvate binding first or the random sequential mechanism are possible mechanisms for DXS as both of these mechanisms support the stability of LThDP intermediate in absence of D-GAP and the requirement of ternary complex for decarboxylation (Patel *et al.* 2012).

1.3.2 Structure

The crystal structure of DXS has been reported from *E. coli* and *Deinococcus radiodurans* (Xiang *et al.* 2007). DXS exists as a tightly associated dimer. Each monomer in the dimeric arrangement shares a surface area of more than 3900 Å in the dimer interface, which is mostly hydrophobic in nature (Xiang *et al.* 2007). The crystal structure shows that the two DXS monomers are positioned side-by-side in the dimeric assembly in a way that each domain of one monomer is in contact with its equivalent in the other monomer (Figure 1.4) (Xiang *et al.* 2007).

Each monomer of DXS is composed of three domains, I, II, and III (Figure 1.4) (Xiang *et al.* 2007). Structurally, DXS is different from the other ThDP-dependent enzymes. The arrangement

of three domains of DXS monomer is different from TK and pyruvate dehydrogenase (PDH). This results in a different dimeric organization and the positioning of the active site for DXS as compared to TK and PDH. In the DXS dimer, domain I of one monomer is located directly above domains II and III of the same monomer (Figure 1.4) whereas in TK and PDH dimers, domain I of one monomer is located above domains II and III of the other monomer (Xiang *et al.* 2007). The different dimeric organization of DXS causes its active site to be located within the same monomer in contrast to TK and PDH, where the active site is located at the interface between the two monomers (Xiang *et al.* 2007). In DXS, the active site is located at the interface between domains I and II of the same monomer without having any direct contribution from the residues in the other monomer of the dimer (Xiang *et al.* 2007). The difference in the domain organization of DXS may be due to the presence of a very short linker (~20 residues) between domains I and II in contrast to the long linker of TK and PDH (~95 residues) (Xiang *et al.* 2007).

1.3.3 Role in MEP pathway regulation

Several studies have suggested that DXS plays a significant role in the regulation of the MEP pathway. It has been shown that the regulation of gene expression is most evident for DXS among all the MEP pathway enzymes along with isoprene synthase in isoprene emitting poplar leaves (Wiberley *et al.* 2009). In support of the regulatory role of DXS, other evidence comes from the observation that Arabidopsis transgenic lines, having higher or lower DXS levels, have increased or decreased amount of different isoprenoids including chlorophylls, carotenoids, tocopherols, gibberellins, and abscisic acid (Estévez *et al.* 2001). Recently, Wright and coworkers have demonstrated using metabolic control analysis that DXS controls the flux

through the MEP pathway in Arabidopsis (Wright *et al.* 2014). Various reports in other plants including tomato (Enfissi *et al.* 2005; Lois *et al.* 2000), potato (Morris *et al.* 2006), and *Ginkgo biloba* (Gong *et al.* 2006) have shown that the level of some end products of the pathway can be manipulated (between 2–7-fold) by modulating the gene expression of DXS. These results suggested that the step catalyzed by DXS has a rate-determining function in the MEP pathway. In addition to plants, the rate-limiting role of DXS has also been demonstrated in several bacteria (Harker & Bramley 1999; Kuzuyama *et al.* 2000; Matthews & Wurtzel 2000).

Another line of evidence indicating a potential regulatory role of DXS in the MEP pathway is the presence of multiple genes that encode DXS in different plant species including conifers, dicots, and monocots (Cordoba *et al.* 2009). Multiple copies of DXS genes are widespread in various plants like Arabidopsis (Araki *et al.* 2000; Estévez *et al.* 2000), *Zea mays* (Walter *et al.* 2000), *Medicago truncatula* (Walter *et al.* 2002), *Oryza sativa* (Kim *et al.* 2005), *Picea abies* (Phillips *et al.* 2007), *Ginkgo biloba* (Kim *et al.* 2006), and *Pinus densiflora* (Kim *et al.* 2009) (Table 1.1). Two or three potential DXS genes are reported in these plants. Each of these genes exhibits particular expression pattern and often different spatial distributions, which is suggestive of their distinct roles in isoprenoid biosynthesis. Functionally each of these different variants of DXS has been correlated with the synthesis of particular isoprenoid compounds. Phylogenetic analysis shows that the different variants of DXS from some of these plants clustered into independent clades (Kim *et al.* 2005; Kim *et al.* 2009; Krushkal *et al.* 2003). Two out of the three different DXS-like genes in Arabidopsis and *Picea abies* cluster into the same clade (Kim *et al.* 2005; Phillips *et al.* 2007). The existence of the representative genes of DXS belonging to different clades during evolution in several species also suggests a particular function for them. Considering the huge number of isoprenoid end products synthesized through this pathway, it is

tempting to speculate that each variant of DXS gene family might contribute to the synthesis of particular products and, thereby, is involved in the independent regulation of their synthesis (Cordoba *et al.* 2009).

1.4 METABOLIC REGULATION OF THE MEP PATHWAY

1.4.1 Background

Metabolic regulation of the MEP pathway has been strongly suggested by Wolfertz and coworkers. They have shown that feeding leaves with dideuterated deoxyxylulose (DOX-d_2) results in the complete displacement of the endogenous, unlabeled isoprene by the exogenous, labeled isoprene with little change in the overall rate of isoprene emission (Wolfertz *et al.* 2004; Wolfertz *et al.* 2003) (Figure 1.5). In this experiment, exogenous DOX-d_2 is absorbed by the cell and phosphorylated to DXP-d_2 in the cytosol (Hemmerlin *et al.* 2006). It is then transported to the chloroplast by a xylulose phosphate transporter (Eicks *et al.* 2002). The transported DXP-d_2 then enters the MEP pathway leading to the synthesis of labeled DMADP. The endogenous supply of DXP gets displaced by the exogenous source after feeding with DOX- d_2 keeping the overall rate of isoprene emission nearly constant (Figure 1.5). This suggests that the concentration of DMADP and DXP remains constant. In order to maintain a constant level of DMADP and DXP, the carbon flow through the endogenous pathway is reduced during the feeding of exogenous DOX. This in turn suggests that regulation may be present in the beginning of the MEP pathway. The overall result can be rationalized by a negative feedback loop from

DXP, DMADP or any other intermediates of the pathway affecting the activity of DXS. The endogenous source of MEP pathway intermediates through DXS is reduced as exogenous DOX begins to supply DXP. Feedback regulation of enzymes downstream of DXP is ruled out because these would regulate both the endogenous and exogenous sources of DMADP. This is shown in Figure 1.6.

1.4.2 Research Goal

The work of Wolfertz and coworkers suggested the presence of metabolic regulation in the MEP pathway. The goal of my research involved the understanding of the specific metabolic regulation of the MEP pathway. My main focus was to study the role of DXS in this metabolic regulation.

APPENDIX

TABLE 1.1 List of multiple genes for DXS. The nomenclature used for each gene is according to their name in the corresponding literature. The extension 'like' is used (as suggested by Phillips *et al.*, 2008) in those genes whose function has not been determined. The number mentioned in the parenthesis beside the protein name denotes the proposed class in which the DXS protein belongs. (Adapted from Cordoba *et al*. 2009)

Plant Species	Gene	Protein	Reference
Arabidopsis thaliana	*DXS*	DXS1 (1)	Estévez *et al.*, 2000
	DXL1	DXS2 (1)	Araki *et al.*, 2000
	DXL2	DXS3 (3)	Araki *et al.*, 2000
Picea abies	*PaDXS1*	PaDXS1 (1)	Phillips *et al.*, 2007
	PaDXS2A	PaDXS2A (2)	Phillips *et al.*, 2007
	PaDXS2B	PaDXS2B (2)	Phillips *et al.*, 2007
Medicago truncatula	*MtDXS1-like*	MtDXS1 (1)	Walter *et al.*, 2002
	MtDXS2-like	MtDXS2 (2)	Walter *et al.*, 2002
Ginkgo biloba	*GbDXS1*	GbDXS1 (1)	Kim *et al.*, 2006
	GbDXS2	GbDXS2 (2)	Kim *et al.*, 2006
Oryza sativa	*dxs1-like*	OsDXS1 (1)	Kim *et al.*, 2005
	dxs2-like	OsDXS2 (3)	Kim *et al.*, 2005
	dxs3	OsDXS3 (2)	Kim *et al.*, 2005
Zea mays	*dxs1-like*	DXS1 (1)	Walter *et al.*, 2000
	dxsL2-like	DXS2 (2)	Walter *et al.*, 2000
Pinus densiflora	*PdDXS1*	PdDXS1 (1)	Kim *et al.*, 2009
	PdDXS2	PdDXS2 (2)	Kim *et al.*, 2009

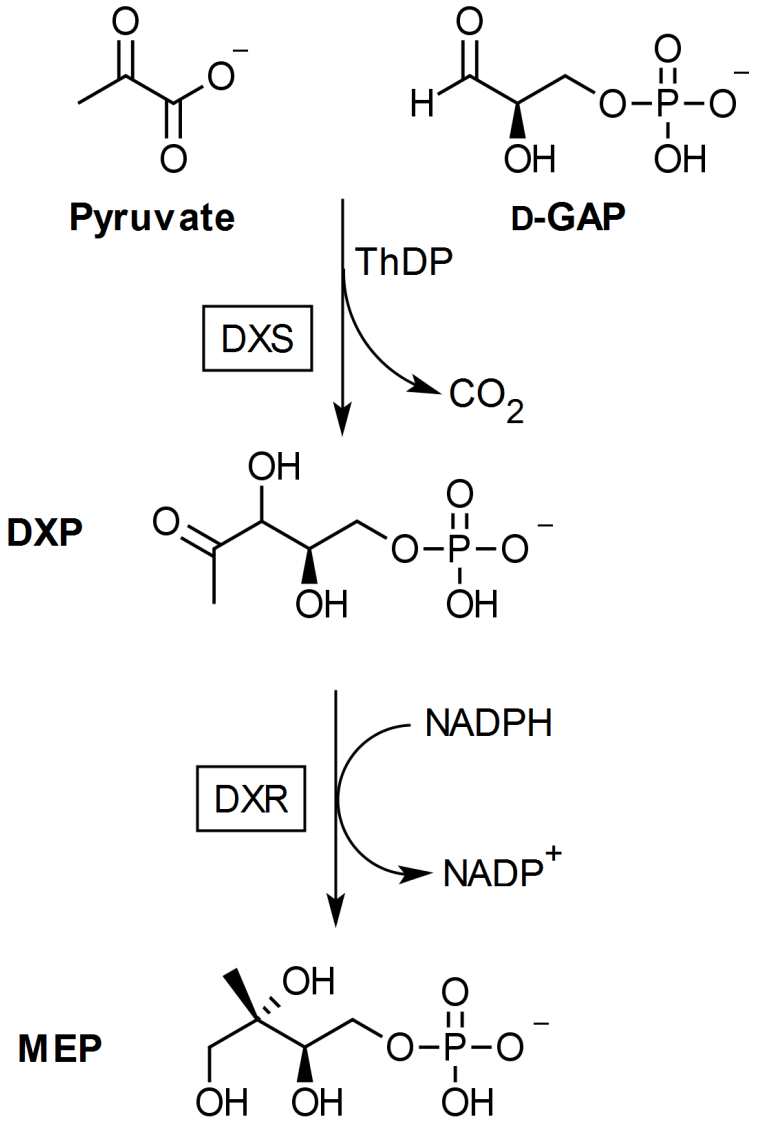

FIGURE 1.1 MEP pathway for biosynthesis of isoprenoids. The steps shown in the blue boxes are not part of MEP pathway and constitute the downstream steps for isoprenoid biosynthesis. *MEP pathway*: 2-*C*-methyl-D-erythritol 4-phosphate pathway; *D-GAP*: D-glyceraldehyde 3-phosphate; *DXS*: 1-deoxy-D-xylulose 5-phosphate (DXP) synthase; *DXR*: DXP reductoisomerase; *MEP*: 2-*C*-methyl-D-erythritol 4-phosphate; *CMS*: 4-(cytidine 5'-diphospho)-2-*C*-methyl-D-erythritol (CDPME) synthase; *CMK*: CDPME kinase; *CDPMEP*: CDPME 2-phosphate; *MCS*: 2-*C*-methyl-D-erythritol 2,4-cyclodiphosphate (MEcDP) synthase; *HDS*: 4-hydroxy-3-methylbut-2-enyl diphosphate (HMBDP) synthase; *HDR*: HMBDP reductase; *IDP*: isopentenyl diphosphate; *DMADP*: dimethylallyl diphosphate; *IDI*: IDP isomerase; *IspS*: isoprene synthase. (Adapted from Sharkey *et al*. 2008)

FIGURE 1.1 (cont'd)

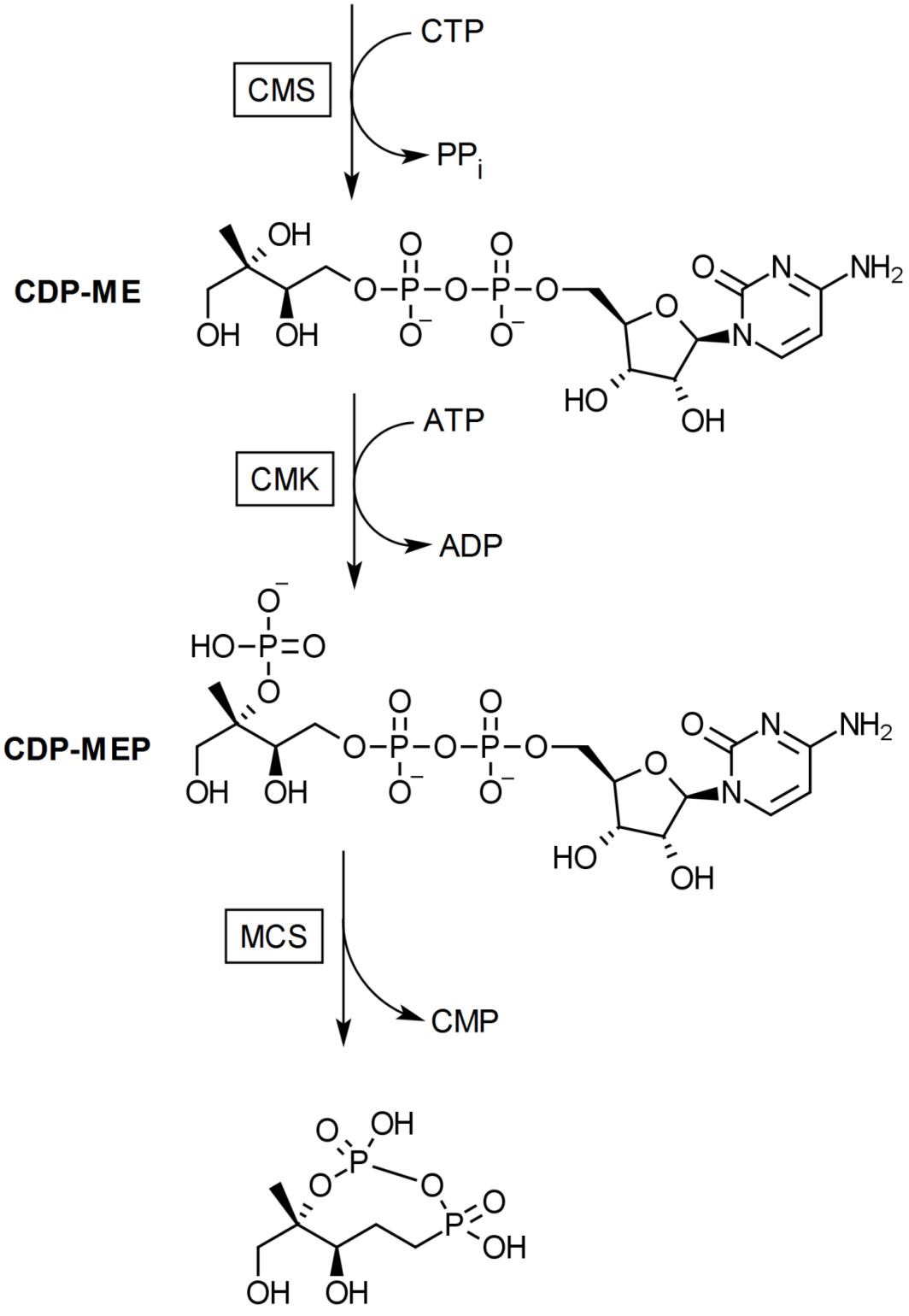

FIGURE 1.1 (cont'd)

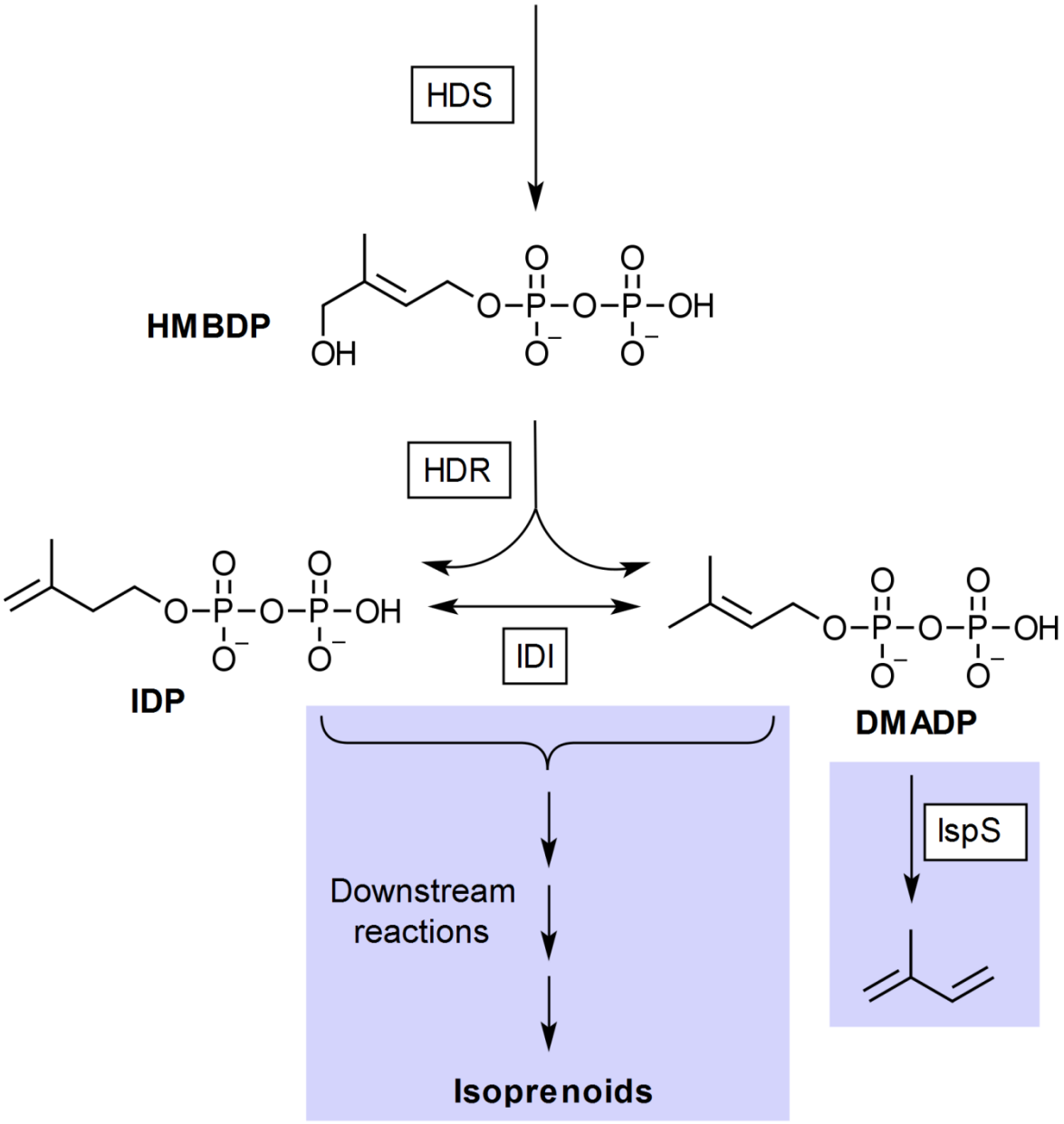

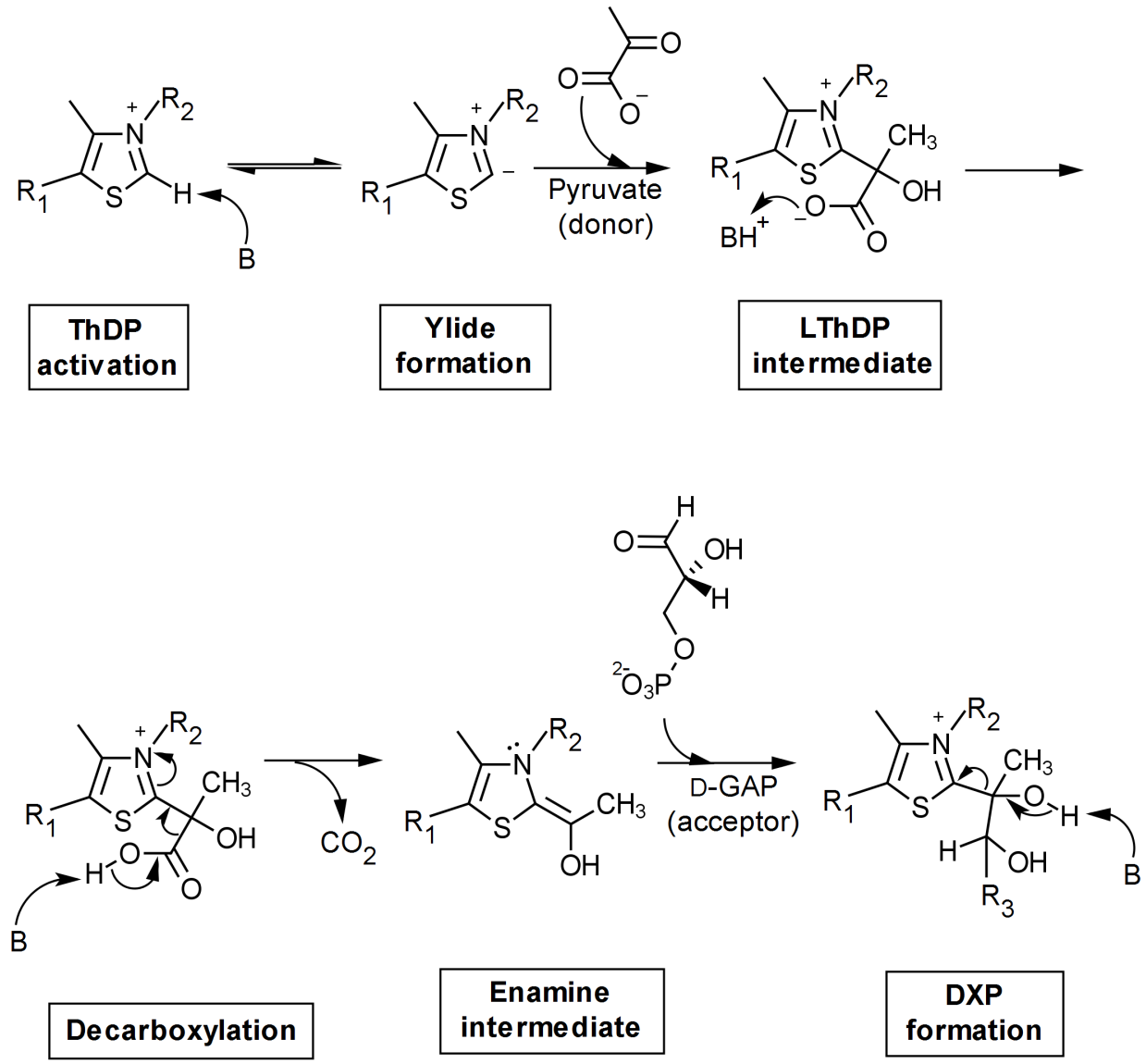

FIGURE 1.2 Proposed mechanism for the catalytic cycle of DXS. *ThDP*: thiamin diphosphate; *LThDP*: C2α-lactylthiamin diphosphate. (Adapted from Eubanks *et al*. 2003).

FIGURE 1.2 (cont'd)

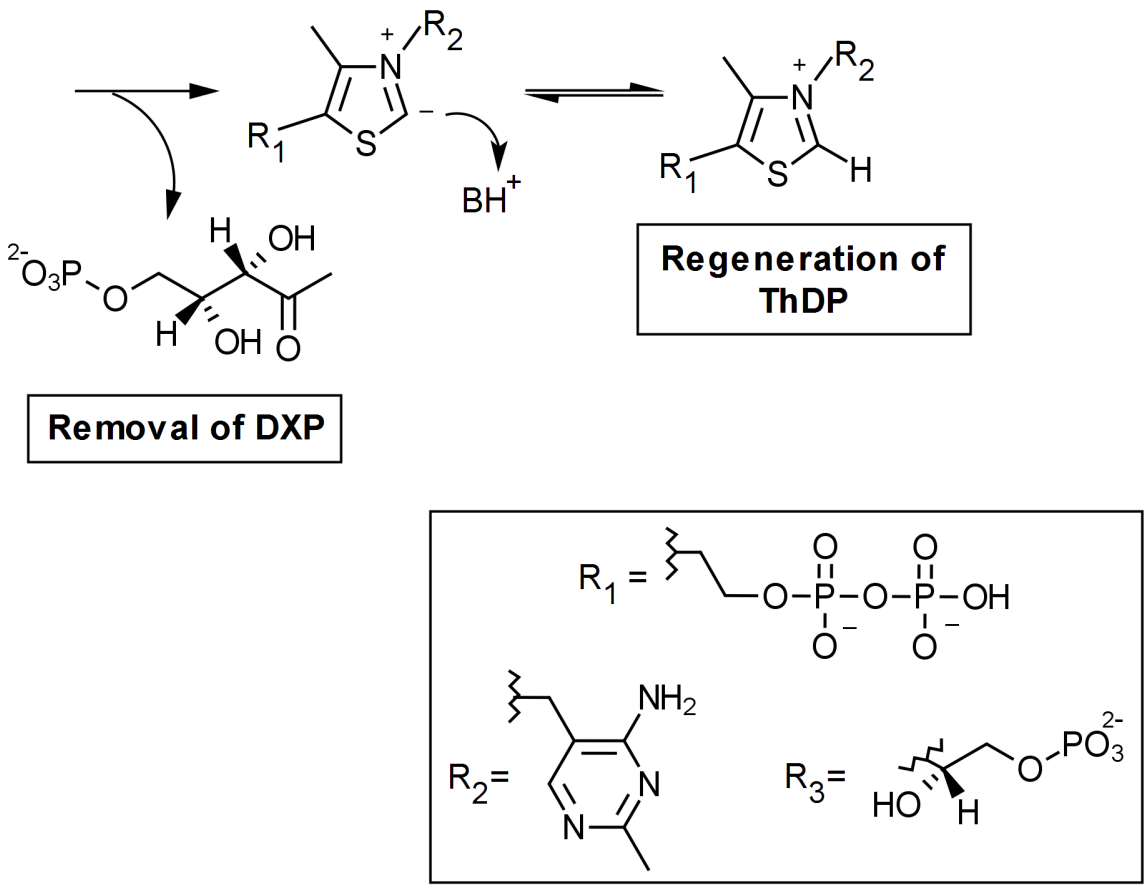

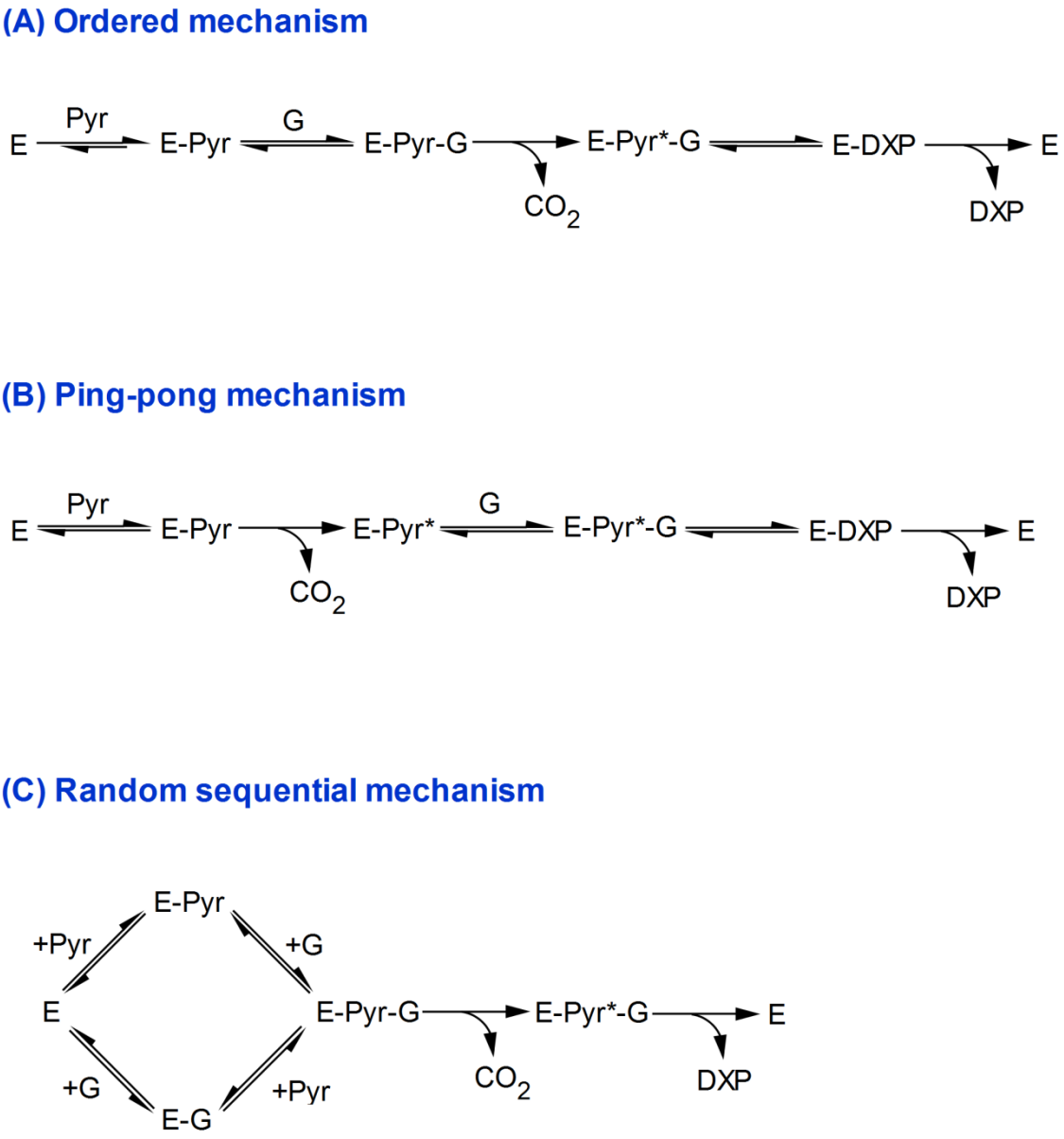

FIGURE 1.3 Different possible mechanisms for DXS activity. (A) Ordered mechanism where pyruvate binds tightly and essentially irreversibly to DXS. (B) Ping-pong mechanism where CO_2 eliminates prior to D-GAP binding. (C) Random sequential mechanism where D-GAP and pyruvate bind reversibly and independently to DXS. *E*: ThDP-bound enzyme; *Pyr:* Pyruvate; *Pyr*:* 2-hydroxyethyl-ThDP; *G*: D-GAP; *E-Pyr-G:* catalytically competent ternary complex. (Adapted from Brammer *et al*. 2011).

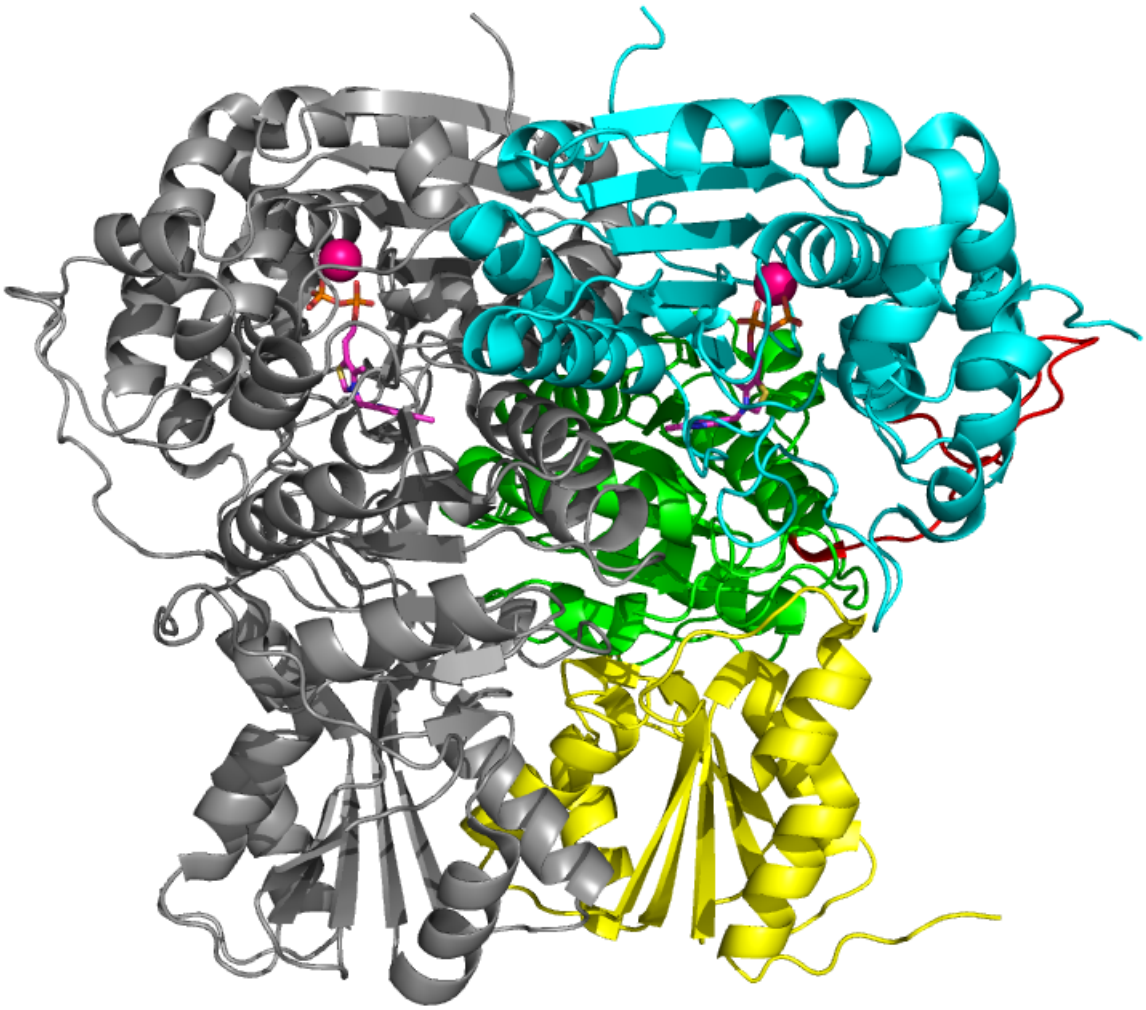

FIGURE 1.4 Crystal structures of DXS from *Deinococcus radiodurans*. The three domains of one monomer are colored cyan, green, and yellow, respectively, and the linker between domains I and II is colored red. The other monomer is colored gray. These two monomers shown here are related by an approximate non-crystallographic two-fold symmetry. ThDP is shown as a stick model in magenta. Mg^{2+} ion is shown as sphere in pink. The image was produced in PyMol (The PyMOL Molecular Graphics System, Schrödinger, LLC) using the Protein Data Bank files (2O1X: code for *D. radiodurans*). (Xiang *et al.* 2007)

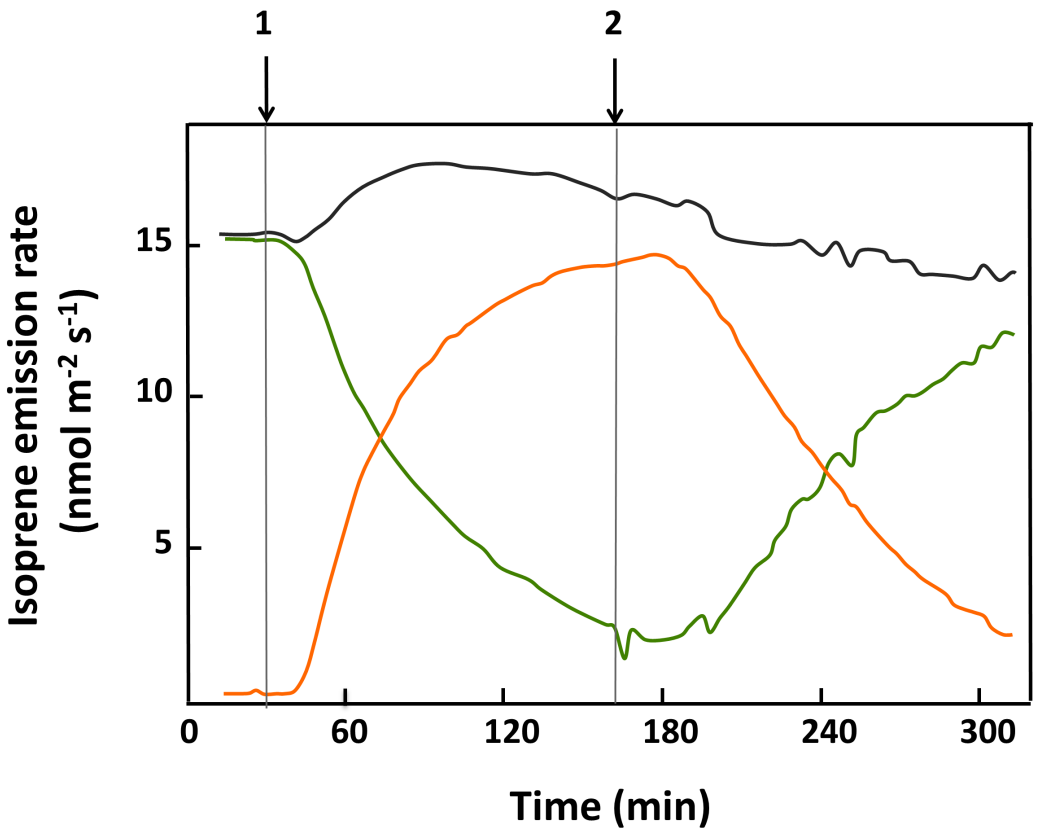

FIGURE 1.5 Time course of the rate of isoprene emission in the DOX-d_2 experiment by Wolfertz and coworkers. DOX-d_2 (2.94 mM) was fed to the leaf at point 1 and the feeding was stopped at point 2. Black curve represents total isoprene emission, green curve represents isoprene not labeled with deuterium, and orange curve represents deuterium-labeled isoprene. (Adapted from Wolfertz *et al*. 2004).

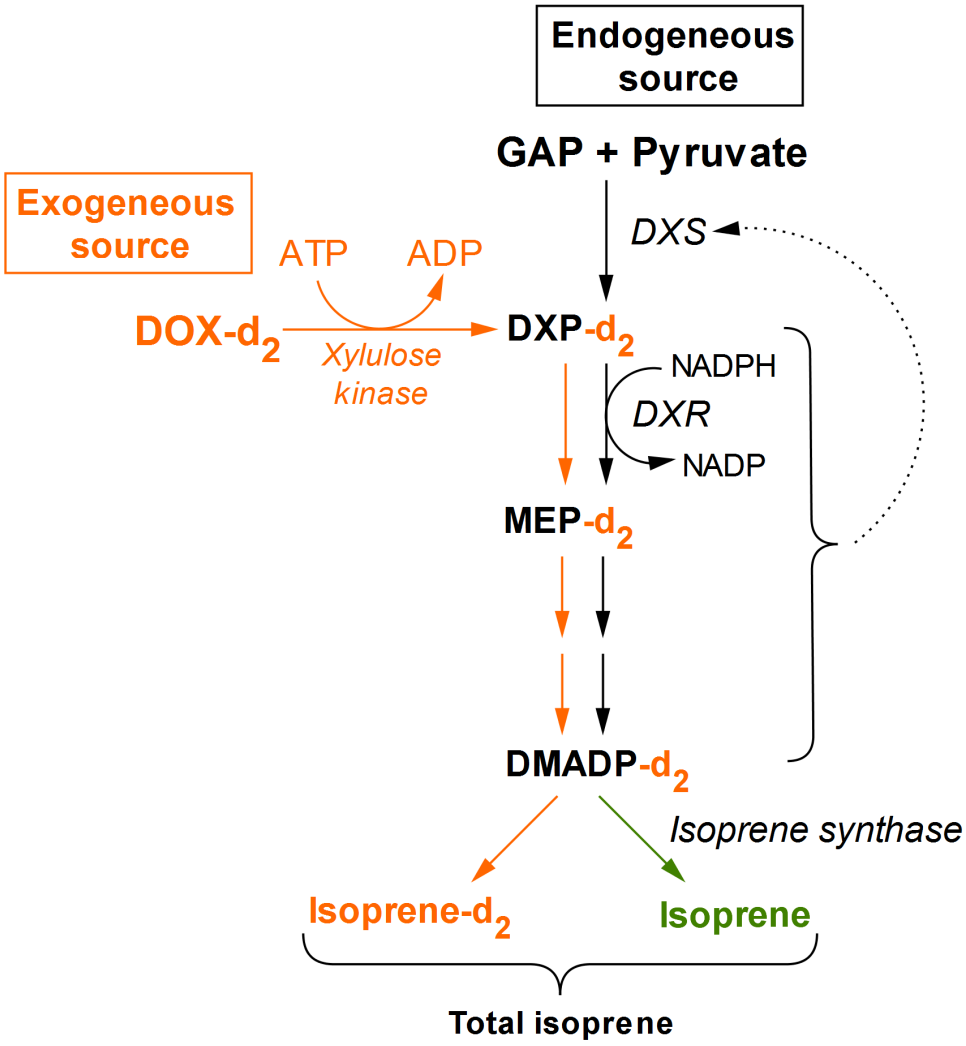

FIGURE 1.6 Possible feedback regulation in DOX-d_2 experiment. Solid black arrows represent the pathway for isoprene synthesis from the endogenous sources (GAP + pyruvate). Green arrow represents the isoprene synthesized from the endogenous source. Orange arrows represent the pathway for isoprene synthesis from the exogenous source of DOX-d_2. Dotted lines represent the hypothesized feedback loops. (Adapted from Wolfertz *et al*., 2004)

LITERATURE CITED

LITERATURE CITED

Ajikumar P.K., Tyo K., Carlsen S., Mucha O., Phon T.H. & Stephanopoulos G. (2008) Terpenoids: opportunities for biosynthesis of natural product drugs using engineered microorganisms. *Molecular Pharmaceutics*, **5**, 167–190.

Araki N., Kusumi K., Masamoto K., Niwa Y. & Iba K. (2000) Temperature-sensitive *Arabidopsis* mutant defective in 1-deoxy-D-xylulose 5-phosphate synthase within the plastid non-mevalonate pathway of isoprenoid biosynthesis. *Physiologia Plantarum*, **108**, 19-24.

Arigoni D., Sagner S., Latzel C., Eisenreich W., Bacher A. & Zenk M.H. (1997) Terpenoid biosynthesis from 1-deoxy-D-xylulose in higher plants by intramolecular skeletal rearrangement. *Proceedings of the National Academy of Sciences of the United States of America*, **94**, 10600-10605.

Brammer Basta L.A., Patel H., Kakalis L., Jordan F. & Freel Meyers C.L. (2014) Defining critical residues for substrate binding to 1-deoxy-D-xylulose 5-phosphate synthase – active site substitutions stabilize the predecarboxylation intermediate C2α-lactylthiamin diphosphate. *FEBS Journal*, **281**, 2820-2837.

Brammer L.A. & Meyers C.F. (2009) Revealing substrate promiscuity of 1-deoxy-D-xylulose 5-phosphate synthase. *Organic Letters*, **11**, 4748-4751.

Brammer L.A., Smith J.M., Wade H. & Meyers C.F. (2011) 1-Deoxy-D-xylulose 5-phosphate synthase catalyzes a novel random sequential mechanism. *Journal of Biological Chemistry*, **286**, 36522-36531.

Caputi L. & Aprea E. (2011) Use of terpenoids as natural flavouring compounds in food industry. *Recent Patents on Food, Nutrition & Agriculture*, **3**, 9-16.

Cordoba E., Salmi M. & León P. (2009) Unravelling the regulatory mechanisms that modulate the MEP pathway in higher plants. *Journal of Experimental Botany*, **60**, 2933-2943.

Cserháti T. & Forgács E. (2001) Liquid chromatographic separation of terpenoid pigments in foods and food products. *Journal of Chromatography A*, **936**, 119-137.

DellaPenna D. & Posgon B.J. (2006) Vitamin synthesis in plants: tocopherols and carotenoids. *Annual Review of Plant Biology*, **57**, 711-738.

Eicks M., Maurino V., Knappe S., Flügge U.-I. & Fischer K. (2002) The plastidic pentose phosphate translocator represents a link between the cytosolic and the plastidic pentose phosphate pathways in plants. *Plant Physiology*, **128**, 512-522.

Eisenreich W., Bacher A., Arigoni D. & Rohdich F. (2004) Biosynthesis of isoprenoids via the non-mevalonate pathway. *Cellular and Molecular Life Sciences*, **61**, 1401-1426.

Eisenreich W., Menhard B., Hylands P.J. & Zenk M.H. (1996) Studies on the biosynthesis of taxol: the taxane carbon skeleton is not of mevalonoid origin. *Proceedings of the National Academy of Sciences of the United States of America*, **93**, 6431-6436.

Eisenreich W., Schwarz M., Cartayrade A., Arigoni D., Zenk M.H. & Bacher A. (1998) The deoxyxylulose phosphate pathway of terpenoid biosynthesis in plants and microorganisms. *Chemistry & Biology*, **5**, R221-R233.

Enfissi E.M.A., Fraser P.D., Lois L.M., Boronat A., Schuch W. & Bramley P.M. (2005) Metabolic engineering of the mevalonate and non-mevalonate isopentenyl diphosphate-forming pathways for the production of health-promoting isoprenoids in tomato. *Plant Biotechnology Journal*, **3**, 17-27.

Estévez J.M., Cantero A., Reindl A., Reichler S. & León P. (2001) 1-Deoxy-D-xylulose-5-phosphate synthase, a limiting enzyme for plastidic isoprenoid biosynthesis in plants. *Journal of Biological Chemistry*, **276**, 22901-22909.

Estévez J.M., Cantero A., Romero C., Kawaide H., Jiménez L.F., Kuzuyama T., Seto H., Kamiya Y. & Léon P. (2000) Analysis of the expression of *CLA1*, a gene that encodes the 1-deoxyxylulose 5-phosphate synthase of the 2-*C*-methyl-D-erythritol-4-phosphate pathway in Arabidopsis. *Plant Physiology*, **124**, 95-103.

Eubanks L.M. & Poulter C.D. (2003) *Rhodobacter capsulatus* 1-deoxy-D-xylulose 5-phosphate synthase: steady-state kinetics and substrate binding. *Biochemistry*, **42**, 1140-1149.

Frank R.A., Leeper F.J. & Luisi B.F. (2007) Structure, mechanism and catalytic duality of thiamine-dependent enzymes. *Cellular and Molecular Life Sciences*, **64**, 892-905.

Gong Y.F., Liao Z.H., Guo B.H., Sun X.F. & Tang K.X. (2006) Molecular cloning and expression profile analysis of *Ginkgo biloba DXS* gene encoding 1-deoxy-D-xylulose 5-phosphate synthase, the first committed enzyme of the 2-*C*-methyl-D-erythritol 4-phosphate pathway. *Planta Medica*, **72**, 329-335.

Guenther A., Karl T., Harley P., Wieldinmyer C., Palmer P.I. & Geron C. (2006) Estimates of global terrestrial isoprene emissions using MEGAN (Model of Emissions of Gases and Aerosols from Nature). *Atmospheric Chemistry Physics*, **6**, 3181-3210.

Harker M. & Bramley P.M. (1999) Expression of prokaryotic 1-deoxy-D-xylulose-5-phosphatases in *Escherichia coli* increases carotenoid and ubiquinone biosynthesis. *FEBS Letters*, **448**, 115-119.

Hemmerlin A., Hoeffler J.-F., Meyer O., Tritsch D., Kagan I.A., Grosdemange-Billiard C., Rohmer M. & Bach T.J. (2003) Cross-talk between the cytosolic mevalonate and the plastidial methylerythritol phosphate pathways in tobacco bright yellow-2 cells. *Journal of Biological Chemistry*, **278**, 26666-26676.

Hemmerlin A., Tritsch D., Hartmann M., Pacaud K., Hoeffler J.-F., van Dorsselaer A., Rohmer M. & Bach T.J. (2006) A cytosolic Arabidopsis D-xylulose kinase catalyzes the phosphorylation of 1-deoxy-D-xylulose into a precursor of the plastidial isoprenoid pathway. *Plant Physiology*, **142**, 441-457.

Hunter W.N. (2007) The non-mevalonate pathway of isoprenoid precursor biosynthesis. *Journal of Biological Chemistry*, **282**, 21573-21577.

Kim B.-R., Kim S.-U. & Chang Y.-J. (2005) Differential expression of three 1-deoxy-D-xylulose-5-phosphate synthase genes in rice. *Biotechnology Letters*, **27**, 997-1001.

Kim S.-M., Kuzuyama T., Chang Y.-J., Song K.-S. & Kim S.-U. (2006) Identification of class 2 1-deoxy-D-xylulose 5-phosphate synthase and 1-deoxy-D-xylulose 5-phosphate reductoisomerase genes from *Ginkgo biloba* and their transcription in embryo culture with respect to ginkgolide biosynthesis. *Planta Medica*, **72**, 234-240.

Kim Y.-B., Kim S.-M., Kang M.-K., Kuzuyama T., Lee J.K., Park S.-C., Shin S.-C. & Kim S.-U. (2009) Regulation of resin acid synthesis in *Pinus densiflora* by differential transcription of genes encoding multiple 1-deoxy-D-xylulose 5-phosphate synthase and 1-hydroxy-2-methyl-2-(*E*)-butenyl 4-diphosphate reductase genes. *Tree Physiology*, **29**, 737-749.

Klein-Marcuschamer D., Ajikumar P.K. & Stephanopoulos G. (2007) Engineering microbial cell factories for biosynthesis of isoprenoid molecules: beyond lycopene. *Trends in Biotechnology*, **25**, 417-424.

Krushkal J., Pistilli M., Ferrell K.M., Souret F.F. & Weathers P.J. (2003) Computational analysis of the evolution of the structure and function of 1-deoxy-D-xylulose-5-phosphate synthase, a key regulator of the mevalonate-independent pathway in plants. *Gene*, **313**, 127-138.

Kuzuyama T., Takagi M., Takahashi S. & Seto H. (2000) Cloning and characterization of 1-deoxy-D-xylulose 5-phosphate synthase from *Streptomyces* sp. strain CL190, which uses both the mevalonate and nonmevalonate pathways for isopentenyl diphosphate biosynthesis. *Journal of Bacteriology*, **182**, 891-897.

Lichtenthaler H.K., Rohmer M. & Schwender J. (1997a) Two independent biochemical pathways for isopentenyl diphosphate and isoprenoid biosynthesis in higher plants. *Physiologia Plantarum*, **101**, 643-652.

Lichtenthaler H.K., Schwender J., Disch A. & Rohmer M. (1997b) Biosynthesis of isoprenoids in higher plant chloroplasts proceeds via a mevalonate-independent pathway. *FEBS Letters*, **400**, 271-274.

Lois L.M., Campos N., Putra S.R., Danielsen K., Rohmer M. & Boronat A. (1998) Cloning and characterization of a gene from *Escherichia coli* encoding a transketolase-like enzyme that catalyzes the synthesis of D-1-deoxyxylulose 5-phosphate, a common precursor for

isoprenoid, thiamin, and pyridoxol biosynthesis. *Proceedings of the National Academy of Sciences of the United States of America*, **95**, 2105-2110.

Lois L.M., Rodríguez-Concepción M., Gallego F., Campos N. & Boronat A. (2000) Carotenoid biosynthesis during tomato fruit development: regulatory role of 1-deoxy-D-xylulose 5-phosphate synthase. *Plant Journal*, **22**, 503-513.

Matsue Y., Mizuno H., Tomita T., Asami T., Nishiyama M. & Kuzuyama T. (2010) The herbicide ketoclomazone inhibits 1-deoxy-D-xylulose 5-phosphate synthase in the 2-*C*-methyl-D-erythritol 4-phosphate pathway and shows antibacterial activity against *Haemophilus influenzae*. *The Journal of Antibiotics*, **63**, 583-588.

Matthews P.D. & Wurtzel E.T. (2000) Metabolic engineering of carotenoid accumulation in *Escherichia coli* by modulation of the isoprenoid precursor pool with expression of deoxyxylulose phosphate synthase. *Applied Microbiology and Biotechnology*, **53**, 396-400.

McGarvey D.J. & Croteau R. (1995) Terpenoid metabolism. *The Plant Cell*, **7**, 1015-1026.

Misawa N. (2011) Pathway engineering for functional isoprenoids. *Current Opinion in Biotechnology*, **22**, 627-633.

Monson R.K., Grote R., Niinemets Ü. & Schnitzler J.-P. (2012) Modeling the isoprene emission rate from leaves. *New Phytologist*, **195**, 541-559.

Morris W.L., Ducreux L.J.M., Hedden P., Millam S. & Taylor M.A. (2006) Overexpression of a bacterial 1-deoxy-D-xylulose 5-phosphate synthase gene in potato tubers perturbs the isoprenoid metabolic network: implications for the control of the tuber life cycle. *Journal of Experimental Botany*, **57**, 3007-3018.

Nakamura A., Shimada H., Masuda T., Ohta H. & Takamiya K. (2001) Two distinct isopentenyl diphosphate isomerases in cytosol and plastid are differentially induced by environmental stresses in tobacco. *FEBS Letters*, **506**, 61-64.

Nemeria N., Binshtein E., Patel H., Balakrishnan A., Vered I., Shaanan B., Barak Z., Chipman D. & Jordan F. (2012) Glyoxylate carboligase: a unique thiamin diphosphate-dependent enzyme that can cycle between the 4'-aminopyrimidinium and 1',4'-iminopyrimidine tautomeric forms in the absence of the conserved glutamate. *Biochemistry*, **51**, 7940-7952.

Patel H., Nemeria N.S., Brammer L.A., Freel Meyers C.L. & Jordan F. (2012) Observation of thiamin-bound intermediates and microscopic rate constants for their interconversion on 1-deoxy-D-xylulose 5-phosphate synthase: 600-fold rate acceleration of pyruvate decarboxylation by D-glyceraldehyde-3-phosphate. *Journal of the American Chemical Society*, **134**, 18374-18379.

Phillips M., Walter M., Ralph S., Dabrowska P., Luck K., Urós E., Boland W., Strack D., Rodríguez-Concepción M., Bohlmann J. & Gershenzon J. (2007) Functional identification and differential expression of 1-deoxy-D-xylulose 5-phosphate synthase in induced terpenoid resin formation of Norway spruce (*Picea abies*). *Plant Molecular Biology*, **65**, 243-257.

Phillips M.A., León P., Boronat A. & Rodríguez-Concepción M. (2008) The plastidial MEP pathway: unified nomenclature and resources. *Trends in Plant Science*, **13**, 619-623.

Roberts S.C. (2007) Production and engineering of terpenoids in plant cell culture. *Nature Chemical Biology*, **3**, 387-395.

Rodríguez-Concepción M. (2004) The MEP pathway: a new target for the development of herbicides, antibiotics and antimalarial drugs. *Current Pharmaceutical Design*, **10**, 2391-2400.

Rodríguez-Concepción M. (2006) Early steps in isoprenoid biosynthesis: multilevel regulation of the supply of common precursors in plant cells. *Phytochemistry Reviews*, **5**, 1-15.

Rodríguez-Concepción M. & Boronat A. (2002) Elucidation of the methylerythritol phosphate pathway for isoprenoid biosynthesis in bacteria and plastids. A metabolic milestone achieved through genomics. *Plant Physiology*, **130**, 1079-1089.

Rohmer M., Knani M., Simonin P., Sutter B. & Sahm H. (1993) Isoprenoid biosynthesis in bacteria: a novel pathway for the early steps leading to isopentenyl diphosphate. *Biochemical Journal*, **295**, 517-524.

Rohmer M., Seemann M., Horbach S., Bringer-Meyer S. & Sahm H. (1996) Glyceraldehyde 3-phosphate and pyruvate as precursors of isoprenic units in an alternative non-mevalonate pathway for terpenoid biosynthesis. *Journal of the American Chemical Society*, **118**, 2564-2566.

Rude M.A. & Schirmer A. (2009) New microbial fuels: a biotech perspective. *Current Opinion in Microbiology*, **12**, 274-281.

Sacchettini J.C. & Poulter C.D. (1997) Creating isoprenoid diversity. *Science*, **277**, 1788-1789.

Schwender J., Seemann M., Lichtenthaler H.K. & Rohmer M. (1996) Biosynthesis of isoprenoids (carotenoids, sterols, prenyl side-chains of chlorophylls and plastoquinone) via a novel pyruvate/glyceraldehyde 3-phosphate non-mevalonate pathway in the green alga *Scenedesmus obliquus*. *Biochemical Journal*, **316**, 73-80.

Schwender J., Zeidler J., Gröner R., Müller C., Focke M., Braun S. & Lichtenthaler H.K. (1997) Incorporation of 1-deoxy-D-xylulose into isoprene and phytol by higher plants and algae. *FEBS Letters*, **414**, 129-134.

Sharkey T.D., Wiberley A.E. & Donohue A.R. (2008) Isoprene emission from plants: why and how. *Annals of Botany*, **101**, 5-18.

Silver G.M. & Fall R. (1991) Enzymatic synthesis of isoprene from dimethylallyl diphosphate in aspen leaf extracts. *Plant Physiology*, **97**, 1588-1591.

Silver G.M. & Fall R. (1995) Characterization of aspen isoprene synthase, an enzyme responsible for leaf isoprene emission to the atmosphere. *Journal of Biological Chemistry*, **270**, 13010-13016.

Takahashi S., Kuzuyama T., Watanabe H. & Seto H. (1998) A 1-deoxy-D-xylulose 5-phosphate reductoisomerase catalyzing the formation of 2-*C*-methyl-D-erythritol 4-phosphate in an alternative nonmevalonate pathway for terpenoid biosynthesis. *Proceedings of the National Academy of Sciences of the United States of America*, **95**, 9879-9884.

Walter M.H., Fester T. & Strack D. (2000) Arbuscular mycorrhizal fungi induce the non-mevalonate methylerythritol phosphate pathway of isoprenoid biosynthesis correlated with accumulation of the 'yellow pigment' and other apocarotenoids. *Plant Journal*, **21**, 571-578.

Walter M.H., Hans J. & Strack D. (2002) Two distantly related genes encoding 1-deoxy-D-xylulose 5-phosphate synthases: differential regulation in shoots and apocarotenoid-accumulating mycorrhizal roots. *Plant Journal*, **31**, 243-254.

Wanke M., Skorupinska-Tudek K. & Swiezewska E. (2001) Isoprenoid biosynthesis via 1-deoxy-D-xylulose 5-phosphate/2-*C*-methyl-D-erythritol 4-phosphate (DOXP/MEP) pathway. *Acta Biochimica Polonica*, **48**, 663-672.

Westfall P.J., Pitera D.J., Lenihan J.R., Eng D., Woolard F.X., Regentin R., Horning T., Tsuruta H., Melis D.J., Owens A., Fickes S., Diola D., Benjamin K.R., Keasling J.D., Leavell M.D., McPhee D.J., Renninger N.S., Newman J.D. & Paddon C.J. (2012) Production of amorphadiene in yeast, and its conversion to dihydroartemisinic acid, precursor to the antimalarial agent artemisinin. *Proceedings of the National Academy of Sciences of the United States of America*, **109**, E111-E118.

Wiberley A.E., Donohue A.R., Westphal M.M. & Sharkey T.D. (2009) Regulation of isoprene emission from poplar leaves throughout a day. *Plant, Cell and Environment*, **32**, 939-947.

Wikner C., Nilsson U., Meshalkina L., Udekwu C., Lindqvist Y. & Schneider G. (1997) Identification of catalytically important residues in yeast transketolase. *Biochemistry*, **36**, 15643-15649.

Wolfertz M., Sharkey T.D., Boland W. & Kühnemann F. (2004) Rapid regulation of the methylerythritol 4-phosphate pathway during isoprene synthesis. *Plant Physiology*, **135**, 1939-1945.

Wolfertz M., Sharkey T.D., Boland W., Kühnemann F., Yeh S. & Weise S.E. (2003) Biochemical regulation of isoprene emission. *Plant, Cell and Environment*, **26**, 1357-1364.

Wright L.P., Rohwer J.M., Ghirardo A., Hammerbacher A., Ortiz-Alcaide M., Raguschke B., Schnitzler J.P., Gershenzon J. & Phillips M.A. (2014) Deoxyxylulose 5-phosphate synthase controls flux through the methylerythritol 4-phosphate pathway in Arabidopsis. *Plant Physiology*, **165**, 1488-1504.

Xiang S., Usunow G., Lange G., Busch M. & Tong L. (2007) Crystal structure of 1-deoxy-D-xylulose 5-phosphate synthase, a crucial enzyme for isoprenoids biosynthesis. *Journal of Biological Chemistry*, **282**, 2676-2682.

Zeidler J.G., Lichtenthaler H.K., May H.U. & Lichtenthaler F.W. (1997) Is isoprene emitted by plants synthesized via the novel isopentenyl pyrophosphate pathway? *Zeitschrift für Naturforschung*, **52c**, 15-23.

CHAPTER 2

Feedback inhibition of deoxy-D-xylulose 5-phosphate synthase regulates the methyl erythritol 4-phosphate pathway

This research was originally published in The Journal of Biological Chemistry. Aparajita Banerjee, Yan Wu, Rahul Banerjee, Yue Li, Honggao Yan and Thomas D. Sharkey. Feedback inhibition of deoxy-D-xylulose-5-phosphate synthase regulates the methylerythritol 4-phosphate pathway. The Journal of Biological Chemistry. 2013; 288:16926-16936.

2.1 SUMMARY

The methylerythritol phosphate (MEP) pathway leads to the biosynthesis of isopentenyl diphosphate (IDP) and dimethylallyl diphosphate (DMADP), the precursors for isoprene and higher isoprenoids. Isoprene has significant effects on atmospheric chemistry, whereas other isoprenoids have diverse roles ranging from various biological processes to applications in commercial uses. Understanding the metabolic regulation of the MEP pathway is important considering the numerous applications of this pathway. The deoxyxylulose-5-phosphate synthase (DXS) enzyme was cloned from *Populus trichocarpa* and the recombinant protein (*Pt*DXS) was purified from *E. coli*. The steady-state kinetic parameters were measured by a coupled enzyme assay. An LC-MS/MS-based assay involving the direct quantification of the end product of the enzymatic reaction, 1-deoxy-D-xylulose 5-phosphate (DXP), was developed. The effect of different metabolites of the MEP pathway on *Pt*DXS activity was tested. *Pt*DXS was inhibited by IDP and DMADP. Both of these metabolites compete with thiamin diphosphate (ThDP) for binding with the enzyme. An atomic structural model of *Pt*DXS in complex with ThDP and Mg^{2+} was built by homology modeling and refined by molecular dynamics simulations. The refined structure was used to model the binding of IDP and DMADP and indicated that IDP and DMADP might bind with the enzyme in a manner very similar to the binding of ThDP. The feedback inhibition of *Pt*DXS by IDP and DMADP constitutes an important mechanism of metabolic regulation of the MEP pathway and indicates that ThDP-dependent enzymes may often be affected by IDP and DMADP.

2.2 INTRODUCTION

The 2-*C*-methyl-D-erythritol 4-phosphate (MEP) pathway has been found to be an important pathway for the biosynthesis of isopentenyl diphosphate (IDP) and its isomer dimethylallyl diphosphate (DMADP), which are the precursors of all isoprenoids. Earlier it was believed that the mevalonic acid (MVA) pathway was the only pathway for the biosynthesis of IDP (Eisenreich *et al.* 2004; Eisenreich *et al.* 1998). The MEP pathway was discovered in early 1990s in bacteria (Eisenreich *et al.* 1998; Rohmer *et al.* 1993; Rohmer *et al.* 1996). Further studies showed that the MEP pathway is also present in green algae (Schwender *et al.* 1996) and higher plants (Arigoni *et al.* 1997; Eisenreich *et al.* 1996; Lichtenthaler *et al.* 1997a; Lichtenthaler *et al.* 1997b; Schwender *et al.* 1997; Zeidler *et al.* 1997). Both the MVA and MEP pathways are present in plants, however, they are localized in the cytosol and the chloroplast respectively (Hemmerlin *et al.* 2003; Lichtenthaler *et al.* 1997a). Extensive research has been carried out since its discovery to elucidate the various genes and enzymes involved in the MEP pathway. However, the regulation of the MEP pathway is not yet completely understood.

Considering its numerous applications it is important to identify key regulatory mechanisms in the MEP pathway. The absence of the MEP pathway in humans and its presence in different eubacteria, various apicomplexa parasites, and photosynthetic eukaryotes make it an attractive target for drug development and herbicides (Cordoba *et al.* 2009; Hale *et al.* 2012; Lange *et al.* 1998). Some isoprenoids also serve as important targets for biotechnological applications because of their nutritional and medicinal benefits (Cordoba *et al.* 2009; DellaPenna & Posgon 2006; Dubey *et al.* 2003). Isoprene, the most abundantly produced isoprenoid in plants, significantly affects atmospheric chemistry (Sharkey *et al.* 2008). In this regard, a mechanistic

model predicting isoprene emission from plants will be of great importance in atmospheric chemistry. A mechanistic model requires a deep understanding of the regulation of the MEP pathway.

Various studies reported that 1-deoxy-D-xylulose 5-phosphate synthase (DXS), the first enzyme of the MEP pathway, could play an important role in the regulation of the 2-*C*-methyl-D-erythritol 4-phosphate (MEP) pathway. Most of these reports are based on gene expression studies demonstrating a potential regulatory role for DXS in the synthesis of DMADP/IDP (Cordoba *et al.* 2009) but metabolic regulation of MEP pathway is not yet understood completely. Wolfertz and coworkers (Wolfertz *et al.* 2004; Wolfertz *et al.* 2003) used deuterium-labeled deoxyxylulose 5-phosphate (DOX-d_2) to show that the carbon flux through the MEP pathway is under strong metabolic regulation. They suggested that a feedback inhibition of DXS enzyme by the metabolites of this pathway downstream of DXP, especially DMADP, plays a critical role in this regulation. However, no direct evidence has been shown so far that can explain the tight control of the carbon flux through the MEP pathway.

In this work, the cloning, and characterization of the recombinant DXS (*Pt*DXS) protein from *Populus trichocarpa* have been described. I also report here a rapid and convenient high-performance liquid chromatography–tandem mass spectrometry (HPLC-MS/MS) based assay for *Pt*DXS. This assay was used to study the activity of *Pt*DXS in presence of different metabolites of the MEP pathway. My results show that IDP and DMADP, the last metabolites of the MEP pathway significantly inhibit *Pt*DXS by competing with ThDP. Computational analysis shows that both of these metabolites bind with the enzyme in a manner similar to that of ThDP. The inhibition of *Pt*DXS by IDP and DMADP constitutes an important regulatory mechanism of the

MEP pathway where the very last metabolite of the pathway regulates the activity of the very first enzyme of the pathway.

2.3 EXPERIMENTAL PROCEDURES

2.3.1 Cloning

(In collaboration with Dr. Honggao Yan)

The cDNA encoding the mature *Pt*DXS was amplified by PCR using the primers 5'-G GAA TTC CAT ATG GCA TCA CTA TCA GAA AGA GGA GAG-3' and 5'-CG GGA TCC TTA TGA TGA CAT AAT CTC CAG AGC-3'. The PCR product was digested with the restriction enzyme *Bam*HI to completion followed by a partial digestion with the restriction enzyme *Nde*I, as the coding DNA of *Pt*DXS contained an *Nde*I site. The partially digested PCR product was ligated with a lab-made vector, pET17b-HR, digested with the same two restriction enzymes. The ligation mixture was transformed into the *E. coli* strain DH5α. The clones that contained the complete cDNA were selected by agarose gel electrophoresis of the isolated DNA constructs. The resultant overexpression plasmid construct was designated as pET17bHR/*Pt*DXS for the production of *Pt*DXS with a tobacco etch virus (TEV) protease-cleavable six-His tag at the N-terminus. An overexpression plasmid construct for the production of *Pt*DXS with a TEV protease-cleavable ten-His tag at the N-terminus was engineered by PCR-based site-directed mutagenesis using pET17bHR/*Pt*DXS as the template. The mutagenesis primers were 5'- G CAT CAC CAT CAC CAT CAT CAC CAT CAC CAT AGC GGT ACC GAG AAC CTG TAC

TTC-3’ and 5’- GAA GTA CAG GTT CTC GGT ACC GCT ATG GTG ATG GTG ATG ATG GTG ATG GTG ATG C-3’. The resulting construct was designated as pET17b10HR/*Pt*DXS.

An overexpression plasmid construct for the production of *Pt*DXS with a TEV protease-cleavable six-His tag at both the N- and the C-termini was engineered in two steps. First, the overexpression construct pET17bHR/*Pt*DXS was digested with *Bam*HI and *Eco*RI and ligated with a synthetic duplex DNA consisting of the oligos 5’-GA TCC GAG AAC CTG TAC TTC CAG GGT CAC CAC CAC CAC CAC CAC TAA-3’ and 5’-AA TT TTA GTG GTG GTG GTG GTG GTG ACC CTG GAA GTA CAG GTT CTC G-3’. The clones with the inserted DNA were selected by *Eco*RI digestion, as the insertion destroyed the *Eco*RI site. Then the stop codon at the end of the *Pt*DXS-coding sequence was converted to Ser by PCR-based site-directed mutagenesis using the primers 5’-CTG GAG ATT ATG TCA TCA TCA GGA TCC GAG AAC CTG TAC-3’ and 5’- GTA CAG GTT CTC GGA TCC TGA TGA TGA CAT AAT CTC CAG -3’. The resultant DNA construct was designated as pET17bHR3’HR/*Pt*DXS. The N-terminal His tag and TEV protease site was removed by PCR-based site-directed mutagenesis using pET17bHR3’HR/*Pt*DXS as the template. The two primers for the mutagenesis were 5’-CT TTA AGA AGG AGA TAT ACC ATG GCA TCA CTA TCA GAA AGA GGA GAG-3’ and 5’- CTC TCC TCT TTC TGA TAG TGA TGC CAT GGT ATA TCT CCT TCT TAA AG -3’. The resultant DNA construct was designated as pET17b3’HR/*Pt*DXS. For all the plasmid constructs, the presence of the correct *Pt*DXS coding sequence, and the absence of any undesired mutation, was confirmed by DNA sequencing.

2.3.2 Overexpression and purification

(In collaboration with Dr. Honggao Yan)

The *E. coli* strain BL21(DE3)pLysS was used to overexpress the various forms of *Pt*DXS. One liter of LB medium containing 100 μg/ml of ampicillin and 20 μg/ml of chloramphenicol was inoculated with colonies of fresh transformants of an overexpression construct and incubated at 37 ºC with vigorous shaking (225 rpm) until the OD_{600} reached 1. The culture was then cooled with ice to room temperature, induced with 0.5 mM (final concentration) of isopropyl β-D-1-thiogalactopyranoside (IPTG), and further incubated with vigorous shaking at room temperature for ~18 h. The *E. coli* cells were harvested by centrifugation and resuspended in 10 mL cold buffer A (50 mM sodium phosphate, 300 mM NaCl, 10% glycerol, pH 8.0) per gram of bacterial paste. $MgCl_2$ was added to a final concentration of 20 mM followed by the addition of DNase I and EDTA-free inhibitors. The cells were lysed with a French press. The cell debris was removed by centrifugation at ~27,000 x g for 20 min. Ammonium sulfate was added to the supernatant in small quantities to 45% saturation under gentle stirring. After 30 min, the suspension was centrifuged at ~27,000 x g for 20 min. The pellet was redissolved in the same volume of cold buffer A. The solution was centrifuged and the ammonium sulfate precipitation was repeated with the supernatant. The pellet of the second ammonium sulfate precipitation was redissolved in cold buffer A and the solution was centrifuged. The supernatant was dialyzed against 2 L of the same buffer for 3 h. The dialyzed protein solution was mixed with Ni-NTA resin with gentle shaking for 1 h and loaded onto a column. The column was washed with 10 mM imidazole in buffer A until OD_{280} of the effluent < 0.05 and eluted with a 10-250 mM linear imidazole gradient in buffer A. Fractions containing *Pt*DXS were identified by SDS-PAGE and

pooled. *Pt*DXS was precipitated with ammonium sulfate (45% saturation) and the pellet redissolved in a minimal volume of a cold buffer containing 50 mM Tris-HCl, 10% glycerol, and 1 mM dithiothreitol (DTT) (pH 7.5). The protein solution was dialyzed against 1 L of the same buffer and centrifuged at ~27,000 x g for 20 min. The supernatant was dispensed into microtubes, frozen in liquid nitrogen, and stored at -80 ºC. All protein purification procedures were carried out at 4 ºC unless specified otherwise.

2.3.3 Coupled enzyme assay

(In collaboration with Dr. Honggao Yan)

The steady-state kinetic constants of *Pt*DXS were measured using a DXR-coupled assay. The assay components in a buffer containing 100 mM HEPES (pH 7.5) included pyruvate, GAP, 5 mM $MgCl_2$, 1 mM ThDP, 50 mM NADPH, 4 μM recombinant *Acinetobacter baumannii* DXR (*Ab*DXR, lab made), and 0.5 μM *Pt*DXS. The reaction was initiated by the addition of GAP at room temperature. For measuring the K_m of pyruvate, GAP was fixed at 0.2 or 0.5 mM and pyruvate varied in the range of 0.05-1.2 mM. For measuring the K_m of GAP, pyruvate was fixed at 2 or 5 mM and GAP varied in the range of 10-175 μM. The kinetic constants were evaluated by nonlinear least squares fitting of the data to the Michaelis-Menten equation using the program Origin (http://www.originlab.com/).

2.3.4 Enzymatic synthesis of DXP and [$^{13}C_2$]DXP

DXP and [$^{13}C_2$]DXP were synthesized enzymatically from pyruvate and 2,3-[$^{13}C_2$]pyruvate, and GAP (produced in situ) using *E. coli* DXS (*Ec*DXS) as described in (Argyrou & Blanchard 2004) with some modifications. The reaction mixture was prepared by dissolving D-fructose 1,6-bisphosphate (406 mg, 25 mM) and pyruvate (or 2,3-[$^{13}C_2$]pyruvate) (~220 mg, 50 mM) in ~39 mL of 50 mM Tris-HCl, pH 7.5 with 1 mM DTT, 5 mM $MgCl_2$, and 0.5 mM ThDP. The reaction mixture also contained recombinant *Staphylococcus aureas* fructose bisphosphate aldolase (*Sa*FBP aldolase) (2.4 μM, lab made), yeast triose phosphate isomerase (TPI) (0.04 μM, lab made), and *Ec*DXS (1.5 μM, lab made). The reaction was then carried out at 37 °C for ~24 h. The enzymes were removed from the reaction mixture by ultrafiltration through YM10 (Millipore) membrane. The filtrate was then loaded on Dowex 1 x 8 column (40 mL, chloride form), which was equilibrated with water. The column was washed with 100 mL of water after collecting the flow-through. DXP was then eluted from the column with 100 mL of 1% NaCl solution. The fractions containing DXP were lyophilized to obtain solid DXP. The solid was then dissolved in ~3 mL of water. The solution was desalted with a Sephadex G10 column by eluting with water. The concentration of the pure DXP solution was obtained from NMR.

2.3.5 Preparation of PtDXS assay mixture for LC-MS/MS based assay

The activity of the purified *Pt*DXS enzyme was studied using an LC-MS/MS-based assay. A mixture of dihydroxyacetone phosphate (DHAP) and TPI from rabbit muscle was used to maintain a constant supply of GAP in the reaction mixture. The ratio of equilibrium

concentration of DHAP and GAP at the temperature of the reaction mixture (37 °C) was calculated to be 18:1. The assay mixture contained 40 mM Tris-HCl buffer at pH 8.0, 10 mM $MgCl_2$, 1 mM DTT, 100 μM ThDP, 1 U/mL rabbit muscle TPI, and 0.25 μM *Pt*DXS in a total volume of 100 μL. The reaction was initiated with a mixture of DHAP and pyruvate. The concentrations used to study the K_m of DHAP and pyruvate were 0-197 μM of DHAP in presence of 5 mM pyruvate and 0-1 mM pyruvate in presence of 260 μM of DHAP respectively. The concentrations used to study the K_m of ThDP were 0-1 mM of ThDP in presence of 260 μM of DHAP and 500 μM pyruvate. The reaction was incubated at 37 °C for 5 min. It was then quenched by freezing in liquid nitrogen followed by the addition of 400 μL of ice-cold acetonitrile keeping the frozen reaction mixture on dry ice. Then the reaction mixture was thawed on ice followed by the addition of 2 μM of [$^{13}C_2$]DXP as an internal standard (IS) for the mass spectrometry. The assay mixture was then centrifuged at 28,000 x g for 10 min and the supernatant was stored at -80 °C until further analysis.

2.3.6 Inhibition studies

Different metabolites of the MEP pathway, namely MEP, 4-(cytidine 5'-diphospho)-2-*C*-methyl-D-erythritol (CDPME), 2-*C*-methyl-D-erythritol 2,4-cyclodiphosphate (MEcDP), 4-hydroxy-3-methylbut-2-enyl diphosphate (HMBDP), IDP, and DMADP were tested to study their effect on *Pt*DXS activity. All the metabolites except IDP and DMADP were purchased from Echelon Biosciences Inc. (Salt Lake City, UT, USA). IDP and DMADP were purchased from Isoprenoids, LC (Tampa, FL, USA). The assay mixture was prepared as mentioned before with 400 μM of the metabolites. The reaction was initiated with a mixture of DHAP (210 μM)

and pyruvate (200 μM). Similarly, the assay mixtures for obtained the Michaelis-Menten plot at different inhibitor concentrations were prepared as mentioned before at different ThDP concentrations in the presence of 0 μM, 100 μM, and 1000 μM of IDP keeping the concentration of DHAP and pyruvate fixed at 210 μM and 200 μM respectively. The reaction was initiated with a mixture of DHAP and pyruvate. In order to calculate the K_i of DMADP and IDP, the assay was done in presence of 25 μM ThDP (~K_m for ThDP) and 0-3 mM of the metabolites. The reaction was initiated with a mixture of DHAP (210 μM) and pyruvate (200 μM). The assay was then carried out as described before.

2.3.7 LC-MS/MS of the PtDXS assay mixture

The assay mixture was analyzed by LC-MS/MS to separate the product DXP from the substrate DHAP. Liquid chromatography was performed using Merck SeQuant™ ZIC®-pHILIC (50 x 2.1 mm, 5 μm, 200 Å, polymeric beads PEEK) column (The Nest Group, Inc., MA, USA) fitted to two LC-20AD HPLC pumps and a SIL-HTc autosampler (Shimadzu, Kyoto, Japan) as described in (Li & Sharkey 2013). The rest of the instrumental setup for the mass spectrometer coupled to this chromatography system was done as described in Sharkey & Li (2013). The assay mixture was filtered through Whatman™ syringeless filter device (Mini-Uniprep™ PTFE filter media) and 5 μL of the sample was injected into the column. The analyte was eluted with a binary gradient consisting of 50 mM ammonium acetate at pH 10 and acetonitrile (composition as shown in the inset of Figure 2.1) at a flow rate of 0.15 mL/min. Mass spectrometry was performed as described in Sharkey & Li (2013). Multiple-reaction-monitoring (MRM) mode was used to acquire the precursor/product ion pairs for DXP, [$^{13}C_2$]DXP, and DHAP. The mass pairs

used for scanning these compounds were (in atomic mass units) 213/97, 215/97, and 169/97 for DXP, [$^{13}C_2$]DXP, and DHAP respectively. The optimized declustering potential used for acquiring the mass spectra was -30 V for DXP and [$^{13}C_2$]DXP, and -20 V for DHAP. The optimized collision energy used for acquiring the mass spectra was -20 V for DXP and [$^{13}C_2$]DXP, and -15 V for DHAP.

2.3.8 Quantification and data analysis

To obtain better quantification of the analytes, an internal standard was used in all the samples to allow a correction for the ionization efficiency. Standard DXP samples containing 2 μM of [$^{13}C_2$]DXP as an internal standard were run to obtain a calibration curve. The calibration curve was used to quantify the amount of DXP produced in the assay samples. After correction for the dilution factor, the amount of DXP produced in the reaction mixture was used to calculate the specific activity of the *Pt*DXS enzyme. The kinetic constants of *Pt*DXS enzyme for different substrates and the IC_{50} curves for IDP and DMADP were obtained by fitting the experimental data with non-linear regression using the program Origin (http://www.originlab.com/). The kinetic constants were evaluated using the Michaelis-Menten equation. Calculation of the IC_{50} values was done using a logistic equation (Shi *et al.* 2012) and described as

$$v = v_{min} + \frac{v_{max} - v_{min}}{1 + \left(\frac{[I]}{IC_{50}}\right)^{H}}$$

where, v is the relative activity, v_{min} is the minimum activity, v_{max} is the maximum activity, $[I]$ is the concentration of the inhibitor, and H is the Hill coefficient. The K_i of the inhibitors were calculated using Cheng-Prusoff equation (Cheng & Prusoff 1973) as follows.

$$K_i = \frac{IC_{50}}{1 + \frac{[S]}{K_m}}$$

The IC_{50} curves were obtained at K_m concentration of ThDP. At $[S] = K_m$, K_i is calculated to be $\frac{IC_{50}}{2}$.

2.3.9 Computational modeling

(In collaboration with Dr. Honggao Yan)

A structural model of *Pt*DXS was first built by homology modeling using the SWISS-MODEL server (http://swissmodel.expasy.org/) with the crystal structure of *Deinococcus radiodurans* DXS (*Dr*DXS; PDB ID: 2O1X) (Xiang *et al.* 2007) as the template. The crystal structure of *Dr*DXS, not that of *E. coli* DXS (*Ec*DXS; PDB ID: 2O1S), was chosen as the template for the homology modeling because *Dr*DXS has only one segment (residues 199–243) with no electron density whereas *Ec*DXS has two segments (residues 183–238 and 292–317) with no electron density (Xiang *et al.* 2007). Each monomer of the modeled homodimeric enzyme contains one Mg^{2+} ion and one coenzyme ThDP. The Mg^{2+} ion is coordinated with four oxygen atoms, two from diphosphate of ThDP and one each from Asp-145 and Asn-174. Two water molecules were placed near each Mg^{2+} ion based on the crystal structure of *Ec*DXS so that

the Mg^{2+} ion is coordinated with six oxygen atoms. The structural model was then refined by molecular dynamics using the AMBER program package (version 10) (Case *et al.* 2008). The modeled homodimeric protein was solvated with ~32,900 transferable intermolecular potential with three point charges (TIP3P) water molecules in a rectangular box with the edges at least 12 Å from the protein. The system was neutralized using 12 Na^{+} ions. Glu-377 was considered protonated as a hydrogen donor to form a hydrogen bond with N1 of the pyrimidine ring of ThDP as in the crystal structures of *Ec*DXS and *Dr*DXS (Xiang *et al.* 2007). Water molecules in the system were minimized first using a combination of steepest descent (15,000 steps) and conjugated gradient (5,000 steps) methods with protein and ligand heavy atoms restrained with a force constant of 100 kcal mol^{-1} $Å^{-2}$. The whole system was then minimized using a combination of steepest descent (5,000 steps) and conjugated gradient (5,000) methods without any positional restraint for any atoms except those interacting with the Mg^{2+} ions and forming the hydrogen bond between ThDP and Glu-377. The restraints for the Mg^{2+} coordination and the hydrogen bond between ThDP and Glu-377 were also enforced during the subsequent heating and equilibration steps. The minimized system was heated from 0 to 300 K in 500,000 steps in 1 ns at constant volume and equilibrated at 300K and constant pressure for 4 ns. The system was further simulated without any distance restraint for 1.5 ns. The minimization, heating and equilibration simulations were carried out using the Sander module in AMBER 10 (Case *et al.* 2008) with the ff99SB force field.

The force field parameters for the coenzyme ThDP were derived using the AMBER antechamber program (Case *et al.* 2008). The PMEMD module in AMBER 10 (Case *et al.* 2008) was used for the subsequent production simulation. The particle mesh Ewald method (Essmann *et al.* 1995) was used to evaluate long-range electrostatic interactions. The nonbonded cutoff was

10 Å. All bonds to hydrogen atoms were constrained in the simulations with the SHAKE algorithm (Ryckaert *et al.* 1977) permitting a time step of 2 fs. Temperature was controlled with Langevin dynamics. The data of the 1.5 ns simulation were analyzed using the PTRAJ module in the program AmberTools (Case *et al.* 2008). The refined structural model of *Pt*DXS in complex with ThDP and Mg^{2+} was used to dock IDP and DMADP molecules. ThDP was mutated to IDP and DMADP using the xleap program in AmberTools (Case *et al.* 2008). The force field parameters for IDP and DMADP were derived using the same procedure as for the coenzyme ThDP. The models of the inhibitor complexes were neutralized with Na^{+} ions, solvated with explicit water molecules, and minimized using essentially the same procedure as for the ThDP complex. All structural illustrations were drawn with the program PyMOL (The PyMOL Molecular Graphics System, Schrödinger, LLC).

2.4 RESULTS

2.4.1 Cloning, overexpression, and purification

(In collaboration with Dr. Honggao Yan)

To produce *Pt*DXS in *E. coli*, the cDNA encoding the mature *Pt*DXS was cloned into a home-made overexpression vector derived from the commercial vector pET17b from Novagen, under the control of an isopropyl β-D-1-thiogalactopyranoside (IPTG)-inducible T7 promoter. A large quantity of *Pt*DXS can be produced using this overexpression construct in the *E. coli* strain BL21(DE3)pLysS at 37 ºC (not shown) but more soluble *Pt*DXS protein could be obtained at

room temperature (data not shown). The recombinant protein contained a six-histidine tag at its N-terminus to facilitate its purification using Ni-NTA resin but the His-tag did not help the purification, as the majority of the protein molecules did not bind to Ni-NTA resin. To address this issue, the His-tag was extended to 10 histidine residues, but the longer His-tag did not improve the binding. Then a six-histidine tag was engineered at the C-terminus of the protein and the N-terminal His-tag was removed as it did not help the purification. The C-terminal His-tag helped the purification of the protein. However, the purified protein could be easily degraded. Ammonium sulfate precipitation effectively removed protease contamination. Two steps of ammonium sulfate precipitation before the Ni-NTA chromatography and one step of ammonium sulfate precipitation after the Ni-NTA chromatography yielded a stable protein preparation. The average yield for the purified protein was ~14 mg/L of *E. coli* culture.

2.4.2 Steady-state kinetic analysis

(In collaboration with Dr. Honggao Yan)

Steady-state kinetic parameters of the recombinant *Pt*DXS were measured by a DXR-coupled enzyme assay. *Ab*DXR was used as a coupling enzyme in the assay as this enzyme is stable. The assay was validated by varying the concentrations of *Pt*DXS and *Ab*DXR. *Ab*DXR at 4 μM was deemed sufficient as the reaction rate doubled as the *Pt*DXS concentration doubled and increasing the *Ab*DXR concentration further did not increase the reaction. The kinetic data are summarized in Table 2.1. The K_m values for pyruvate and GAP (87.8 and 18.5 μM, respectively) were both higher than those of *Mycobacterium tuberculosis* DXS (40 and 6.1 μM,

respectively) (Bailey *et al.* 2002) but significantly smaller than those of *Rhodobacter capsulatus* DXS (440 and 68 μM, respectively) (Eubanks & Poulter 2003).

2.4.3 Development of LC-MS/MS based assay for PtDXS enzyme

The effect of different MEP pathway metabolites on the activity of *Pt*DXS enzyme was studied by measuring the amount of DXP produced by the *in vitro* reaction of the enzyme in presence of those metabolites. The chromatogram of the assay mixture is shown in Figure 2.1. Manual addition of substrates to the assay mixture followed by its quenching in liquid nitrogen involves a time lag. This leads to the production of small amount of DXP at 0 min. Study of the time course of the *Pt*DXS enzymatic reaction showed that it was linear for the initial 10 minutes (data not shown). Samples were collected at 5 minutes to calculate the specific activity of the enzyme. Table 2.1 shows the kinetic constants of *Pt*DXS enzyme for different substrates measured by this method.

2.4.4 Effect of pH on PtDXS activity

The activity of the *Pt*DXS enzyme was monitored at different pH using Bis-tris propane buffer. The useful pH range for this buffer is 6.3-9.5. The activity of the enzyme was found to be highly sensitive to the pH of the assay mixture (Figure 2.1). The enzyme did not show substantial activity below pH 6.5 and above pH 8.5. The highest activity of this enzyme is obtained at pH 8.0. This is typical for a chloroplastic enzyme.

2.4.5 Effect of different metabolites of the MEP pathway using LC-MS/MS method

DMADP was selected for testing based on previous suggestions of its role in metabolic regulation of the MEP pathway (Wolfertz *et al.* 2004; Wolfertz *et al.* 2003). The rest of the intermediates of the MEP pathway were screened for potential effects on *Pt*DXS activity (Figure 2.3A). The intermediate 4-(cytidine 5'-diphospho)-2-*C*-methyl-D-erythritol 2-phosphate (CDPMEP) could not be tested due to its instability. Figure 2.3B shows the effect of MEP on *Pt*DXS activity. Because the molecular weight of MEP is the same as the internal standard ([$^{13}C_2$]DXP) used for the LC-MS/MS based assay, I could not normalize the data for MEP with respect to the internal standard. I compared the effect of MEP relative to the control instead of using absolute values because the ion suppression effect could not be eliminated in this case. Analysis of variance (ANOVA) followed by Bonferroni posttest indicated that IDP alone showed statistically significant inhibition ($p = 0.0036$). HMBDP also showed some effect, although it was not statistically significant in this experiment. Li and Sharkey found that the physiological concentration of HMBDP under normal conditions is very low (~4.2 μM) (Li & Sharkey 2013). Therefore, I believe that HMBDP plays little or no role in feedback within the MEP pathway.

2.4.6 Mechanism of inhibition

The next goal was to study the mode of inhibition of *Pt*DXS by IDP. The effect of each of the substrates on the inhibition of *Pt*DXS by IDP was tested. In each case, the concentration of a particular substrate was doubled as compared to the control, keeping the concentration of the inhibitor (400 μM) same as that in the control. It was observed that the extent of inhibition was

reduced in presence of higher concentration of ThDP (Figure 2.4). Use of higher concentration of pyruvate and DHAP did not affect the inhibition significantly. A two way ANOVA followed by Bonferroni posttest indicated that doubling the concentration of each metabolite had no effect on the rate in the absence of inhibitor and the inhibition by IDP is significantly reduced ($p < 0.01$) only in the presence of twice the amount of ThDP. This suggests that IDP acts as a competitive inhibitor of ThDP. The inhibitory effect of IDP on *Pt*DXS enzyme was tested by varying the concentration of IDP in presence of different concentration of ThDP and fixed concentration of pyruvate and DHAP. The Michaelis-Menten plot of *Pt*DXS activity at different ThDP concentration showed that the activity was decreased in presence of higher concentration of IDP (Figure 2.5). This also indicates that IDP acts as a competitive inhibitor of ThDP. Regression of the experimental data points was done using the method of least squares. The Michaelis-Menten plot for the activity of the enzyme at different substrate concentration with varying inhibitor concentration could not be fitted well by assuming the equation for standard competitive inhibition kinetics. A better curve-fitting was obtained by incorporating a Hill coefficient in the rate equation (Figure 2.5). The H value obtained from the least squares regression was 0.68.

The activity of *Pt*DXS enzyme was studied over a broad range of concentration of IDP and DMADP in presence of ~K_m concentration of ThDP (Figure 2.6). The K_i of IDP and DMADP for *Pt*DXS enzyme were found to be 65.4 ± 4.3 μM and 81.3 ± 10.5 μM respectively. The IC_{50} curves of IDP and DMADP were not easily modeled by standard competitive inhibition kinetics. I applied the logistic equation (as mentioned in the experimental procedure section) to the experimental data points using two different approaches: fitting using a fixed value of H = 1 or a fixed value of $v_{min} = 0$. A better fitting of the IC_{50} curve was obtained using the second approach. This approach resulted in the H values less than 1. The Hill coefficients of the

inhibitor binding as obtained from the non-linear curve fitting using Origin (www.originlab.com) were $H = 0.69 \pm 0.03$ for IDP and $H = 0.61 \pm 0.06$ for DMADP. These H values are consistent with both the inhibitors exhibiting negative cooperativity of binding for the enzyme, in other words, binding of one inhibitor to a dimer reduces the binding of a second inhibitor molecule to the other member of the dimer. One part of the IDP and DMADP molecules that they have in common with ThDP is the diphosphate group. Therefore, the effect of pyrophosphate was tested (inset of Figure 2.6). Sodium pyrophosphate did not show any effect on *Pt*DXS activity even at a concentration of 1 mM. This suggests that the inhibitory effect of IDP and DMADP on *Pt*DXS activity is not due to a nonspecific effect of diphosphate part of the molecules.

2.4.7 Computational modeling

(In collaboration with Dr. Honggao Yan)

To understand substrate and inhibitor binding, a three-dimensional atomic structure of *Pt*DXS in complex with ThDP and Mg^{2+} was built by homology modeling based on the crystal structures of *Dr*DXS and *Ec*DXS (Xiang *et al.* 2007) and refined by molecular dynamics simulations. The modeled structure was stable with an average root-mean-squares fluctuation (RMSF) of 0.75 Å (Figure 2.7A). Significant fluctuations are located mainly in the region that was not observed in the crystal structure of *Dr*DXS (residues 199–243), the template used for the homology modeling, and where *Pt*DXS has an eight-residue insertion. The core structure of *Pt*DXS aligns well with the crystal structures of *Ec*DXS and *Dr*DXS (Figure 2.7B). The interactions between the enzyme and the coenzyme ThDP and the metal ion Mg^{2+} are illustrated in Figure 2.8A and are essentially the same as in the crystal structures of *Ec*DXS and *Dr*DXS

(Xiang *et al.* 2007). The Mg^{2+} ion is coordinated with Asp-145 and Asn1-74 of the ThDP-binding motif of $GDGX_{25–30}N$ (Hawkins *et al.* 1989), the diphosphate moiety of ThDP, and two water molecules. The Mg^{2+} coordination is stable during the production phase of the molecular dynamics simulation without any restraint. The coenzyme ThDP is anchored at the active site mainly by its diphosphate and pyrimidine moieties (Figure 2.8A) as in *Ec*DXS and *Dr*DXS. In addition to the interaction with the Mg^{2+} ion, the diphosphate moiety of ThDP is hydrogen bonded to the side chains of His-73 and Lys-291 and the main-chain amides of Gly-146 and Ala-147. In addition to many van der Waals interactions, the pyrimidine ring of ThDP is hydrogen bonded to Gly-114, Ser-116, and Glu-377. The protonation of Glu-377 is crucial for the interaction with N1 of the pyrimidine ring. The interactions of IDP or DMADP with the enzyme are very similar to those of ThDP (Figure 2.8B). The binding of IDP or DMADP to the enzyme is mainly through the interactions of its diphosphate moiety, very similar to the binding of ThDP (Figure 2.8C) but several van der Waals interactions are also predicted.

2.5 DISCUSSION

To study potential feedback regulation in the MEP pathway required a kinetic study of DXS in presence of different MEP pathway metabolites. The most common assay for this enzyme involves the measurement of radioactivity incorporated into the product DXP from radiolabeled pyruvate (Bouvier *et al.* 1998; Hahn *et al.* 2001; Lange *et al.* 1998; Lois *et al.* 1998; Sprenger *et al.* 1997). However, this assay involves a laborious separation of the precursors from products. Another useful method to study DXS activity involves a coupled spectrophotometric assay

exploiting the consumption of NADPH by DXR enzyme, which uses DXP as a substrate (Altincicek *et al.* 2000). I found some ambiguities in early results because of potential effects of tested metabolites on DXR. A fluorometric assay for DXS was developed using a fluorescent derivative of the product DXP (Querol *et al.* 2001). This assay suffered from the lack of selectivity. Another assay for DXS has been reported using HPLC based separation of derivatized DXP with a fluorophore using fluorescence detection (Han *et al.* 2003). This assay still involved an additional step for derivatization of the product. Recently, an assay based on circular dichroism, has been reported for DXS (Patel *et al.* 2012). This assay appeared to be extremely important for studying the mechanistic behavior of DXS illustrating detailed insights about different ThDP-bound intermediates involved in the DXS catalyzed reaction. Enzymatic synthesis of DXP from pyruvate and GAP by yeast transketolase has been successfully monitored by an HPLC-electrospray ionization (ESI)-MS-MS based technique (Feurle *et al.* 1998). Here I report another DXS assay in which DXP produced in the enzymatic reaction is measured by LC-MS/MS. This method is well suited for studying inhibitors of DXS activity.

Recombinant *Pt*DXS enzyme from *Populus trichocarpa* exhibited a K_m for pyruvate of 87.8 ± 3.2 μM and 119.2 ± 14.2 μM by coupled assay and LC-MS/MS-based assay respectively (Table 1). The K_m for GAP obtained from the coupled assay (18.5 ± 0.7 μM) was higher than that obtained from the LC-MS/MS-based assay (5.9 ± 0.9 μM). This could be because of the consumption of GAP in the coupled assay and in situ production of GAP from DHAP and TPI in LC-MS/MS-based assay. The k_{cat} values (~0.5 sec^{-1}) obtained from different measurements by the coupled assay were higher than the values obtained from the LC-MS/MS-based assay (~0.2 sec^{-1}) (Table 1). Use of a substantially lower concentration of ThDP (100 μM) in LC-MS/MS-based assay compared to 1 mM ThDP in the coupled assay may have caused this variation. The

k_{cat} value of ~0.5 sec^{-1} for *Pt*DXS is lower than the reported k_{cat} value of ~1.9 sec^{-1} from *Rhodobacter capsulatus* (Eubanks & Poulter 2003).

The feeding experiment with labeled DOX-d_2 by Wolfertz and coworkers (2004) indicated that a feedback regulation controls the carbon flux through the MEP pathway but did not provide evidence for a specific mechanism. My results show that DMADP and IDP, the very last metabolites of the MEP pathway, inhibit *Pt*DXS, the first enzyme of this pathway. The inhibitors are effective competitors with thiamin diphosphate for binding with the enzyme. It is interesting that inhibitors can compete with ThDP, which is generally thought to be an integral part of the enzyme. The results reported here indicate that IDP and DMADP have the potential to inhibit other ThDP-dependent enzymes.

The absolute physiological concentrations of chloroplastic IDP and DMADP are not known. Non-aqueous fractionation to measure the chloroplastic DMADP pool of kudzu leaves has estimated a range of ~0.25 mM to ~3.5 mM (Wolfertz *et al.* 2003). Measurement of chloroplastic DMADP pool by post illumination isoprene emission measurements estimated a concentration of ~43 μM in oak leaves (Li *et al.* 2011; Winter *et al.* 1994). Metabolic profiling studies by LC-MS/MS estimated the chloroplastic IDP/DMADP pool to be ~30 μM in poplar leaves (Li & Sharkey 2013). Considering the variability in the measurement of the metabolites by these methods, the physiological concentration for DMADP/IDP can certainly be assumed in the range of K_i of these metabolites for *Pt*DXS. Therefore, the inhibition of *Pt*DXS by IDP and DMADP at physiological concentrations constitutes a significant feedback regulation of the MEP pathway that can play an important role in regulating the amount of carbon lost by plants as isoprene.

The inhibition of DXS appeared to be cooperative and the crystal structure of DXS from *E. coli* and *D. radiodurans* shows that the enzyme exists as dimer (Xiang *et al.* 2007). The apparent

cooperativity of inhibitor binding causes *Pt*DXS activity to be very sensitive to low concentrations of inhibitor but relatively less sensitive when the inhibitor concentration is above the K_i. Therefore, the inhibitor cooperativity would ensure some DXS activity even in the presence of high levels of DMADP and IDP. This could be important because DXP is also the substrate for thiamin and pyridoxol synthesis (Lois *et al.* 1998; Rodríguez-Concepción & Boronat 2002; Sprenger *et al.* 1997). If DXS were too effectively shut off by IDP and DMADP it could interfere with thiamin and pyridoxol synthesis.

Wolfertz *et al.* observed (2004) that a very large reduction in DXS activity could be seen with little increase in the rate of isoprene synthesis. This work was done with Eucalyptus and the enzyme kinetics of Eucalyptus isoprene synthase has recently been published (Sharkey *et al.* 2013). Eucalyptus isoprene synthase has a K_m^{DMADP} of 0.16 mM, k_{cat} of 0.195 s^{-1}, and substrate inhibition (K_{is} = 0.9 mM). The inhibition of DXS by IDP and DMADP alone would not be sufficient to reduce DXS activity to such an extent that could explain the constant overall rate of isoprene emission. The complex kinetics of isoprene synthase also plays a significant role in this case. A combination of inhibition of DXS by IDP and DMADP and substrate inhibition of isoprene synthase by DMADP can satisfactorily account for the constant overall rate of isoprene emission using physiologically realistic assumptions (not shown).

Computational modeling shows that the binding of IDP/DMADP to *Pt*DXS is mainly through the diphosphate moiety. Figure 2.8A and 2.8B show that the oxygen atoms of the diphosphate moiety of both ThDP and IDP have polar interactions with Lys-291, His-73, Gly-146, and Ala-147 residues of *Pt*DXS. The diphosphate oxygen atoms from both ThDP and IDP interact with Asn-174 and Asp-145 residues of *Pt*DXS through the Mg^{2+} ion. However, the polar interaction of ThDP through the pyrimidine N1 and N5 atoms with Glu-377 and Ser-116,

nitrogen atom of NH_2 group of pyrimidine C4 with Gly-114, and thiazolium sulfur atom with Ser-178 residue of *Pt*DXS is absent for the binding of IDP with the enzyme. The van der Waals interactions of the carbon chain of IDP/DMADP with Leu-179, Ala-352, Gly-146, and Ala-147 orients the pyrophosphate group in the appropriate position for binding with the enzyme. This interaction is important for binding of the molecule with the enzyme as pyrophosphate alone does not show any inhibitory effect (Figure 2.6, inset).

Several studies indicated that DXS could have a role in the regulation of the MEP pathway. The regulation of gene transcription and translation by different developmental and environmental cues is most evident for DXS (Guevara-García *et al.* 2005; Lois *et al.* 2000; Wiberley *et al.* 2009). Posttranscriptional regulation of DXS was observed by the level of the end product of the pathway (Guevara-García *et al.* 2005). Higher or lower accumulation of isoprenoid end products in transgenic species having an over or under expressed DXS gene respectively was observed both in bacteria (Harker & Bramley 1999; Matthews & Wurtzel 2000; Miller *et al.* 2000) and plants (Enfissi *et al.* 2005; Estévez *et al.* 2001; Morris *et al.* 2006). DXS gene expression is strongly regulated with different developmental stages and strongly correlated with carotenoid accumulation in tomato fruits (Lois *et al.* 2000). The DXS gene expression pattern under the influence of various exogenous elicitors in *Ginkgo biloba* is strongly correlated with ginkgolide accumulation (Gong *et al.* 2006). All of this evidence suggests a regulatory role for DXS in MEP pathway. Recently, a feed-forward activation of IspF enzyme (2-*C*-methyl-D-erythritol 2,4-cyclodiphosphate synthase) by MEP and a feedback inhibition of IspF-MEP complex by a downstream isoprenoid farnesyl diphosphate have been reported in *E. coli* (Bitok & Freel Meyers 2012). This explains a new regulatory mechanism that modulates the synthesis of one of the key intermediates of MEP pathway. It has also been shown that the steps using

reducing power (steps involving DXR, HDS and HDR enzymes) act as strong regulatory points of the MEP pathway under different environmental conditions (Li & Sharkey 2013). This suggests the presence of a regulatory mechanism at the middle of the pathway. My work shows the connection between the beginning and the end of the pathway. It suggests that the beginning of the pathway can control the flow of carbon through the pathway, coordinating with the signals provided by the end of the pathway.

2.6 CONCLUSION

In conclusion, *Pt*DXS activity was monitored in presence of different MEP pathway metabolites. Only IDP and DMADP were found to have significant inhibitory effect on *Pt*DXS activity. Both IDP and DMADP compete with ThDP for binding with the enzyme. The inhibitors also exhibit negative cooperativity for binding with the enzyme. Computational modeling shows that IDP/DMADP use similar polar and non-polar contacts as ThDP for binding with the enzyme. Inhibition of *Pt*DXS by IDP and DMADP shows a potentially important metabolic regulation within the MEP pathway that plays significant role in controlling the carbon flow through this pathway. Beyond its role in regulation of the MEP pathway, the competition among IDP, DMADP and ThDP could affect nearly any other ThDP-dependent reaction, depending on the relative affinities for these compounds.

2.7 ACKNOWLEDGEMENTS

I would like to thank Michigan State University RTSF Mass Spectrometry Core for providing me the facility for doing the LC-MS/MS work. I would also like to thank Dr. A. Daniel Jones for his valuable suggestions for the LC-MS/MS work and Yichen Tang for his help to do the NMR of DXP and [$^{13}C_2$]DXP.

2.8 NOTES

This material is based upon work supported by the National Science Foundation under Grant No. IOS-0950574 to TDS and CHE-0957201 to HY. Any opinions, findings, and conclusions or recommendations expressed in this material are those of the authors and do not necessarily reflect the views of the National Science Foundation.

APPENDIX

TABLE 2.1 Kinetic constants of the *Pt*DXS enzyme measured by the DXR-coupled assay and LC-MS/MS based assay. Each number represents mean ± SE, n = 6 for DXR-coupled assay and mean ± SE, n = 3 for LC-MS/MS based assay. Kinetic constants were obtained from the non-linear curve fitting of the Michaelis-Menten plot in Origin.

Substrate	DXR-coupled assay		LC-MS/MS based assay	
	K_m (μM)	k_{cat} (sec^{-1})	K_m (μM)	k_{cat} (sec^{-1})
Pyruvate	87.8 ± 3.2	0.53 ± 0.01	119.2 ± 14.2	0.16 ± 0.01
GAP	18.5 ± 0.7	0.64 ± 0.01	5.9 ± 0.9	0.22 ± 0.02
ThDP	–	–	26.8 ± 4.3	0.55 ± 0.02

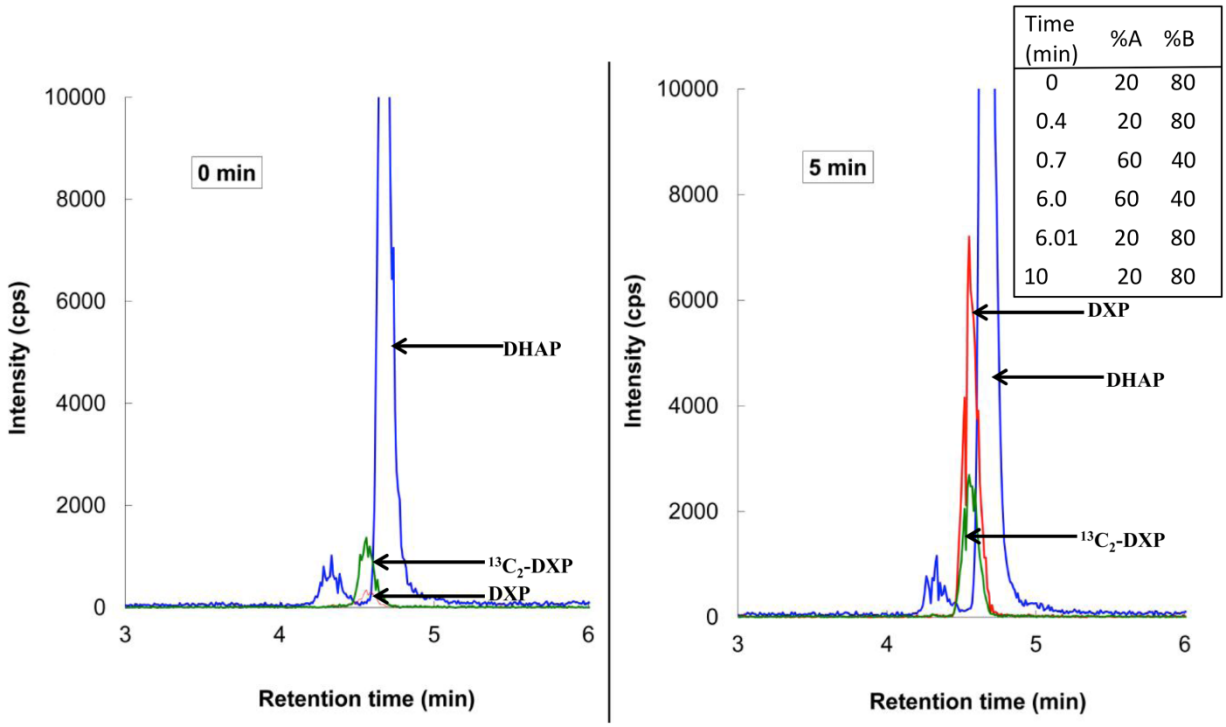

FIGURE 2.1 Chromatogram of *Pt*DXS assay mixture at 0 min and 5 min. DHAP, DXP, and [$^{13}C_2$]DXP are represented by blue, red, and green color respectively. [$^{13}C_2$]DXP was used to quantify the amount of DXP produced. The inset shows the composition of the solvents used in the binary gradient for the elution of DXP and DHAP. Solvent A is 50 mM ammonium acetate, pH 10 and Solvent B is acetonitrile.

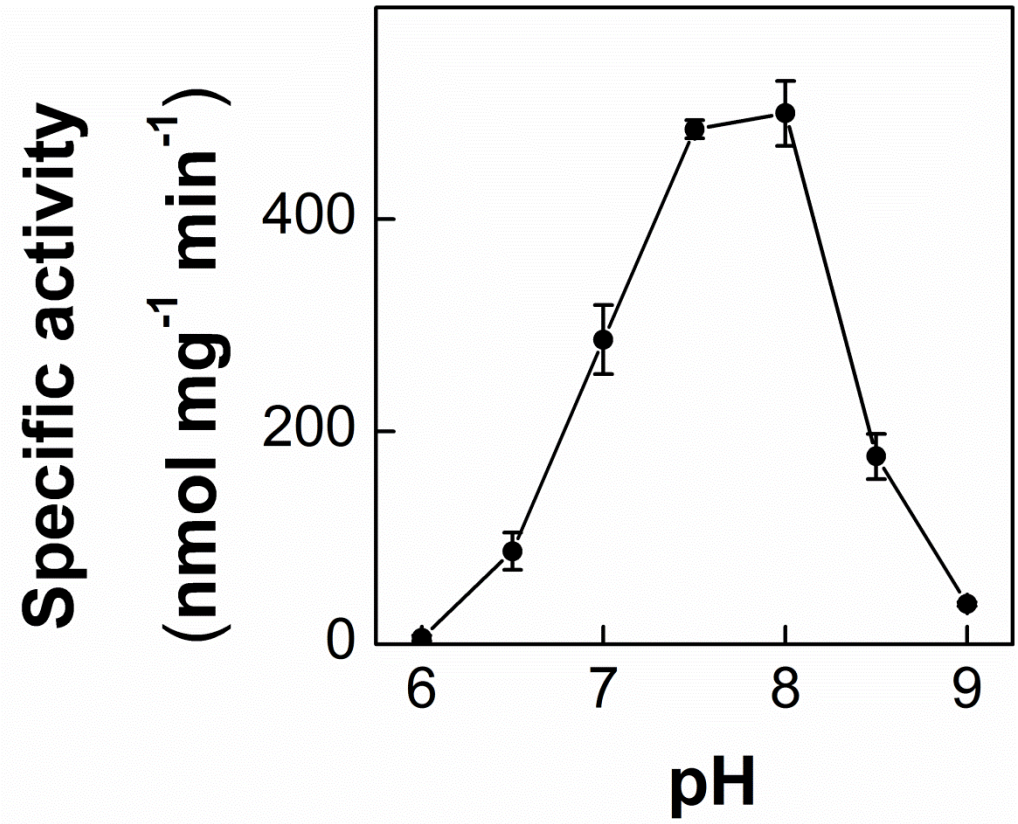

FIGURE 2.2 pH optimum for *Pt*DXS enzyme. Specific activity of the *Pt*DXS enzyme at different pH was monitored using LC-MS/MS based assay. Different pH of the assay mixture was maintained using bis-tris propane buffer. Each data point represents mean ± SD, n = 3. The enzyme is most active at pH 8.0.

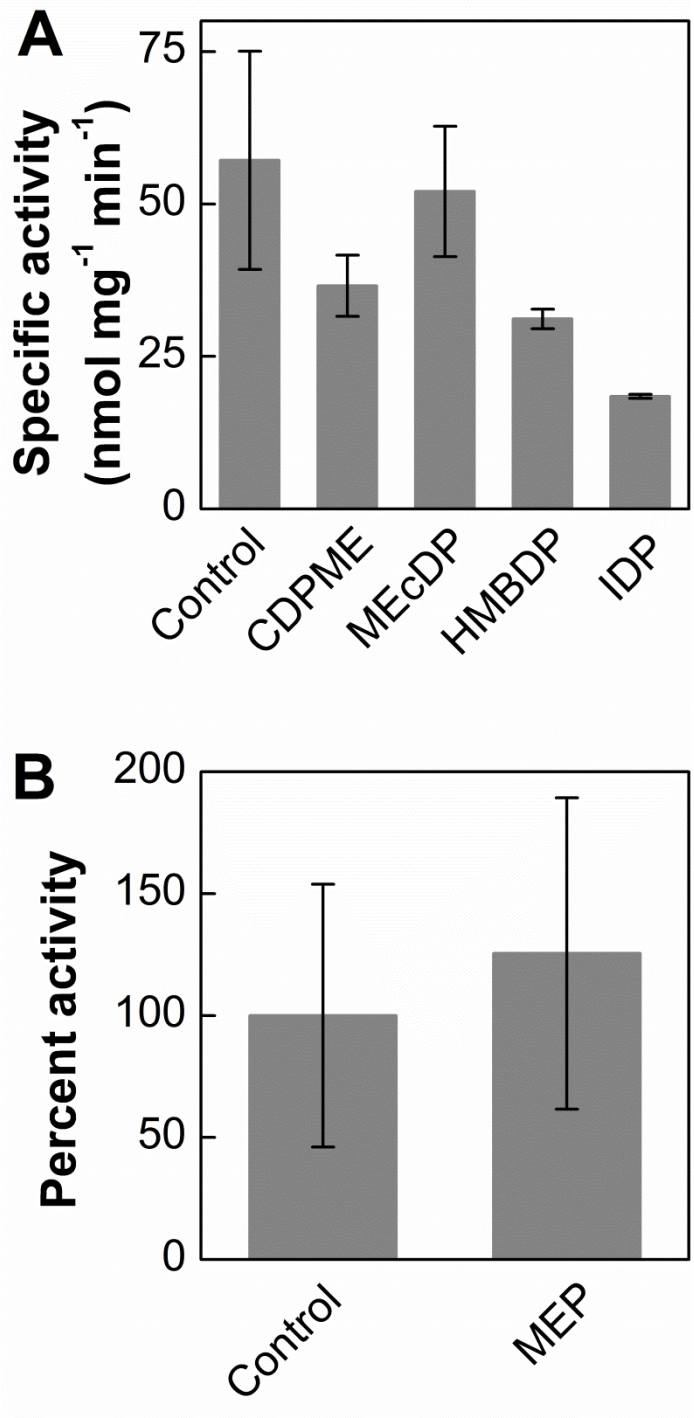

FIGURE 2.3 Effect of different metabolites of MEP pathway on *Pt*DXS activity based on LC-MS/MS based assay. Panel A. Effect of different metabolites except MEP on *Pt*DXS activity. Each bar represents mean ± SD, n = 3. The effect is most significant for IDP (p = 0.0036). Panel B. The effect of MEP on *Pt*DXS activity based on LC-MS/MS based assay without using any internal standard. MEP does not have any inhibitory effect on *Pt*DXS activity.

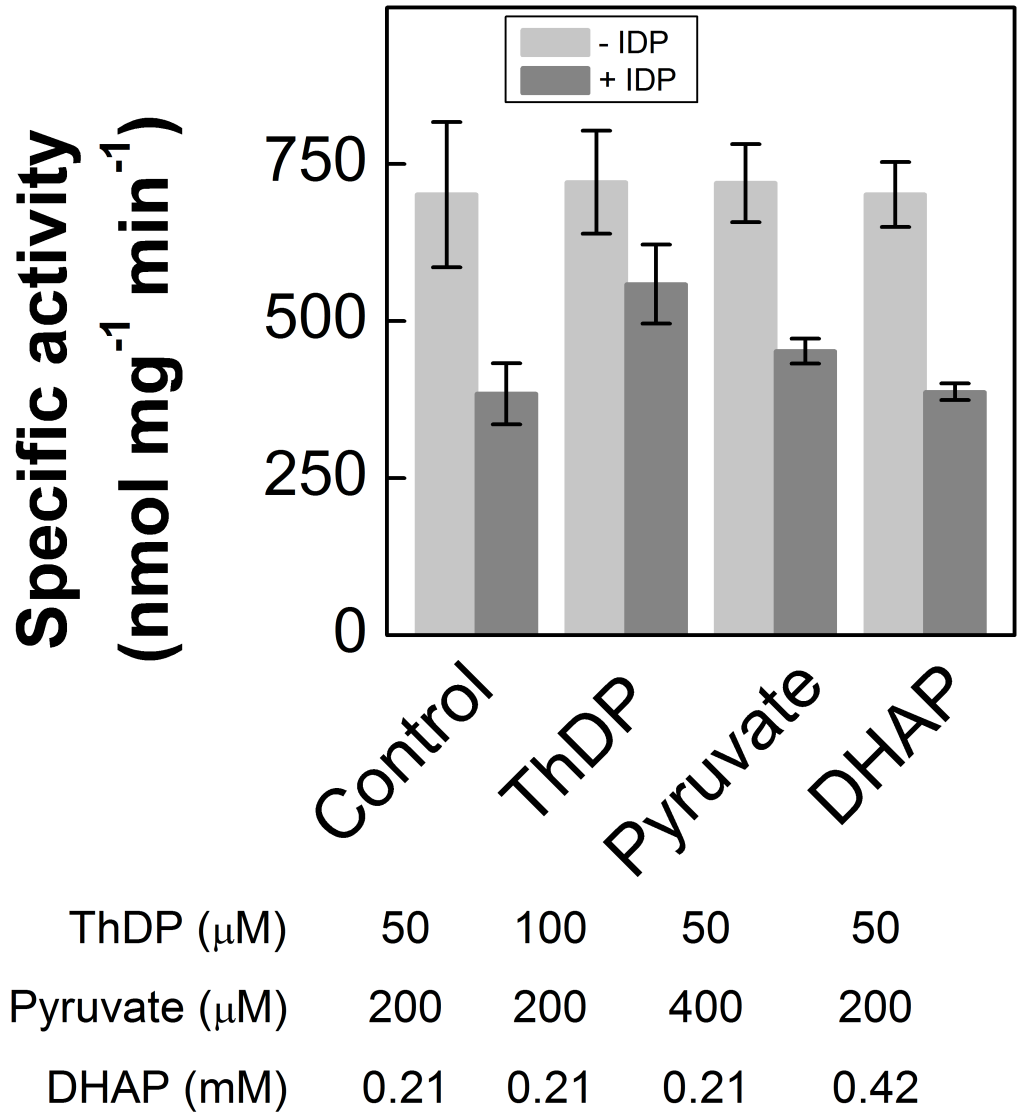

FIGURE 2.4 Effect of IDP on *Pt*DXS activity in presence of increased amount of each of the substrates. The light and dark gray bars represent the enzymatic activity in absence and presence of IDP respectively. The different categories represent the activity in presence of twice the amount of a particular substrate (as designated below) compared to that present in the control. Each bar represents mean ± SD, n = 3. Inhibition by IDP is significantly less ($p < 0.01$) in presence of twice the amount of ThDP.

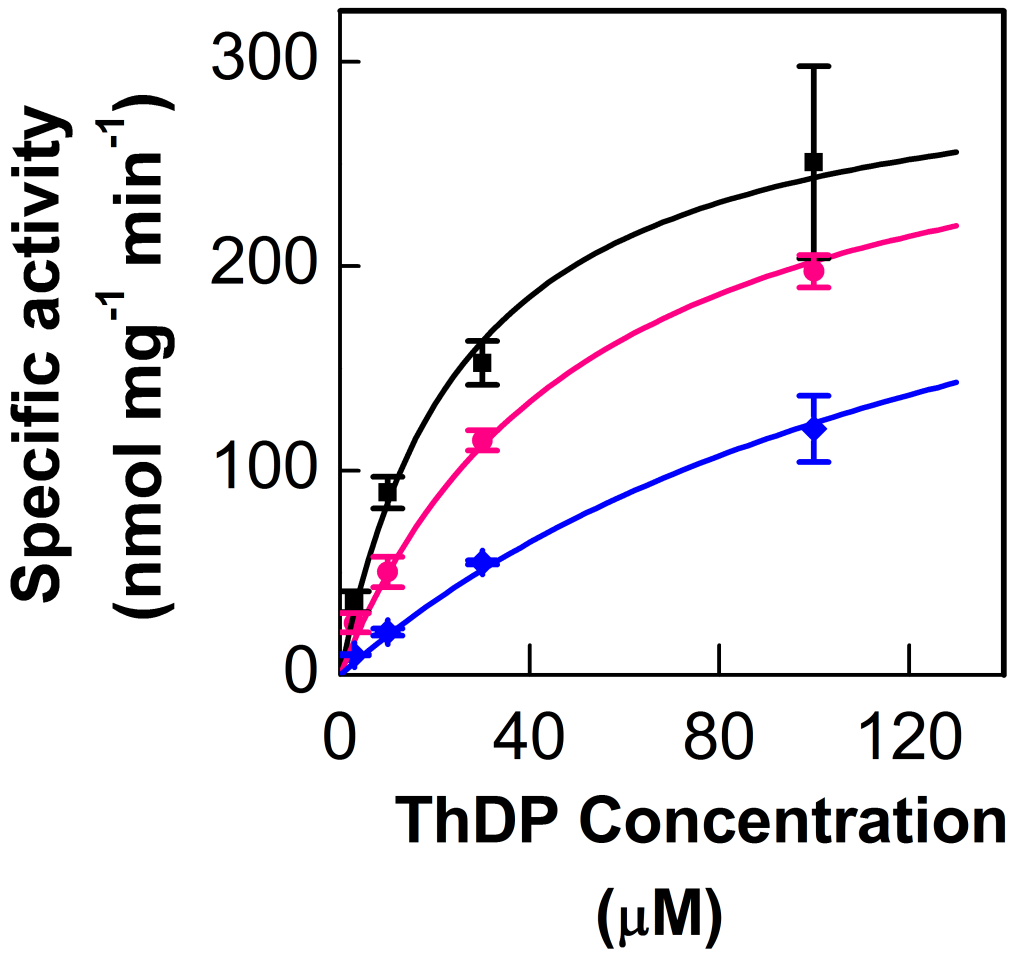

FIGURE 2.5 Michaelis-Menten plot for *Pt*DXS activity at different concentration of ThDP and fixed concentration of pyruvate and DHAP in presence of varying concentration of IDP. Each data point represents mean ± SD, n = 3. Different symbols represent the experimental data points. The solid lines represent the regression of the experimental data points using the method of least squares. The black, pink and blue colors represent the *Pt*DXS activity in presence of 0, 100, and 1000 μM of IDP respectively. *Pt*DXS activity decreases with increasing concentration of IDP.

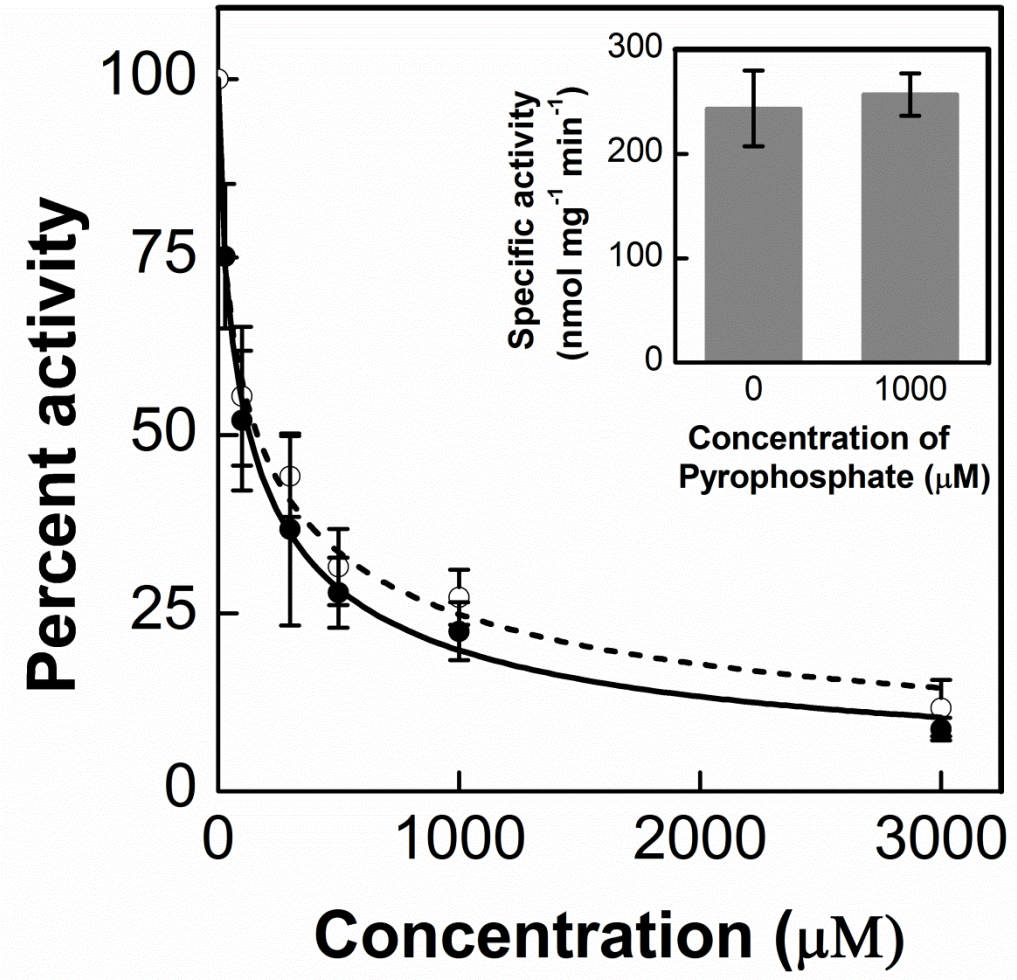

FIGURE 2.6 IC_{50} curve of DMADP and IDP for the *Pt*DXS enzyme in presence of K_m concentration of ThDP. Each data point represents mean ± SD, n = 3. The IC_{50} curves were obtained from the non-linear curve fitting of the experimental data points using Origin. The solid and empty circles represent the experimental data points for IDP and DMADP respectively and the solid and dotted lines represent the fitted IC_{50} curve for IDP and DMADP respectively. The K_i values of IDP and DMADP were calculated to be ~65 μM and ~81 μM respectively. The inset shows the effect of sodium pyrophosphate on *Pt*DXS activity. Each bar represents mean ± SD, n = 3. Sodium pyrophosphate did not show any inhibitory effect on *Pt*DXS activity even at a concentration of 1 mM.

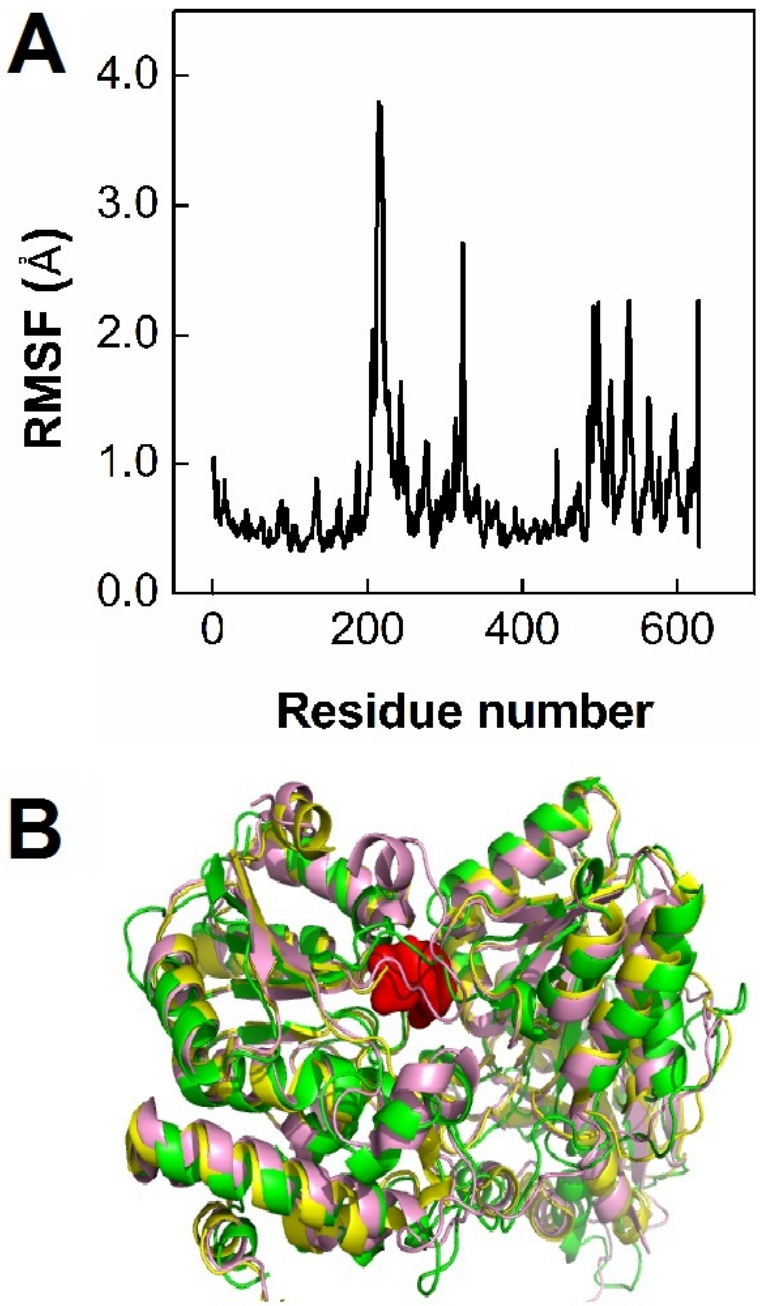

FIGURE 2.7 Panel A. Root-mean-square fluctuations of Cα atoms of the first subunit of *Pt*DXS during 1.5-ns production phase of the molecular dynamics simulation. Panel B. Structural alignment of *Pt*DXS (green) with *Ec*DXS (yellow) and *Dr*DXS (pink). The ligand binding site of *Pt*DXS is shown in red contour.

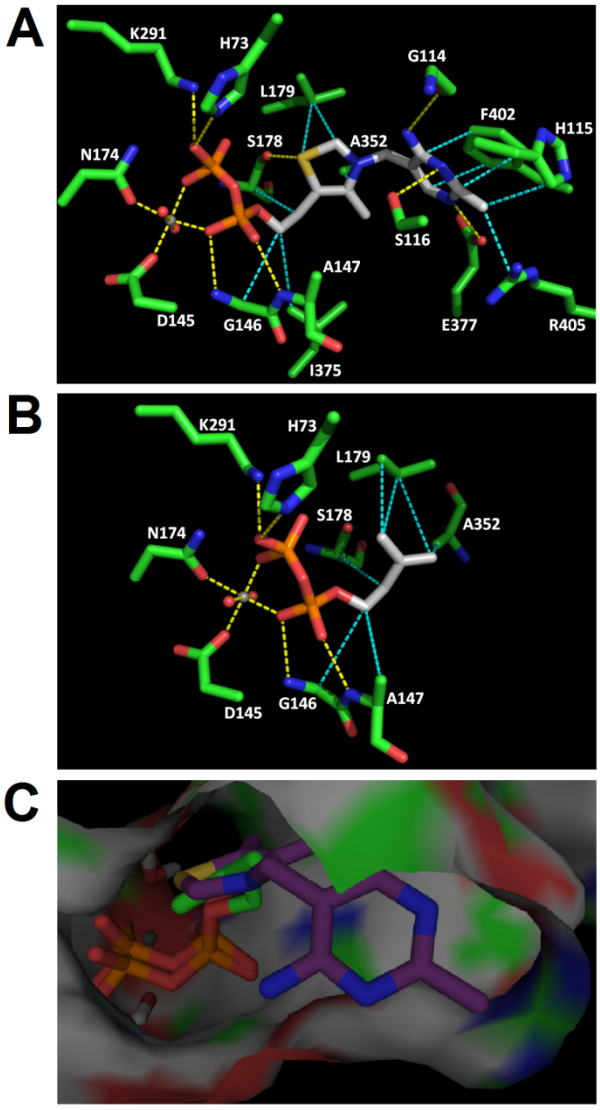

FIGURE 2.8 Interactions of *Pt*DXS with ThDP and IDP. Interactions of *Pt*DXS with the coenzyme ThDP (A) and IDP (B). The Mg^{2+} ion is shown as a gray sphere. Mg^{2+} coordination and hydrogen bonds are shown in yellow dashed lines and van der Waals interactions in cyan dashed lines. Two Mg^{2+}-coordinated water molecules are also shown. (C) Simulated binding pose of IDP (Carbon in green) in the *Pt*DXS active site as compared to that of ThDP. The Mg^{2+} ion is shown as a gray sphere. Two Mg^{2+}-coordinated water molecules are also shown.

LITERATURE CITED

LITERATURE CITED

Altincicek B., Hintz M., Sanderbrand S., Wiesner J., Beck E. & Jomaa H. (2000) Tools for discovery of inhibitors of the 1-deoxy-D-xylulose 5-phosphate (DXP) synthase and DXP reductoisomerase: an approach with enzymes from the pathogenic bacterium *Pseudomonas aeruginosa*. *FEMS Microbiology Letters*, **190**, 329-333.

Argyrou A. & Blanchard J.S. (2004) Kinetic and chemical mechanism of *Mycobacterium tuberculosis* 1-deoxy-D-xylulose-5-phosphate isomeroreductase. *Biochemistry*, **43**, 4375-4384.

Arigoni D., Sagner S., Latzel C., Eisenreich W., Bacher A. & Zenk M.H. (1997) Terpenoid biosynthesis from 1-deoxy-D-xylulose in higher plants by intramolecular skeletal rearrangement. *Proceedings of the National Academy of Sciences of the United States of America*, **94**, 10600-10605.

Bailey A.M., Mahapatra S., Brennan P.J. & Crick D.C. (2002) Identification, cloning, purification, and enzymatic characterization of *Mycobacterium tuberculosis* 1-deoxy-D-xylulose 5-phosphate synthase. *Glycobiology*, **12**, 813-820.

Bitok J.K. & Freel Meyers C. (2012) 2*C*-Methyl-D-erythritol 4-phosphate enhances and sustains cyclodiphosphate synthase IspF activity. *ACS Chemical Biology*, **7**, 1702-1710.

Bouvier F., d'Harlingue A., Suire C., A. Backhaus R.A. & Camara B. (1998) Dedicated roles of plastid transketolases during the early onset of isoprenoid biogenesis in pepper fruits. *Plant Physiology*, **117**, 1423-1431.

Case D.A., Darden T.A., Cheatham I., Simmerling C.L., Wang J., Duke R.E., Luo R., Crowley M., Walker R.C., Zhang W., Merz K.M., Wang B., Hayik S., Roitberg A., Seabra G., Kolossváry I., Wong K.F., Paesani F., Vanicek J., Wu X., Brozell S.R., Steinbrecher T., Gohlke H., Yang L., Tan C., Mongan J., Hornak V., Cui G., Mathews D.H., Seetin M.G., Sagui C., Babin V. & Kollman P.A. (2008) AMBER 10. University of California, San Francisco.

Cheng Y. & Prusoff W.H. (1973) Relationship between the inhibition constant (K_I) and the concentration of inhibitor which causes 50 per cent inhibition (I_{50}) of an enzymatic reaction. *Biochemical Pharmacology*, **22**, 3099-3108.

Cordoba E., Salmi M. & León P. (2009) Unravelling the regulatory mechanisms that modulate the MEP pathway in higher plants. *Journal of Experimental Botany*, **60**, 2933-2943.

DellaPenna D. & Posgon B.J. (2006) Vitamin synthesis in plants: tocopherols and carotenoids. *Annual Review of Plant Biology*, **57**, 711-738.

Dubey V.S., Bhalla R. & Luthra R. (2003) An overview of the non-mevalonate pathway for terpenoid biosynthesis in plants. *Journal of Bioscience*, **28**, 637-646.

Eisenreich W., Bacher A., Arigoni D. & Rohdich F. (2004) Biosynthesis of isoprenoids via the non-mevalonate pathway. *Cellular and Molecular Life Sciences*, **61**, 1401-1426.

Eisenreich W., Menhard B., Hylands P.J. & Zenk M.H. (1996) Studies on the biosynthesis of taxol: the taxane carbon skeleton is not of mevalonoid origin. *Proceedings of the National Academy of Sciences of the United States of America*, **93**, 6431-6436.

Eisenreich W., Schwarz M., Cartayrade A., Arigoni D., Zenk M.H. & Bacher A. (1998) The deoxyxylulose phosphate pathway of terpenoid biosynthesis in plants and microorganisms. *Chemistry & Biology*, **5**, R221-R233.

Enfissi E.M.A., Fraser P.D., Lois L.M., Boronat A., Schuch W. & Bramley P.M. (2005) Metabolic engineering of the mevalonate and non-mevalonate isopentenyl diphosphate-forming pathways for the production of health-promoting isoprenoids in tomato. *Plant Biotechnology Journal*, **3**, 17-27.

Essmann U., Perera L., Berkowitz M.L., Darden T., Lee H. & Pedersen L.G. (1995) A smooth particle mesh ewald method. *The Journal of Chemical Physics*, **103**, 8577-8593.

Estévez J.M., Cantero A., Reindl A., Reichler S. & León P. (2001) 1-Deoxy-D-xylulose-5-phosphate synthase, a limiting enzyme for plastidic isoprenoid biosynthesis in plants. *Journal of Biological Chemistry*, **276**, 22901-22909.

Eubanks L.M. & Poulter C.D. (2003) *Rhodobacter capsulatus* 1-deoxy-D-xylulose 5-phosphate synthase: steady-state kinetics and substrate binding. *Biochemistry*, **42**, 1140-1149.

Feurle J., Jomaa H., Wilhelm M., Gutsche B. & Herderich M. (1998) Analysis of phosphorylated carbohydrates by high-performance liquid chromatography–electrospray ionization tandem mass spectrometry utilising a β-cyclodextrin bonded stationary phase. *Journal of Chromatography A*, **803**, 111-119.

Gong Y.F., Liao Z.H., Guo B.H., Sun X.F. & Tang K.X. (2006) Molecular cloning and expression profile analysis of *Ginkgo biloba DXS* gene encoding 1-deoxy-D-xylulose 5-phosphate synthase, the first committed enzyme of the 2-*C*-methyl-D-erythritol 4-phosphate pathway. *Planta Medica*, **72**, 329-335.

Guevara-García A., Román C.S., Arroyo A., Cortés M., Gutiérrez-Nava M.d.l.L. & León P. (2005) Characterization of the Arabidopsis *clb6* mutant illustrates the importance of posttranscriptional regulation of the methyl-D-erythritol 4-phosphate pathway. *The Plant Cell*, **17**, 628-643.

Hahn E.M., Eubanks L.M., Testa C.A., Blagg B.S.J., Baker J.A. & Poulter C.D. (2001) 1-Deoxy-D-xylulose 5-phosphate synthase, the gene product of open reading frame (ORF) 2816 and ORF 2895 in *Rhodobacter capsulatus*. *Journal of Bacteriology*, **183**, 1-11.

Hale I., O'Neill P.M., Berry N.G., Odom A. & Sharma R. (2012) The MEP pathway and the development of inhibitors as potential anti-infective agents. *Medicinal Chemistry Communications*, **3**, 418-433.

Han Y.-S., Sabbioni C., Heijden R.V.D. & Verpoorte R. (2003) High-performance liquid chromatography assay for 1-deoxy-D-xylulose 5-phosphate synthase activity using fluorescence detection. *Journal of Chromatography A*, **986**, 291-296.

Harker M. & Bramley P.M. (1999) Expression of prokaryotic 1-deoxy-D-xylulose-5-phosphatases in *Escherichia coli* increases carotenoid and ubiquinone biosynthesis. *FEBS Letters*, **448**, 115-119.

Hawkins C.F., Borges A. & Perham R.N. (1989) A common structural motif in thiamin pyrophosphate-binding enzymes. *FEBS Letters*, **255**, 77-82.

Hemmerlin A., Hoeffler J.-F., Meyer O., Tritsch D., Kagan I.A., Grosdemange-Billiard C., Rohmer M. & Bach T.J. (2003) Cross-talk between the cytosolic mevalonate and the plastidial methylerythritol phosphate pathways in tobacco bright yellow-2 cells. *Journal of Biological Chemistry*, **278**, 26666-26676.

Lange B.M., Wildung M.R., Mccaskill D. & Croteau R. (1998) A family of transketolases that directs isoprenoid biosynthesis via a mevalonate-independent pathway. *Proceedings of the National Academy of Sciences of the United States of America*, **95**, 2100-2104.

Li Z., Ratliff E.A. & Sharkey T.D. (2011) Effect of temperature on postillumination isoprene emission in oak and poplar. *Plant Physiology* **155**, 1037-1046.

Li Z. & Sharkey T.D. (2013) Metabolic profiling of the methylerythritol phosphate pathway reveals the source of post-illumination isoprene burst from leaves. *Plant, Cell and Environment*, **36**, 429-437.

Lichtenthaler H.K., Rohmer M. & Schwender J. (1997a) Two independent biochemical pathways for isopentenyl diphosphate and isoprenoid biosynthesis in higher plants. *Physiologia Plantarum*, **101**, 643-652.

Lichtenthaler H.K., Schwender J., Disch A. & Rohmer M. (1997b) Biosynthesis of isoprenoids in higher plant chloroplasts proceeds via a mevalonate-independent pathway. *FEBS letters*, **400**, 271-274.

Lois L.M., Campos N., Putra S.R., Danielsen K., Rohmer M. & Boronat A. (1998) Cloning and characterization of a gene from *Escherichia coli* encoding a transketolase-like enzyme that catalyzes the synthesis of D-1-deoxyxylulose 5-phosphate, a common precursor for

isoprenoid, thiamin, and pyridoxol biosynthesis. *Proceedings of the National Academy of Sciences of the United States of America*, **95**, 2105-2110.

Lois L.M., Rodríguez-Concepción M., Gallego F., Campos N. & Boronat A. (2000) Carotenoid biosynthesis during tomato fruit development: regulatory role of 1-deoxy-D-xylulose 5-phosphate synthase. *Plant Journal*, **22**, 503-513.

Matthews P.D. & Wurtzel E.T. (2000) Metabolic engineering of carotenoid accumulation in *Escherichia coli* by modulation of the isoprenoid precursor pool with expression of deoxyxylulose phosphate synthase. *Applied Microbiology and Biotechnology*, **53**, 396-400.

Miller B., Heuser T. & Zimmer W. (2000) Functional involvement of a deoxy-D-xylulose 5-phosphate reductoisomerase gene harboring locus of *Synechococcus leopoliensis* in isoprenoid biosynthesis. *FEBS Letters*, **481**, 221-226.

Morris W.L., Ducreux L.J.M., Hedden P., Millam S. & Taylor M.A. (2006) Overexpression of a bacterial 1-deoxy-D-xylulose 5-phosphate synthase gene in potato tubers perturbs the isoprenoid metabolic network: implications for the control of the tuber life cycle. *Journal of Experimental Botany*, **57**, 3007-3018.

Patel H., Nemeria N.S., Brammer L.A., Freel Meyers C.L. & Jordan F. (2012) Observation of thiamin-bound intermediates and microscopic rate constants for their interconversion on 1-deoxy-D-xylulose 5-phosphate synthase: 600-fold rate acceleration of pyruvate decarboxylation by D-glyceraldehyde-3-phosphate. *Journal of the American Chemical Society*, **134**, 18374-18379.

Querol J., Besumbes O., Lois M.L., Boronat A. & Imperial S. (2001) A fluorometric assay for the determination of 1-deoxy-D-xylulose 5-phosphate synthase activity. *Analytical Biochemistry*, **296**, 101-105.

Rodríguez-Concepción M. & Boronat A. (2002) Elucidation of the methylerythritol phosphate pathway for isoprenoid biosynthesis in bacteria and plastids. A metabolic milestone achieved through genomics. *Plant Physiology*, **130**, 1079-1089.

Rohmer M., Knani M., Simonin P., Sutter B. & Sahm H. (1993) Isoprenoid biosynthesis in bacteria: a novel pathway for the early steps leading to isopentenyl diphosphate. *Biochemical Journal*, **295**, 517-524.

Rohmer M., Seemann M., Horbach S., Bringer-Meyer S. & Sahm H. (1996) Glyceraldehyde 3-phosphate and pyruvate as precursors of isoprenic units in an alternative non-mevalonate pathway for terpenoid biosynthesis. *Journal of the American Chemical Society*, **118**, 2564-2566.

Ryckaert J.-P., Ciccotti G. & Berendsen H.J.C. (1977) Numerical integration of the cartesian equations of motion of a system with constraints: molecular dynamics of *n*-alkanes. *Journal of Computational Physics*, **23**, 327-341.

Schwender J., Seemann M., Lichtenthaler H.K. & Rohmer M. (1996) Biosynthesis of isoprenoids (carotenoids, sterols, prenyl side-chains of chlorophylls and plastoquinone) via a novel pyruvate/glyceraldehyde 3-phosphate non-mevalonate pathway in the green alga *Scenedesmus obliquus*. *Biochemical Journal*, **316**, 73-80.

Schwender J., Zeidler J., Gröner R., Müller C., Focke M., Braun S. & Lichtenthaler H.K. (1997) Incorporation of 1-deoxy-D-xylulose into isoprene and phytol by higher plants and algae. *FEBS letters*, **414**, 129-134.

Sharkey T.D., Gray D.W., Pell H.K., Breneman S.R. & Topper L. (2013) Isoprene synthase genes form a monophyletic clade of acyclic terpene synthases in the Tps-b terpene synthase family. *Evolution*, **67**, 1026–1040.

Sharkey T.D., Wiberley A.E. & Donohue A.R. (2008) Isoprene emission from plants: why and how. *Annals of Botany*, **101**, 5-18.

Shi G., Shaw G., Li Y., Wu Y., Yan H. & Ji X. (2012) Bisubstrate analog inhibitors of 6-hydroxymethyl-7,8-dihydropterin pyrophosphokinase: new lead exhibits a distinct binding mode. *Bioorganic & Medicinal Chemistry*, **20**, 4303-4309.

Sprenger G.A., Schörken U., Wiegert T., Grolle S., Graaf A.A.D., Taylor S.V., Begley T.P., Bringer-Meyer S. & Sahm H. (1997) Identification of a thiamin-dependent synthase in *Escherichia coli* required for the formation of the 1-deoxy-D-xylulose 5-phosphate precursor to isoprenoids, thiamin, and pyridoxol. *Proceedings of the National Academy of Sciences of the United States of America*, **94**, 12857-12862.

Wiberley A.E., Donohue A.R., Westphal M.M. & Sharkey T.D. (2009) Regulation of isoprene emission from poplar leaves throughout a day. *Plant, Cell and Environment*, **32**, 939-947.

Winter H., Robinson D. & Heldt H. (1994) Subcellular volumes and metabolite concentrations in spinach leaves. *Planta*, **193**, 530-535.

Wolfertz M., Sharkey T.D., Boland W. & Kühnemann F. (2004) Rapid regulation of the methylerythritol 4-phosphate pathway during isoprene synthesis. *Plant Physiology*, **135**, 1939-1945.

Wolfertz M., Sharkey T.D., Boland W., Kühnemann F., Yeh S. & Weise S.E. (2003) Biochemical regulation of isoprene emission. *Plant, Cell and Environment*, **26**, 1357-1364.

Xiang S., Usunow G., Lange G., Busch M. & Tong L. (2007) Crystal structure of 1-deoxy-D-xylulose 5-phosphate synthase, a crucial enzyme for isoprenoids biosynthesis. *Journal of Biological Chemistry*, **282**, 2676-2682.

Zeidler J.G., Lichtenthaler H.K., May H.U. & Lichtenthaler F.W. (1997) Is isoprene emitted by plants synthesized via the novel isopentenyl pyrophosphate pathway? *Zeitschrift für Naturforschung*, **52c**, 15-23.

CHAPTER 3

Engineering of recombinant poplar deoxy-D-xylulose-5-phosphate synthase (*Pt*DXS) by site-directed mutagenesis to improve its activity

3.1 SUMMARY

Deoxyxylulose 5-phosphate synthase (DXS) plays a regulatory role in the methylerythritol 4-phosphate (MEP) pathway. Isopentenyl diphosphate (IDP) and dimethylallyl diphosphate (DMADP), the end products of this pathway, inhibit DXS by competing with thiamin diphosphate (ThDP). I have designed and tested modifications of recombinant poplar DXS (*Pt*DXS) in an attempt to reduce inhibition by IDP and DMADP, thereby removing a feedback that limits the usefulness of the MEP pathway in biotechnological applications. A predicted enzyme structure was examined to find ligand-enzyme interactions relatively more important for inhibitor-enzyme binding than ThDP-enzyme binding. Two alanine residues important for binding ThDP and the inhibitors were mutated to glycine. In one case the IDP/DMADP inhibition was reduced and the overall activity was increased. This provides proof of concept that it is possible to reduce the feedback from IDP and DMADP on DXS activity.

3.2 INTRODUCTION

1-Deoxy-D-xylulose-5-phosphate synthase (DXS) is the first enzyme of the 2-methyl-3-erythritol-4-phosphate (MEP) pathway that leads to the biosynthesis of isopentenyl diphosphate (IDP) and dimethylallyl diphosphate (DMADP) (Lichtenthaler 1999; Lichtenthaler *et al.* 1997; Rodríguez-Concepción & Boronat 2002; Rohmer 1999). These metabolites are the building blocks of isoprenoids, also called terpenoids or terpenes (Eisenreich *et al.* 1998). Isoprenoids constitute an important and diverse group of natural products occurring in all different forms of life including animals, plants as well as bacteria and archea. Over 40,000 different isoprenoids have been reported and they have a huge diversity in their structures and functions (Misawa 2011). Structurally, all isoprenoids are based on the C5, branched chain isoprenoid unit and the complex arrangements of this unit give rise to the structural diversity among the isoprenoids (Cordoba *et al.* 2009; Hemmerlin *et al.* 2003; Rodríguez-Concepción 2006).

In addition to various biological roles, many isoprenoids have important commercial applications as drugs, natural polymers, pigments, flavor and fragrance molecules, agrichemicals, cosmetics, biofuels etc. (Klein-Marcuschamer *et al.* 2007; Misawa 2011; Phillips *et al.* 2008; Roberts 2007; Rodríguez-Concepción 2006; Rude & Schirmer 2009). Natural sources of some isoprenoids is limited (Martin *et al.* 2003; Misawa 2011; Phillips *et al.* 2008), therefore, the biotechnological production of commercially important isoprenoids has attracted widespread attention as a valuable industrial target (Klein-Marcuschamer *et al.* 2007).

Metabolic engineering of the MEP pathway has become a focus to improve the bio-production of downstream isoprenoids (Maury *et al.* 2005). DXS has been one of the main targets for engineering increases in the flux through this pathway in both bacteria and plants.

Overexpression of DXS has been found to increase the biosynthesis of carotenoids and ubiquinone in *E. coli* (Harker & Bramley 1999). It has also been shown that coexpression of DXS with other downstream enzymes improved the yield of taxadiene, lycopene, sesquiterpenes, various mono and diterpenes, carotenoids including β-carotene, and zeaxanthin in *E. coli* (Albrecht *et al.* 1999; Huang *et al.* 2001; Kim & Keasling 2001; Martin *et al.* 2001; Matthews & Wurtzel 2000; Reiling *et al.* 2004; Wang *et al.* 2000). Overexpression of bacterial DXS increased the amount of carotenoid in transgenic tomato lines and potato tubers (Enfissi *et al.* 2005; Morris *et al.* 2006). A transgenic Arabidopsis line with overexpressed DXS was shown to have increased amounts of various isoprenoids such as chlorophylls, tocopherols, carotenoids, abscisic acid, and gibberellins (Estévez *et al.* 2001). In addition to DXS, 1-deoxy-D-xylulose-5-phosphate reductoisomerase (DXR) and isopentenyl diphosphate isomerase (IDI) have also been targeted for metabolic engineering of the MEP pathway to improve its carbon flux to obtain higher yield of isoprenoids (Albrecht *et al.* 1999; Huang *et al.* 2001; Kajiwara *et al.* 1997; Kim & Keasling 2001; Reiling *et al.* 2004; Wang *et al.* 1999).

Efforts have also been made to improve the MEP pathway by other approaches. Overexpression of the entire pathway has been attempted either by chromosomal promoter replacement throughout the core pathway or by the introduction of a complete heterologous pathway onto the chromosome (Vickers *et al.* 2014; Yuan *et al.* 2006). The outcome of these approaches in improving the yield of isoprenoids is promising, but still limited for its use in industrial applications. However, the best yield outcome with an engineered MEP pathway in *E. coli* is still much less than that obtained with an imported mevalonate acid (MVA) pathway (Vickers *et al.* 2014). Attempts have been made to bypass MEP pathway in *E. coli* with an engineered MVA pathway from *S. cerevisiae* (Martin *et al.* 2003). This was done to overcome

the limitation of the regulatory control mechanism of MEP pathway in the native host and resulted in increased production of isoprenoid precursors. This indicates that efforts are needed to improve the MEP pathway by manipulating regulatory mechanisms of this pathway.

Genetic regulation of the MEP pathway has been studied extensively (Cordoba *et al.* 2009). On the other hand, study of the metabolic regulation of the MEP pathway is only recently receiving the same degree of attention (Banerjee & Sharkey 2014). DXS catalyzes the formation of 1-deoxy-D-xylulose 5-phosphate (DXP) from glyceraldehyde 3-phosphate and pyruvate in presence of the cofactor thiamin diphosphate (ThDP) and divalent ions Mg^{2+} or Mn^{2+}. For a long time, DXS has been suggested to be a rate-limiting enzyme and thus have a potential regulatory role in this pathway (Estévez *et al.* 2001; Guevara-García *et al.* 2005; Lois *et al.* 2000; Miller *et al.* 2000; Wiberley *et al.* 2009; Wright *et al.* 2014). A recent study has demonstrated that DXS is inhibited by both IDP and DMADP resulting in feedback regulation (Banerjee *et al.* 2013; Ghirardo *et al.* 2014). Both of these isoprenoid precursors compete with ThDP for binding at the active site of the enzyme (Banerjee *et al.* 2013). The importance of DXS in the metabolic regulation of the MEP pathway makes it a critical target for engineering so that the manipulated enzyme can overcome the regulatory limitation to achieve an improved MEP pathway for industrial use.

The aim of this work was to obtain a DXS enzyme with good ThDP binding to maintain its activity but reduced binding of IDP and DMADP to partially or completely relieve the feedback regulation of this pathway. In this study, I have engineered a recombinant DXS enzyme from *Populus trichocarpa* (*Pt*DXS) by site-directed mutagenesis in such a way that it can selectively bind ThDP over IDP and DMADP. Two residues at the active site, Ala-147 and Ala-352, were selected for mutation as they were critical for binding the carbon chain of IDP and DMADP.

These residues were either individually or simultaneously mutated to Gly to generate A147G*Pt*DXS, A352G*Pt*DXS and A147G/A352G*Pt*DXS. A147G*Pt*DXS was found to have improved activity compared to the WT enzyme in presence of excess amount of the substrates. In addition, both IDP and DMADP exhibited reduced inhibition of A147G*Pt*DXS compared to the WT enzyme.

3.3 EXPERIMENTAL PROCEDURES

3.3.1 Site-directed mutagenesis

For A147G*Pt*DXS and A352G*Pt*DXS, PCR-based site-directed mutagenesis was done using the plasmid construct for C-terminally His-tagged WT*Pt*DXS (pET17b3'HR/*Pt*DXS) as template (Banerjee *et al.* 2013). The primers used for A147G*Pt*DXS mutation were 5'-CCT GCT GTC ATA CCT CCA TCA CC-3' and 5'-GGT GAT GGA GGT ATG ACA GCA GG-3'. The primers used for A352G*Pt*DXS mutation were 5'-CCT CCT CCC ATA CCA GCA TGA ATT GC-3' and 5'-GCA ATT CAT GCT GGT ATG GGA GGA GG-3'. For the double mutant A147G/A352G*Pt*DXS, PCR-based site-directed mutagenesis was done using the plasmid construct of A352G*Pt*DXS as the template and the primer pairs for A147G*Pt*DXS as primers. The PCR reaction mixture was then subjected to DpnI digestion. PCR-clean up of the reaction mixture from DpnI digestion was done using Promega PCR-clean up kit. The resulting plasmids for different mutants were initially transformed in *E. coli* strain DH5α to verify the sequence of

the mutants. The presence of appropriate sequence of the mutants and the absence of any undesired mutation were confirmed by DNA-sequencing.

3.3.2 Overexpression and purification of WT and the different mutant of PtDXS enzyme

The WT and the different mutants of *Pt*DXS enzymes were overexpressed and purified following the reported procedure with some modifications (Banerjee *et al.* 2013). The correct plasmid constructs for WT and the various mutants of *Pt*DXS were overexpressed in *E. coli* strain BL21(DE3)pLysS. In each case, 1 liter of LB medium containing appropriate antibiotics was used for protein expression. Cells were grown and induced as reported before (Banerjee *et al.* 2013). The *E. coli* cells were harvested by centrifugation after overnight (~18 h) induction at room temperature. Cell pellets were resuspended in cold lysis buffer (5 mL lysis buffer/gm of pellet; 50 mM sodium phosphate, 300 mM NaCl, 10% glycerol, pH 8.0) containing 20 mM $MgCl_2$ and 100 U of DNAseI (from Qiagen). The cells were lysed on ice by sonication (Qsonica sonicator ultrasonic processor, Part No. Q500, Misonix sonicator). The sonicator was set at an amplitude of 35% and the sonication was done for 5 min with pulses of 15 s ON and 15 s OFF. EDTA-free protease inhibitor cocktail (Sigma, catalog number S8830) was added to the cell suspension (final concentration of ~1X the concentration recommended by the manufacturer) right before sonication. The lysed cell suspension was centrifuged at ~27,000 g for 30 min at 4 ºC and the supernatant was collected as crude lysate. The crude lysate was slowly supplemented with ammonium sulfate to 45% saturation under gentle stirring at 4 ºC. The suspension was stirred for 30 min followed by centrifugation at ~27,000 g for 20 min at 4 ºC. Same volume of cold lysis buffer (same as the volume of crude lysate used for the first ammonium sulfate

precipitation) was used to resuspend the pellet and the solution was centrifuged again at 4 ºC. The ammonium sulfate precipitation was then repeated with the supernatant as described before. Next, ~20 mL of cold lysis buffer was used to resuspend the pellet from the second ammonium sulfate precipitation. This solution was then centrifuged at ~27,000 g for 20 min at 4 ºC and the supernatant was dialyzed against 2 L of the lysis buffer for overnight at 4 ºC. Ni-NTA resin (Qiagen) was added to the dialyzed protein solution (1 mL resin used for every 4 mL dialyzed protein solution) with gentle stirring for 1 h at 4 ºC. The mixture was then loaded to a column and the flow-through was collected. The column was then washed with wash buffer (50 mM sodium phosphate, 300 mM NaCl, 10 mM imidazole, 10% glycerol, pH 8.0) containing EDTA-free protease inhibitor cocktail (final concentration of ~1X the concentration recommended by the manufacturer) until OD_{280} of the effluent reached less than 0.05. The protein was then eluted with elution buffer containing 50 mM sodium phosphate, 300 mM NaCl, 50-500 mM imidazole, 10% glycerol, pH 8.0. SDS-PAGE was carried out to identify the fractions containing the most protein. Most of the protein was eluted with 100-150 mM of imidazole. A minor difference in procedure was used for A147G*Pt*DXS. For this mutant, the column was very slow during the washing step with the wash buffer. A gradient elution buffer could not be used for this mutant and the protein was eluted with the elution buffer containing 250 mM imidazole. The Ni-NTA column purification was performed in the cold room at 4 ºC. Fractions containing the maximum amount of the protein were combined together and a final ammonium sulfate (45% saturation) precipitation was done as described before. The suspension was centrifuged at ~27,000 g for 20 min at 4 ºC and the protein pellet was dissolved in minimum volume of cold storing buffer containing 50 mM Tris-HCl, 1 mM DTT, 10% glycerol, pH 7.5. The solution was centrifuged again at ~27,000 g for 20 min at 4 ºC and the supernatant was dialyzed against 1 L of the storage

buffer overnight at 4 ºC. The dialyzed protein solution was then dispensed into microtubes, frozen in liquid nitrogen, and stored at -80 ºC.

3.3.3 LC-MS/MS-based activity assay for WT and mutant PtDXS enzyme

The activity of the purified WT and various *Pt*DXS mutants were tested using LC-MS/MS based assay as reported before (Banerjee *et al.* 2013). Enzymatic assays for the WT and mutant *Pt*DXS were carried out in the presence of a large excess (~20 × K_m) of all the substrates. Briefly, the assay was done in 40 mM Tris-HCl buffer at pH 8.0 containing 10 mM $MgCl_2$, 1 mM dithiothreitol (DTT), appropriate concentration of ThDP, 1 U/mL rabbit muscle triose phosphate isomerase (TPI), and 0.25 μM WT/mutant *Pt*DXS in a total volume of 100 μL. The reaction was initiated with a mixture of appropriate concentration of DHAP and pyruvate. For WT, the concentration of ThDP, DHAP, and pyruvate used was 300 μM, 2.2 mM, and 2 mM respectively. For A147G*Pt*DXS, the concentration of ThDP, DHAP, and pyruvate used was 700 μM, 2.2 mM, and 4 mM respectively. For A352G*Pt*DXS, the concentration of ThDP, DHAP, and pyruvate used was 1.2 mM, 2.2 mM, and 4 mM respectively. For A147G/A352G*Pt*DXS, the concentration of ThDP, DHAP, and pyruvate used was 1.2 mM, 2.2 mM, and 5 mM respectively. In each case, the assay mixture was incubated at 37 °C for 5 min. It was then quenched by freezing in liquid nitrogen followed by the addition of 400 μL of ice-cold acetonitrile. The amount of DXP produced was determined in presence of the internal standard ($^{13}C_2$-DXP) by LC-MS/MS as reported before (Banerjee *et al.* 2013).

3.3.4 Kinetic characterization

In order to determine the kinetic parameters of the WT and the various mutants of *Pt*DXS, the enzymatic assays were carried out as described earlier except the use of different concentrations of the substrates. For the different variants of *Pt*DXS, the concentrations used to study the K_m of ThDP, DHAP, and pyruvate were 0-1 mM of ThDP in presence of 263 μM DHAP and 1 mM of pyruvate; 0-197 μM DHAP in presence of 100 μM ThDP and 5 mM pyruvate; 0-1 mM pyruvate in presence of 263 μM DHAP and 100 μM ThDP respectively. The K_m values of various *Pt*DXS enzymes for different substrates were obtained by fitting the experimental data with non-linear regression in Origin (http://www.originlab.com/).

3.3.5 Inhibition studies

IDP and DMADP were purchased from Isoprenoids, LC (Tampa, FL, USA). The inhibition assay for each of the enzymes was carried out as described before in presence of ~K_m concentration of ThDP and ~2 × K_m concentration of DHAP and pyruvate. The concentration of IDP and DMADP used in the inhibition assay was 0-1 mM. The non-linear fitting of the IC_{50} curves was done using the program Origin (http://www.originlab.com/) and the determination of K_i of each of the enzymes for both IDP and DMADP were done as reported earlier (Banerjee *et al.* 2013).

3.3.6 Analysis of the activity of A147GPtDXS relative to WTPtDXS

The activity of WT*Pt*DXS and A147G*Pt*DXS was calculated according to the following equation

$$v = \frac{k_{cat} \times \left(\frac{[E] \times [T]}{K_m^T \left(1 + {[I]}/{K_i^I} + {[D]}/{K_i^D}\right) + [T]} \right) \times [P]}{K_m^P + [P]}$$

where, v is the rate of the enzyme, k_{cat} is the turnover number of the enzyme, $[E]$ is the concentration of the enzyme, $[T]$ is the concentration of ThDP, $[P]$ is the concentration of pyruvate, $[I]$ is the concentration of IDP, $[D]$ is the concentration of DMADP, K_m^T is the Michaelis constant for ThDP, K_m^P is the Michaelis constant for pyruvate, K_i^I is the inhibition constant for IDP, K_i^D is the inhibition constant for DMADP. This equation is based on Michaelis-Menten kinetics for both ThDP and pyruvate and also considering the competitive inhibition of ThDP by both IDP and DMADP. The rate of WT*Pt*DXS and A147G*Pt*DXS was calculated in presence of unit enzyme concentration and typical bacterial *in vivo* concentrations of IDP and DMADP (Zhou *et al.* 2013; Volkmer & Heinemann 2011). A range of 0-500 μM for the concentration of each of the substrates, ThDP and pyruvate, was used in the calculation of the rate of the enzymes. The difference between the rate of A147G*Pt*DXS and WT*Pt*DXS was calculated as described by the following equation

$$v_{difference} = \frac{v_{A147G} - v_{WT}}{v_{WT}} \times 100$$

where, $v_{difference}$ is the difference in rate of the mutant relative to the WT (in per cent), v_{A147G} is the rate of A147G*Pt*DXS, v_{WT} is the rate of WT*Pt*DXS. The graph (Figure 3.7) was generated by plotting the isolines corresponding to the concentrations of ThDP and pyruvate that gave an equivalent change in $v_{difference}$.

3.4 RESULTS

3.4.1 Site-directed mutation, overexpression, and purification of PtDXS

In the previous work computational modeling studies showed that both ThDP and IDP use similar polar interactions for binding of the diphosphate moiety with the enzyme (Banerjee *et al.* 2013). Therefore, any mutations involving these polar interactions may affect the binding of ThDP as well as IDP. It was important to select interactions essential for IDP binding, but not so important for the binding of ThDP. It was observed from the mechanistic studies of the inhibition that the interactions of the carbon chain of IDP and DMADP with the enzyme were pivotal in holding these molecules in place in the active site. Therefore, to affect the binding of IDP/DMADP selectively over ThDP, I focused on those residues of the enzyme that are important for binding the carbon chain of IDP/DMADP.

The computational modeling study predicted that the carbon chain of IDP/DMADP would have non-polar interactions with Leu-179, Ala-352, Gly-146, and Ala-147 (Figure 3.1). These interactions of the carbon chain of IDP/DMADP are important in orienting the diphosphate group in the appropriate position for binding with the enzyme. Among these residues, Gly-146 is

also involved in the polar interaction with the diphosphate group (Banerjee *et al.* 2013) and Leu-179 has several nonpolar interactions with the C2 atom and the sulfur atom of the thiazolium ring of ThDP (Figure 3.2). Therefore, Ala-147 and Ala-352 were chosen to be mutated to glycine to selectively reduce binding of IDP/DMADP more than ThDP. Computational modeling studies in the previous work (Banerjee *et al.* 2013) showed that the methyl side chain of both of these alanine residues has van der Waals interactions with carbon atoms at the beginning and end of the carbon chain of IDP/DMADP. Therefore, mutations involving these alanine residues to glycine might affect these van der Waals interactions resulting in poor binding of IDP/DMADP with the enzyme. These mutations, therefore, could lead to selective binding of ThDP over IDP/DMADP. Site-directed mutagenesis was carried out to generate A147G*Pt*DXS, A352G*Pt*DXS, and the double mutant A147G/A352G*Pt*DXS. For all the mutated plasmid constructs, the presence of the correct mutations was confirmed by DNA sequencing. The *E. coli* strain BL21(DE3)pLysS was used to overexpress the various mutants of *Pt*DXS as was done for WT*Pt*DXS (Banerjee *et al.* 2013). Purification of the different mutant proteins was also carried out as it was done for WT*Pt*DXS (Banerjee *et al.* 2013). The purified mutant proteins have similar molecular weight as the WT as observed by SDS-PAGE (Figure 3.3).

3.4.2 Enzymatic activity of different mutants of PtDXS

Enzymatic activity of the mutant *Pt*DXS was tested using LC-MS/MS-based assay as described previously (Banerjee *et al.* 2013). All of the mutants were enzymatically active. The time course of the enzymatic reactions for the various mutants of *Pt*DXS was found to be linear for the initial 15 min (data not shown). The specific activity of the various mutants was

calculated using the samples collected at 5 min. In the presence of saturating amounts of each of the substrates, A147G*Pt*DXS showed the highest activity and A147G/A352G*Pt*DXS showed the lowest activity (Figure 3.4). A147G*Pt*DXS was found to have twice as much activity compared to the WT (P = 0.0034). On the other hand, A352G*Pt*DXS showed comparable activity as WT and A147G/A352G*Pt*DXS was slightly less active than the WT (P = 0.0313).

3.4.3 Characterization of different mutants of PtDXS

The kinetic parameters of the various mutants of *Pt*DXS were determined using a LC-MS/MS-based assay. For these experiments, concentrations of substrates were 2-5 times the K_m except for the substrate being tested. The only exception was the use of pyruvate in large excess for the determination of the K_m for GAP. Table 3.1 shows the K_m and k_{cat} values of the WT and the various mutants of *Pt*DXS for different substrates. The K_m values of the current batch of WT enzyme for different substrates are comparable with those reported in the previous work (Banerjee *et al.* 2013). Interestingly, the k_{cat} value obtained for the current batch of WT is consistently found to be ~0.2 s^{-1} which is likely to be more accurate than one condition reported in the previous work that gave a value of ~0.5 s^{-1} (Banerjee *et al.* 2013). It was found that all of the mutants have comparable K_m values for GAP as that of the WT. For pyruvate, the K_m values of the mutants were found to be higher than that of the WT (~1.9-fold higher for A147G*Pt*DXS, ~2-fold higher for A352G*Pt*DXS, and ~2.6-fold higher for A147G/A352G*Pt*DXS). The K_m values of the mutants were also found to be higher for ThDP than that of the WT (~2.5-fold higher for A147G*Pt*DXS, ~4.3-fold higher for A352G*Pt*DXS, and ~4.2-fold higher for A147G/A352G*Pt*DXS). The k_{cat} value of A147G*Pt*DXS (~0.5 s^{-1}) is higher than the WT.

A352G*Pt*DXS had a slightly higher k_{cat} and A147G/A352G*Pt*DXS had a slightly lower k_{cat} except when pyruvate was the varied metabolite (Table 3.1).

3.4.4 Inhibitory effect of IDP and DMADP on different mutants of PtDXS

The next aim was to study the inhibitory effect of IDP and DMADP on the various mutants of *Pt*DXS. I showed that IDP and DMADP inhibit WT*Pt*DXS by competing with ThDP for binding at the active site of the enzyme (Banerjee *et al.* 2013). Assuming the same competitive inhibition of the mutant enzymes by IDP and DMADP, I tested whether the mutants are less sensitive to these inhibitors. Figure 3.5 shows the activity of different mutants of *Pt*DXS over a broad range of concentration of IDP and DMADP in the presence of K_m concentration of ThDP for each of the enzymes. The K_i and H values of IDP and DMADP for each of the enzymes were calculated from the non-linear fitting of the IC_{50} curve as described in the previous work (Banerjee *et al.* 2013). Table 3.2 summarizes the K_i and H values of IDP and DMADP for WT and different mutants of *Pt*DXS. The batch of the WT*Pt*DXS used in the current study was found to have slightly higher K_i (~2-fold) values for IDP and DMADP compared to the reported (Banerjee *et al.* 2013) values (shown with the asterisks (*) in Table 3.2). The K_i values for the WT enzyme obtained in this work was used to compare the inhibition of the mutant enzymes as these mutants were isolated simultaneously with the current batch of the WT enzyme. Figure 3.5 shows that A147G*Pt*DXS is much less sensitive to both IDP and DMADP as compared to the WT. The K_i values of IDP and DMADP for A147G*Pt*DXS were found to be 177 ± 11 μM and 319 ± 109 μM respectively and these values are ~1.7 (for IDP) and ~2.0 (for DMADP) times higher than the corresponding values for the WT enzyme. The double mutant

A147G/A352G*Pt*DXS was also shown to have slightly less inhibition by both IDP and DMADP as compared with the WT enzyme (Figure 3.5). For this mutant, the K_i values of IDP and DMADP were found to be 125 ± 1 μM and 253 ± 46 μM respectively, which are also ~1.2 (for IDP) and ~1.6 (for DMADP) times higher than the corresponding values for the WT enzyme. On the contrary, A352G*Pt*DXS was found to have stronger inhibition than the WT enzyme (Figure 3.5) with the K_i values of 65 ± 0.03 μM for IDP and 104 ± 0.4 μM for DMADP, which are ~0.6 (for IDP) and ~0.7 (for DMADP) times of that of the WT enzyme.

3.4.5 Effect of monophosphates on WTPtDXS activity

I observed in the previous work that WT*Pt*DXS is specifically inhibited by IDP and DMADP. The pyrophosphate moiety (in sodium pyrophosphate) alone is not sufficient to inhibit the enzyme indicating that the carbon chain of IDP and DMADP helps these metabolites to bind at the active site of the enzyme (Banerjee *et al.* 2013). Here, I have explored whether the monophosphate-containing metabolites inhibit WT*Pt*DXS. Two related metabolites isopentenyl monophosphate (IMP) and thiamin monophosphate (ThMP) were chosen to test their effect on WT*Pt*DXS activity. None of these monophosphate-containing metabolites showed significant effect on WT*Pt*DXS activity (Figure 3.6). This indicates that the diphosphate moiety is essential for the inhibition of WT*Pt*DXS.

3.5 DISCUSSION

Both modifications increased the k_{cat} of DXS, but only one reduced binding of the inhibitors IDP and DMADP. However, the K_m for ThDP was also increased and so it was not possible to preferentially reduce binding of the inhibitors relative to ThDP. The higher k_{cat} and reduced binding of inhibitors make A147G a potentially useful enzyme in biotechnological applications, especially if the concentration of ThDP is enhanced in the engineered organism. The activity of WT*Pt*DXS and A147G*Pt*DXS was analyzed across a range of concentrations of ThDP and pyruvate in the presence of typical bacterial *in vivo* concentrations of IDP and DMADP (Zhou *et al.* 2013). It showed that the WT has higher activity only at the very low range of concentrations of both ThDP and pyruvate (Figure 3.7). At higher concentrations of the substrates, A147G*Pt*DXS always has higher activity than the WT (Figure 3.7). At the higher range of substrate concentrations, A147G*Pt*DXS exhibited twice as much activity as that of the WT. Higher concentrations of inhibitors or the absence of inhibitors was also tested with similar results. This analysis supports the usefulness of A147G*Pt*DXS in biotechnological applications.

The structural models described in the previous work (Banerjee *et al.* 2013) were used to analyze the experimental observations in the current study. Figure 3.2A shows that C2 atom of the thiazolium ring of ThDP is accessible through a channel while the rest of the molecule is well buried inside. The carbanion generated from this C2 atom initiates the catalytic reaction by reacting with pyruvate (Xiang *et al.* 2007). Mechanistic studies on DXS revealed that the catalytic reaction requires the formation of a ternary complex between GAP and C2α-lactylthiamin diphosphate (LThDP) intermediate, which is the predecarboxylation complex formed between pyruvate and ThDP (Brammer Basta *et al.* 2014; Brammer *et al.* 2011; Eubanks

& Poulter 2003; Patel *et al.* 2012). It has been observed that LThDP is a stable intermediate and its association with GAP facilitates the subsequent decarboxylation step to generate the enamine (Brammer Basta *et al.* 2014; Patel *et al.* 2012). It is likely that the mutations did not affect the interaction between LThDP and GAP as there was no change in the K_m for GAP. Figure 3.2A shows that the methyl group of Ala-147 is sticking out towards this open channel maintaining a distance of about 7.2 Å (Figure 3.2B) from the C2 atom of the thiazolium ring. On the other hand, the methyl group of Ala-352 is much closer (4.6 Å; Figure 3.2B) to the C2 atom of the thiazolium ring. Therefore, it is highly possible that in the WT enzyme, LThDP followed by the enamine adduct after decarboxylation would be oriented towards Ala-147 resulting in steric interaction between the bulky enamine adduct with the methyl group of Ala-147. Mutation of Ala-147 to Gly can be favorable for accommodating both the LThDP intermediate as well as the subsequent enamine adduct. This could explain the higher activity of A147G*Pt*DXS than the WT enzyme (Figure 3.4).

Loss of the methyl group of Ala-147 will also result in the loss of van der Waals interaction of the carbon backbone of ThDP (4.9 Å; Figure 3.2B). This loss of the hydrophobic interaction does not have a severe impact in the binding of ThDP as there is another hydrophobic interaction (the backbone carbon of Gly-146, 4.0 Å; Figure 3.2B), which might be sufficient to keep the carbon backbone of ThDP in place. However, this might require a higher concentration of ThDP at the active site to compensate for the loss of this important interaction in its binding with ThDP. This could explain the higher K_m value of this mutant for ThDP.

The mutation of Ala-147 to Gly also causes an increase in the K_m of this mutant for pyruvate compared to WT. The methyl group of Ala-147 might help pyruvate orient properly at the active site through a hydrophobic interaction. Thus, the loss of this methyl group could require more

pyruvate at the active site to form the LThDP intermediate resulting in higher K_m of the mutant for pyruvate. However, in presence of excess concentration of both ThDP and pyruvate, this mutant exhibits higher activity than the WT. This could make this modification of DXS very useful in bioengineered organisms where substrates may be increased by genetic modifications to make some product of the MEP pathway. It has been reported that altering GAP and pyruvate concentration by genetic modification increased lycopene production in *E. coli* (Farmer & Liao 2001). The C2 atom of the thiazolium ring is strongly held in the appropriate position for catalytic reaction through the hydrophobic interactions with the methyl group of Ala-352 (4.6 Å; Figure 3.2B) and the side chain methyl group of Leu-179 (4.1 Å; Figure 3.2B). Mutation of Ala-352 to Gly can be compensated by the other hydrophobic interaction and therefore does not significantly disturb the positioning of the thiazolium ring. This results in the comparable activity of A352G*Pt*DXS with the WT enzyme (Figure 3.4). However, in the double mutant A147G/A352G*Pt*DXS, the loss of some hydrophobic interactions causes ThDP to be held somewhat loosely in its active site compared to the WT. This could explain why the double mutant exhibited lower activity compared to the WT (Figure 3.4).

The inhibitory effect of IDP on various mutants can also be explained from the modeled structures. The C1 atom of IDP has hydrophobic interactions with both the methyl group of Ala-147 (4.5 Å; Figure 3.1) and the backbone carbon of Gly-146 (4.2 Å; Figure 3.1). Both of these residues help anchor the beginning of the carbon chain of IDP. Mutation of Ala-147 to Gly can lead to the sloppy binding of the beginning of the carbon chain of IDP resulting in inefficient binding of this inhibitor. This is exhibited by the poor inhibition of A147G*Pt*DXS by IDP compared to WT (Figure 3.5). The K_i value of A147G*Pt*DXS is ~1.7 and ~2.0 times higher for IDP and DMADP respectively than those of the WT. Interestingly, the increase in the K_i value of

A147G*Pt*DXS for IDP and DMADP is comparable to the increase in the K_m value for pyruvate (~1.9 times) but lower than the increase in the K_m value for ThDP (~2.5 times).

One of the terminal carbons of the carbon chain of IDP is very close to the methyl group of Ala-352 (3.7 Å; Figure 3.1). This particular terminal carbon of IDP, however, has other hydrophobic interactions with the side chain methyl group of Leu-179 (4.6 Å, 4.5 Å; Figure 3.1). The other terminal carbon of the carbon chain of IDP also has hydrophobic interactions with the side chain methyl group of Leu-179 (3.8 Å; Figure 3.1). Mutation of Ala-352 to Gly does not impair the binding of this terminal carbon of the carbon chain of IDP because of the presence of Leu-179 which can provide anchoring sites for the terminal carbons of IDP. On the other hand, this mutation may relieve the steric interaction between Ala-352 and the terminal carbon of IDP resulting in better binding of IDP and hence, more inhibition than the WT (Figure 3.5). The K_i value of A352G*Pt*DXS is ~0.6 (for IDP) and ~0.7 (for DMADP) times of those of the WT. This mutant is also found to have ~4.3 and ~2 times higher K_m values for ThDP and pyruvate respectively than those of the WT. Overall, the mutation of Ala-352 by Gly has made it a worse enzyme than the WT.

In the case of the double mutant A147G/A352G*Pt*DXS, both the beginning and the end of the carbon chain of IDP suffer from inefficient binding because of the loss of key interactions of the termini of IDP with the methyl groups of Ala-147 and Ala-352. Consequently, this double mutant was also found to have reduced inhibition by both IDP and DMADP. This explains ~1.2 and ~1.6 times higher K_i value of this mutant for IDP and DMDP respectively than those of the WT.

The residues Ala-147 and Ala-352, which have been mutated to glycine to improve the activity of the engineered *Pt*DXS, are well conserved in bacteria and plants as observed from the

amino acid sequence alignment of various DXS enzyme from a group of widely divergent bacteria and two plant species (Figure 3.8). It has been observed that Ala-352 of *Pt*DXS is completely conserved among all of these organisms. The absence of any natural mutation of this residue is evolutionary critical and indicates the importance of this residue in the catalytic activity of the enzyme. This is also supported by this work as the mutation of Ala-352 to Gly makes the engineered enzyme worse. *Deinococcus radiodurans* and *Desulfobacterium autotrophicum* have Ser instead of Ala at the corresponding position of Ala-147 of *Pt*DXS. The absence of any natural mutation of Ala-147 of *Pt*DXS to Gly underscores the importance of its engineering to Gly to improve its activity.

3.6 CONCLUSION

The overall goal for this work was engineering of *Pt*DXS by point mutation to improve its activity and future application of the engineered enzyme for biotechnological uses. The binding pattern of both the cofactor ThDP and the inhibitors IDP/DMADP renders the engineering of *Pt*DXS for avoiding the feedback regulation really challenging (Vickers *et al.* 2014). This study shows that it is possible to improve the DXS enzyme for future biotechnological applications. Appropriate metabolic engineering could help maintain the high levels of pyruvate and ThDP to maximize the performance enhancement of this mutation.

3.7 ACKNOWLEDGEMENTS

I would like to thank Michigan State University RTSF Mass Spectrometry Core for providing me the facility for doing the LC-MS/MS work.

3.8 NOTES

This material is based upon work supported by the National Science Foundation under Grant No. IOS-0950574 to TDS. Salary for TDS is provided in part by Michigan AgBioResearch. Any opinions, findings, and conclusions or recommendations expressed in this material are those of the authors and do not necessarily reflect the views of the National Science Foundation.

APPENDIX

TABLE 3.1 Kinetic constants of the mutant *Pt*DXS enzymes measured by LC-MS/MS-based assay. Each number represents the mean ± S. E. (n = 3). Kinetic constants were obtained from the non-linear curve fitting of the Michaelis-Menten plot in Origin.

	Substrate	Enzyme			
		WT	A147G	A352G	A147G/A352G
K_m (μM)	Pyruvate	105 ± 63	201 ± 47	208 ± 45	268 ± 71
	GAP	5 ± 1	5 ± 1	7 ± 1	5 ± 2
	ThDP	14 ± 8	35 ± 17	60 ± 32	59 ± 8
k_{cat} (s^{-1})	Pyruvate	0.15 ± 0.04	0.44 ± 0.03	0.32 ± 0.02	0.17 ± 0.02
	GAP	0.28 ± 0.03	0.55 ± 0.04	0.38 ± 0.04	0.17 ± 0.03
	ThDP	0.23± 0.03	0.48 ± 0.06	0.37 ± 0.05	0.18 ± 0.01

TABLE 3.2 The K_i and H values of IDP and DMADP for various mutants of *Pt*DXS. These values are determined from the IC_{50} curves shown in Figure 3.5. Each number represents the calculated value from the non-linear fitting of the IC_{50} curve ± S. E. (n = 3). Non-linear curve fitting was done as described in the previous work (Banerjee *et al.* 2013). (* values reported in the previous work (Banerjee *et al.* 2013))

*Pt*DXS	IDP		DMADP	
	K_i (μM)	*H*	K_i (μM)	*H*
WT	102 ± 0.7 *(65.4 ± 4.3)*	1.02 ± 0.01 *(0.69 ± 0.03)*	156 ± 18 *(81.3 ± 10.5)*	0.67 ± 0.09 *(0.61 ± 0.06)*
A147G	177 ± 11	0.59 ± 0.04	319 ± 109	0.51 ± 0.17
A352G	65 ± 0.03	1.07 ± 0.001	104 ± 0.4	0.98 ± 0.004
A47G/A352G	125 ± 1	0.89 ± 0.01	253 ± 46	1.14 ± 0.29

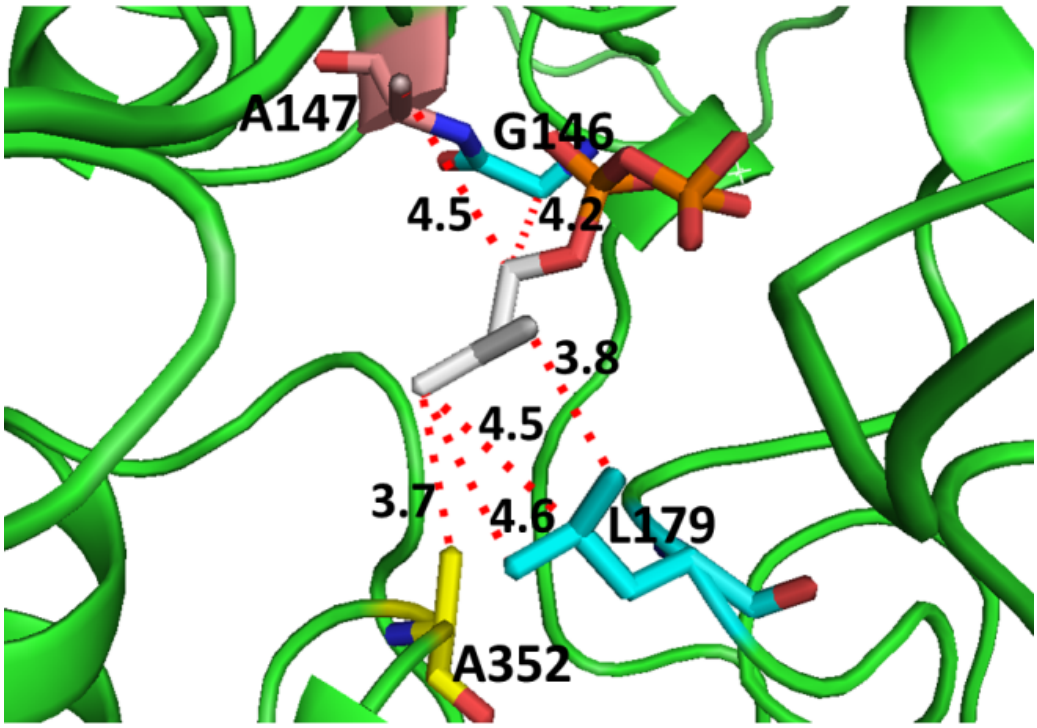

FIGURE 3.1 Cartoon view of the interactions of different residues of WT*Pt*DXS with IDP and their relevant distances from the carbon chain of IDP. The image was produced in PyMol (The PyMOL Molecular Graphics System, Schrödinger, LLC).

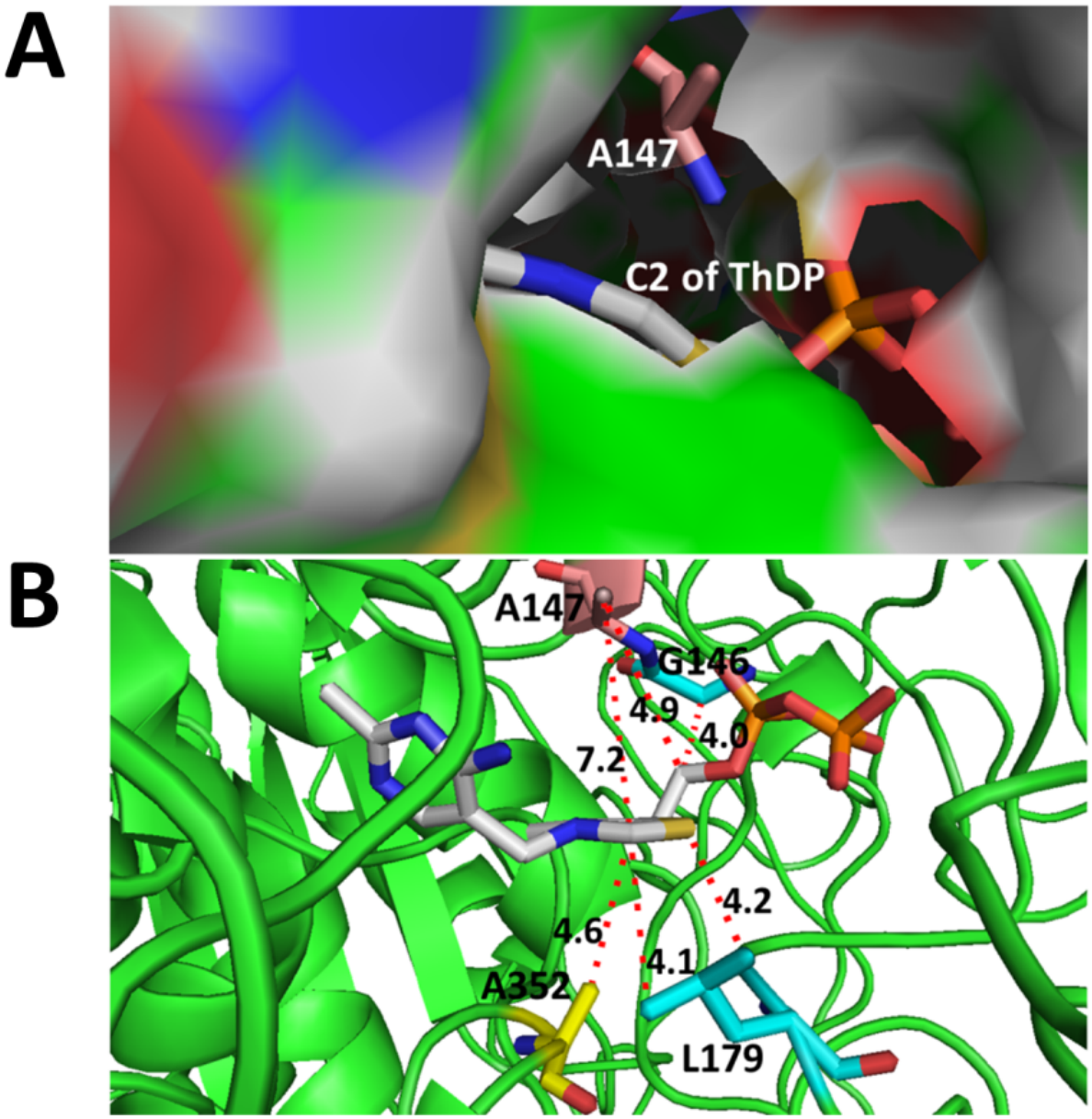

FIGURE 3.2 A. Zoomed in surface view of the orientation of Ala-147 residue of WT*Pt*DXS and the thiazolium ring of ThDP in the enzyme active site. B. Cartoon view of the interactions of different residues of WT*Pt*DXS with ThDP and their relevant distances from the thiazolium ring and the carbon chain of ThDP. The image was produced in PyMol (The PyMOL Molecular Graphics System, Schrödinger, LLC).

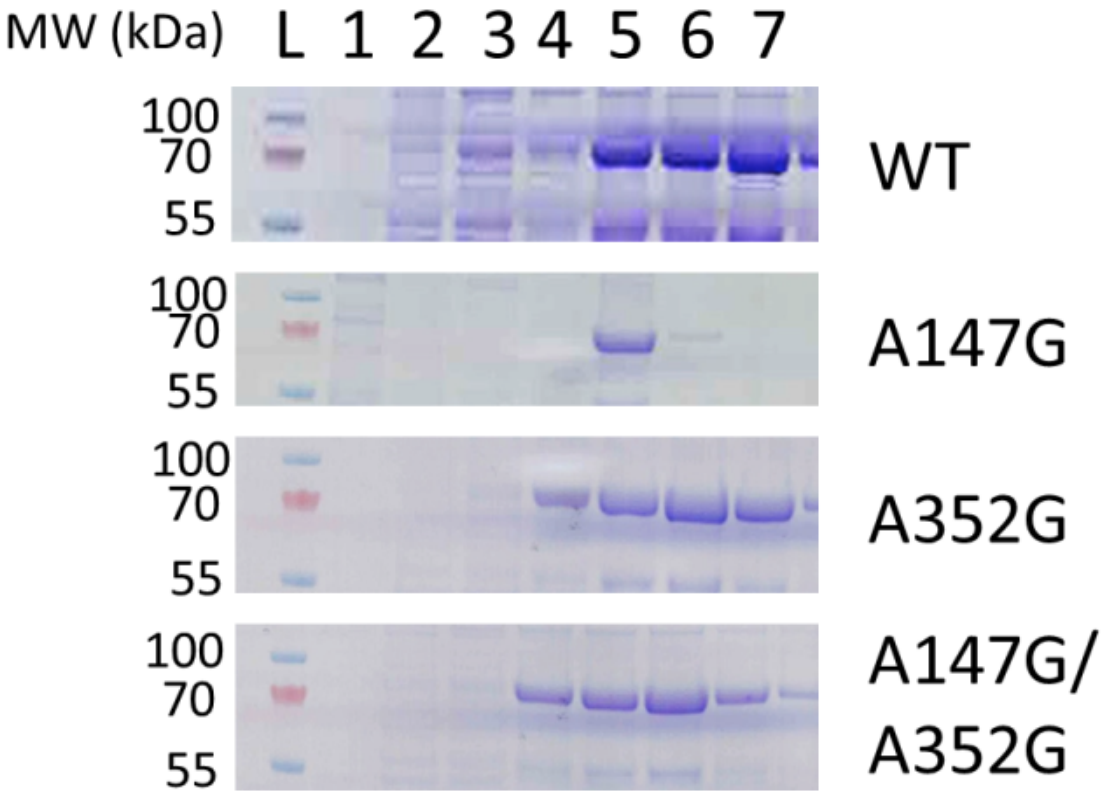

FIGURE 3.3 SDS-PAGE of the different fractions from the Ni-NTA column purification of recombinant WT and the various mutants of *Pt*DXS. For WT panel, lane 1-3: elution fraction containing 50 mM imidazole; lane 4-5: elution fraction containing 100 mM imidazole; lane 6-7: elution fraction containing 150 mM imidazole. For A147G panel, lane 1: flow-through; lane 2- 4: wash fraction containing 10 mM imidazole; lane 5-6: elution fraction containing 250 mM imidazole, lane 7: blank. For A352G panel and A147G/A352G panel, lane 1-2: elution fraction containing 50 mM imidazole; lane 3-4: elution fraction containing 100 mM imidazole; lane 5-6: elution fraction containing 150 mM imidazole; lane 7: elution fraction containing 200 mM imidazole. L: protein marker. The molecular weight of WT and all the mutant enzymes is ~73 kDa.

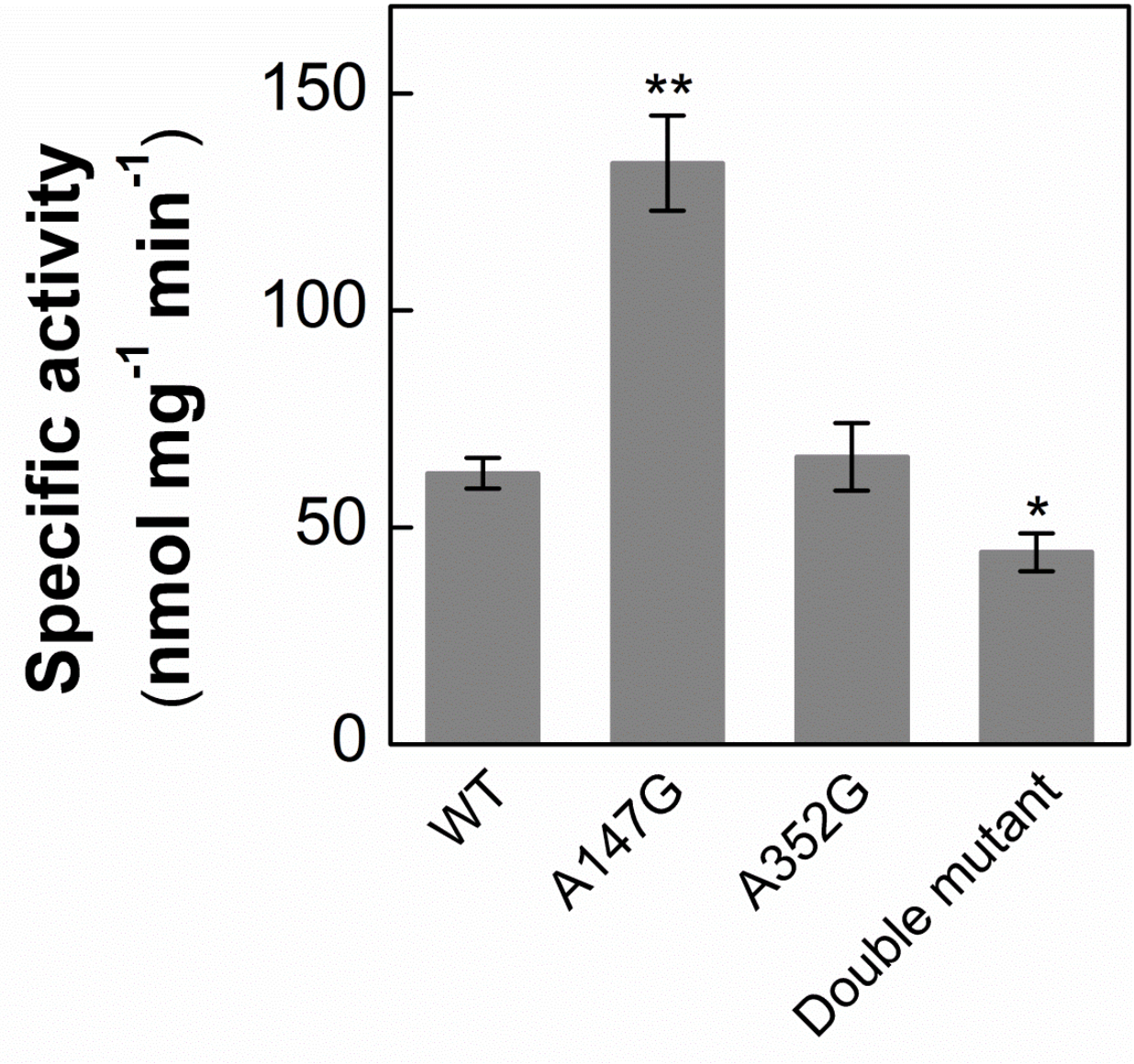

FIGURE 3.4 Comparison of the specific activity of WT and various mutants of *Pt*DXS based on LC-MS/MS based assay. Each bar represents mean, error bars represent S.E. (n = 3). A147G*Pt*DXS showed highest activity among all of them. Data with an asterisk (*) are significantly different from WT as determined by Student's *t*-test. (*P < 0.05 and **P < 0.01).

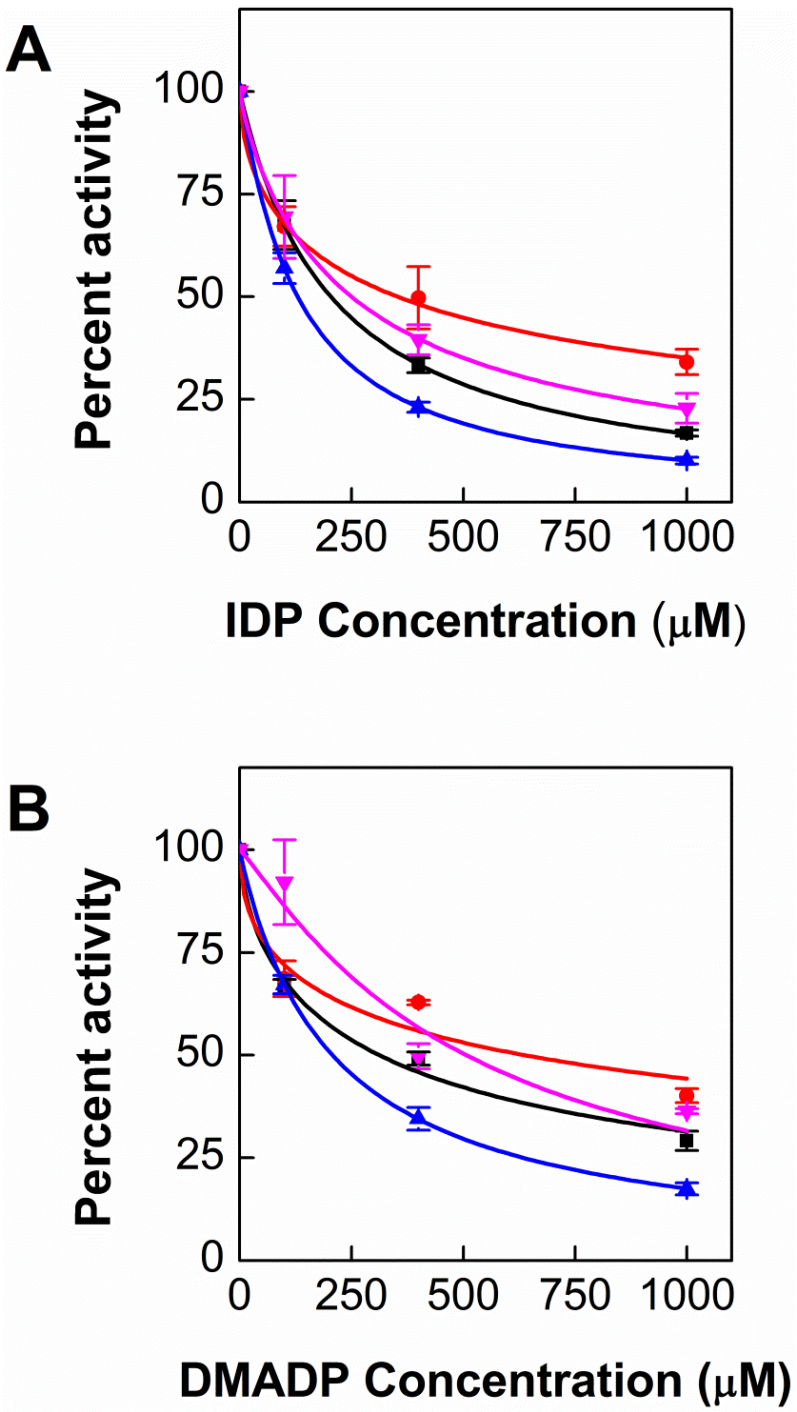

FIGURE 3.5 Effect of IDP (A) and DMADP (B) on different mutants of *Pt*DXS. Each data point represents mean, error bars represent S.E. (n = 3). Different symbols represent the experimental data points. The solid lines represent the fitted IC_{50} curves. Black, red, blue, and pink represent the activity of WT, A147G, A352G and A147G/A352G*Pt*DXS respectively. A147G*Pt*DXS showed least inhibition by both IDP and DMADP.

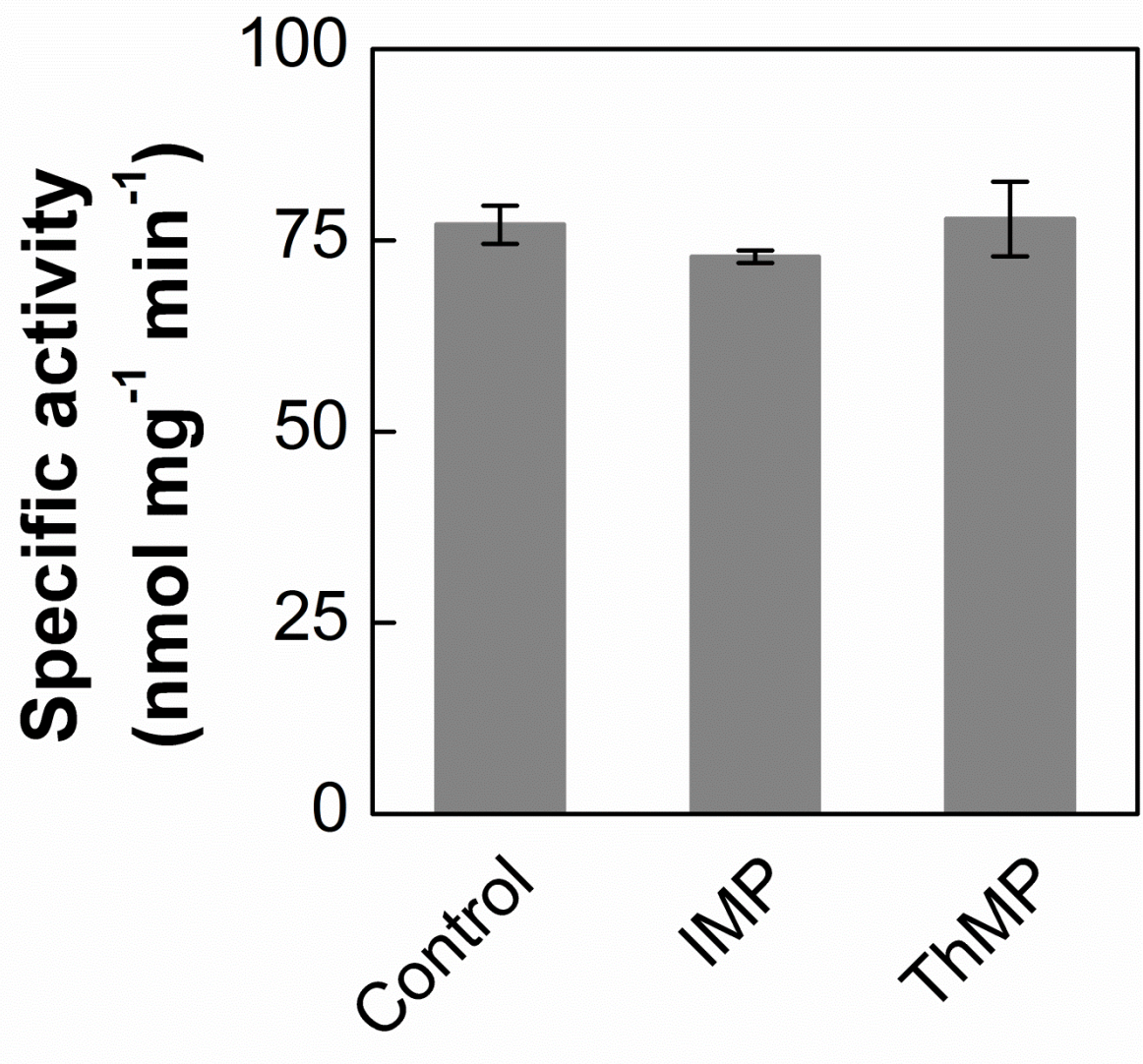

FIGURE 3.6 Effect of monophosphate containing metabolites on WT*Pt*DXS activity based on the LC-MS/MS based assay. Each bar represents mean, error bars represent S.E. (n = 3). None of these monophosphates showed any significant effect on WT*Pt*DXS activity. IMP, isopentenyl monophosphate; TMP, thiamin monophosphate.

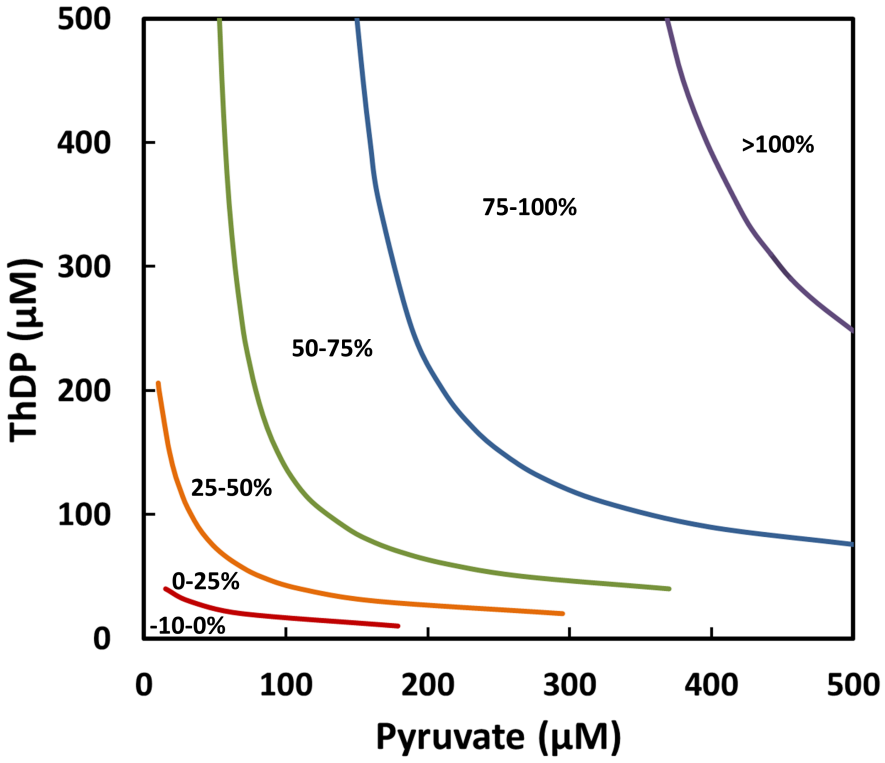

Figure 3.7 Analysis of the difference of rate of A147G*Pt*DXS relative to WT*Pt*DXS. The activity of A147G*Pt*DXS was compared relative to WT*Pt*DXS in presence of various concentrations of pyruvate, ThDP and concentrations of IDP and DMADP found in *E. coli;* IDP: 0.3 µM; DMADP: 0.7 µM. The difference in rate of mutant with respect to the WT was calculated as described in section 3.3.6. At very low substrate concentrations the mutant enzyme has a lower predicted activity (< 0%, lower left corner). At modest to high concentration of pyruvate or ThDP the mutant enzyme has a higher predicted rate, exceeding 100% stimulation in the upper right corner. Each isoline represents the border of the indicated improvement in activity of the mutant relative to WT.

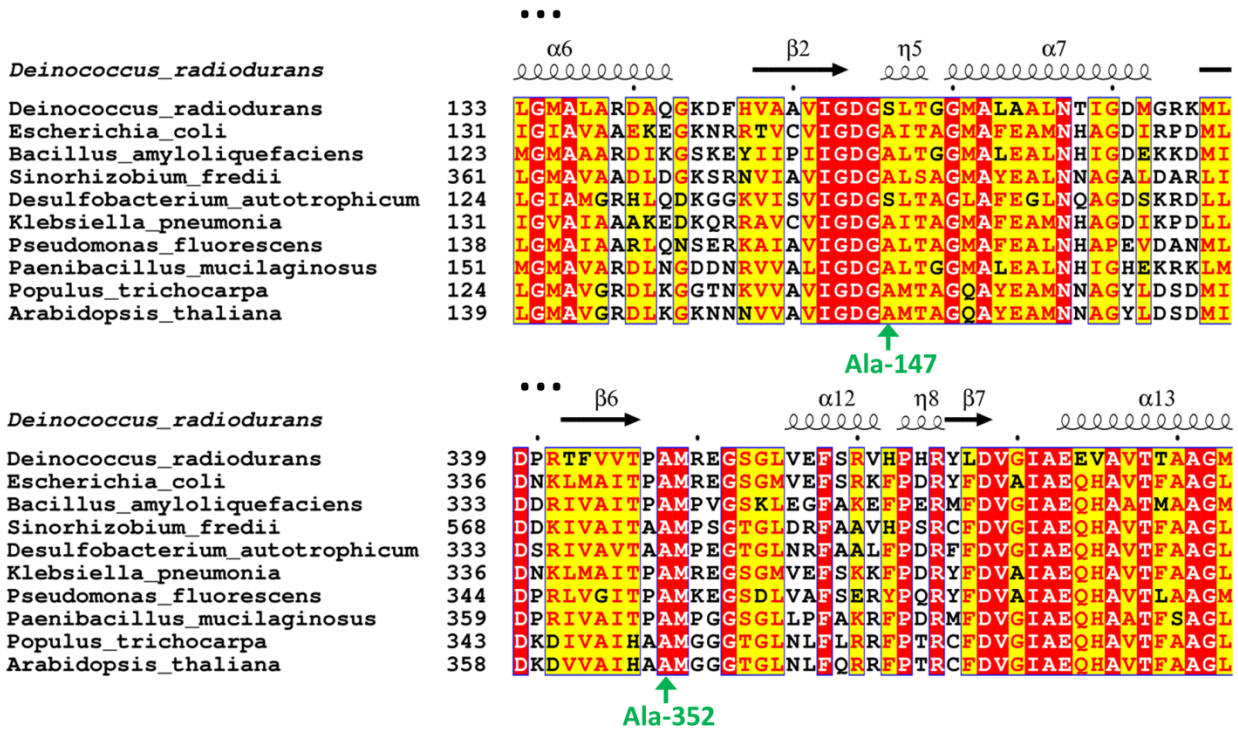

FIGURE 3.8 Excerpt from amino acid sequence alignment of DXS from a group of widely divergent bacteria and two plant species. The secondary structure elements of *D. radiodurans* enzyme are indicated on the top of the sequences. Conserved and similar residues are highlighted in red and yellow box respectively. The two Ala residues mutated in *Pt*DXS are indicated by green arrow. The sequence alignment has been generated using ESPript online server (Robert & Gouet 2014).

LITERATURE CITED

LITERATURE CITED

Albrecht M., Misawa N. & Sandmann G. (1999) Metabolic engineering of the terpenoid biosynthetic pathway of *Escherichia coli* for production of the carotenoids β-carotene and zeaxanthin. *Biotechnology Letters*, **21**, 791-795.

Banerjee A. & Sharkey T.D. (2014) Methylerythritol 4-phosphate (MEP) pathway metabolic regulation. *Natural Product Reports*, **31**, 1043-1055.

Banerjee A., Wu Y., Banerjee R., Li Y., Yan H. & Sharkey T.D. (2013) Feedback inhibition of deoxy-D-xylulose-5-phosphate synthase regulates the methylerythritol 4-phosphate pathway. *Journal of Biological Chemistry*, **288**, 16926-16936.

Brammer Basta L.A., Patel H., Kakalis L., Jordan F. & Freel Meyers C.L. (2014) Defining critical residues for substrate binding to 1-deoxy-D-xylulose 5-phosphate synthase – active site substitutions stabilize the predecarboxylation intermediate C2α-lactylthiamin diphosphate. *FEBS Journal*, **281**, 2820-2837.

Brammer L.A., Smith J.M., Wade H. & Meyers C.F. (2011) 1-Deoxy-D-xylulose 5-phosphate synthase catalyzes a novel random sequential mechanism. *Journal of Biological Chemistry*, **286**, 36522-36531.

Cordoba E., Salmi M. & León P. (2009) Unravelling the regulatory mechanisms that modulate the MEP pathway in higher plants. *Journal of Experimental Botany*, **60**, 2933-2943.

Eisenreich W., Schwarz M., Cartayrade A., Arigoni D., Zenk M.H. & Bacher A. (1998) The deoxyxylulose phosphate pathway of terpenoid biosynthesis in plants and microorganisms. *Chemistry & Biology*, **5**, R221-R233.

Enfissi E.M.A., Fraser P.D., Lois L.M., Boronat A., Schuch W. & Bramley P.M. (2005) Metabolic engineering of the mevalonate and non-mevalonate isopentenyl diphosphate-forming pathways for the production of health-promoting isoprenoids in tomato. *Plant Biotechnology Journal*, **3**, 17-27.

Estévez J.M., Cantero A., Reindl A., Reichler S. & León P. (2001) 1-Deoxy-D-xylulose-5-phosphate synthase, a limiting enzyme for plastidic isoprenoid biosynthesis in plants. *Journal of Biological Chemistry*, **276**, 22901-22909.

Eubanks L.M. & Poulter C.D. (2003) *Rhodobacter capsulatus* 1-deoxy-D-xylulose 5-phosphate synthase: steady-state kinetics and substrate binding. *Biochemistry*, **42**, 1140-1149.

Farmer W.R. & Liao J.C. (2001) Precursor balancing for metabolic engineering of lycopene production in *Escherichia coli*. *Biotechnology Progress*, **17**, 57-61.

Ghirardo A., Wright L.P., Bi Z., Rosenkranz M., Pulido P., Rodríguez-Concepción M., Niinemets Ü., Brüggemann N., Gershenzon J. & Schnitzler J.-P. (2014) Metabolic flux analysis of plastidic isoprenoid biosynthesis in poplar leaves emitting and non-emitting isoprene. *Plant Physiology*, **165**, 37-51.

Guevara-García A., Román C.S., Arroyo A., Cortés M., Gutiérrez-Nava M.d.l.L. & León P. (2005) Characterization of the Arabidopsis *clb6* mutant illustrates the importance of posttranscriptional regulation of the methyl-D-erythritol 4-phosphate pathway. *The Plant Cell*, **17**, 628-643.

Harker M. & Bramley P.M. (1999) Expression of prokaryotic 1-deoxy-D-xylulose-5-phosphatases in *Escherichia coli* increases carotenoid and ubiquinone biosynthesis. *FEBS Letters*, **448**, 115-119.

Hemmerlin A., Hoeffler J.-F., Meyer O., Tritsch D., Kagan I.A., Grosdemange-Billiard C., Rohmer M. & Bach T.J. (2003) Cross-talk between the cytosolic mevalonate and the plastidial methylerythritol phosphate pathways in tobacco bright yellow-2 cells. *Journal of Biological Chemistry*, **278**, 26666-26676.

Huang Q., Roessner C.A., Croteau R. & Scott A.I. (2001) Engineering *Escherichia coli* for the synthesis of taxadiene, a key intermediate in the biosynthesis of taxol. *Bioorganic and Medicinal Chemistry*, **9**, 2237-2242.

Kajiwara S., Fraser P.D., Kondo K. & Misawa N. (1997) Expression of an exogenous isopentenyl diphosphate isomerase gene enhances isoprenoid biosynthesis in *Escherichia coli*. *Biochemical Journal*, **324**, 421-426.

Kim S.W. & Keasling J.D. (2001) Metabolic engineering of the nonmevalonate isopentenyl diphosphate synthesis pathway in *Escherichia coli* enhances lycopene production. *Biotechnology and Bioengineering*, **72**, 408-415.

Klein-Marcuschamer D., Ajikumar P.K. & Stephanopoulos G. (2007) Engineering microbial cell factories for biosynthesis of isoprenoid molecules: beyond lycopene. *Trends in Biotechnology*, **25**, 417-424.

Lichtenthaler H.K. (1999) The 1-Deoxy-D-xylulose-5-phosphate pathway of isoprenoid biosynthesis in plants. *Annual Review Plant Physiology Plant Molecular Biology*, **50**, 47-65.

Lichtenthaler H.K., Rohmer M. & Schwender J. (1997) Two independent biochemical pathways for isopentenyl diphosphate and isoprenoid biosynthesis in higher plants. *Physiologia Plantarum*, **101**, 643-652.

Lois L.M., Rodríguez-Concepción M., Gallego F., Campos N. & Boronat A. (2000) Carotenoid biosynthesis during tomato fruit development: regulatory role of 1-deoxy-D-xylulose 5-phosphate synthase. *Plant Journal*, **22**, 503-513.

Martin V.J., Pitera D.J., Withers S.T., Newman J.D. & Keasling J.D. (2003) Engineering a mevalonate pathway in *Escherichia coli* for production of terpenoids. *Nature Biotechnology*, **21**, 796-802.

Martin V.J., Yoshikuni Y. & Keasling J.D. (2001) The in vivo synthesis of plant sesquiterpenes by *Escherichia coli*. *Biotechnology and Bioengineering*, **75**, 497-503.

Matthews P.D. & Wurtzel E.T. (2000) Metabolic engineering of carotenoid accumulation in *Escherichia coli* by modulation of the isoprenoid precursor pool with expression of deoxyxylulose phosphate synthase. *Applied Microbiology and Biotechnology*, **53**, 396-400.

Maury J., Asadollahi M.A., Moller K., Clark A. & Nielsen J. (2005) Microbial isoprenoid production: an example of green chemistry through metabolic engineering. *Advances in Biochemical Engineering/Biotechnology*, **100**, 19-51.

Miller B., Heuser T. & Zimmer W. (2000) Functional involvement of a deoxy-D-xylulose 5-phosphate reductoisomerase gene harboring locus of *Synechococcus leopoliensis* in isoprenoid biosynthesis. *FEBS Letters*, **481**, 221-226.

Misawa N. (2011) Pathway engineering for functional isoprenoids. *Current Opinion in Biotechnology*, **22**, 627-633.

Morris W.L., Ducreux L.J.M., Hedden P., Millam S. & Taylor M.A. (2006) Overexpression of a bacterial 1-deoxy-D-xylulose 5-phosphate synthase gene in potato tubers perturbs the isoprenoid metabolic network: implications for the control of the tuber life cycle. *Journal of Experimental Botany*, **57**, 3007-3018.

Patel H., Nemeria N.S., Brammer L.A., Freel Meyers C.L. & Jordan F. (2012) Observation of thiamin-bound intermediates and microscopic rate constants for their interconversion on 1-deoxy-D-xylulose 5-phosphate synthase: 600-fold rate acceleration of pyruvate decarboxylation by D-glyceraldehyde-3-phosphate. *Journal of the American Chemical Society*, **134**, 18374-18379.

Phillips M.A., León P., Boronat A. & Rodríguez-Concepción M. (2008) The plastidial MEP pathway: unified nomenclature and resources. *Trends in Plant Science*, **13**, 619-623.

Reiling K.K., Yoshikuni Y., Martin V.J., Newman J., Bohlmann J. & Keasling J.D. (2004) Mono and diterpene production in *Escherichia coli*. *Biotechnology and Bioengineering*, **87**, 200-212.

Robert X. & Gouet P. (2014) Deciphering key features in protein structures with the new ENDscript server. *Nucleic Acids Res*, **42**, W320-W324.

Roberts S.C. (2007) Production and engineering of terpenoids in plant cell culture. *Nature Chemical Biology*, **3**, 387-395.

Rodríguez-Concepción M. (2006) Early steps in isoprenoid biosynthesis: multilevel regulation of the supply of common precursors in plant cells. *Phytochemistry Reviews*, **5**, 1-15.

Rodríguez-Concepción M. & Boronat A. (2002) Elucidation of the methylerythritol phosphate pathway for isoprenoid biosynthesis in bacteria and plastids. A metabolic milestone achieved through genomics. *Plant Physiology*, **130**, 1079-1089.

Rohmer M. (1999) The discovery of a mevalonate-independent pathway for isoprenoid biosynthesis in bacteria, algae and higher plants. *Natural Product Reports*, **16**, 565-574.

Rude M.A. & Schirmer A. (2009) New microbial fuels: a biotech perspective. *Current Opinion in Microbiology*, **12**, 274-281.

Vickers C.E., Bongers M., Liu Q., Delatte T. & Bouwmeester H. (2014) Metabolic engineering of volatile isoprenoids in plants and microbes. *Plant, Cell and Environment*, **37**, 1753-1775.

Volkmer B. & Heinemann M. (2011) Condition-dependent cell volume and concentration of *Escherichia coli* to facilitate data conversion for systems biology modeling. *PLoS One*, **6**, e23126.

Wang C., Oh M.K. & Liao J.C. (2000) Directed evolution of metabolically engineered *Escherichia coli* for carotenoid production. *Biotechnology Proggress*, **16**, 922-926.

Wang C.W., Oh M.K. & Liao J.C. (1999) Engineered isoprenoid pathway enhances astaxanthin production in *Escherichia coli*. *Biotechnoogy and Bioengineering*, **62**, 235-241.

Wiberley A.E., Donohue A.R., Westphal M.M. & Sharkey T.D. (2009) Regulation of isoprene emission from poplar leaves throughout a day. *Plant, Cell and Environment*, **32**, 939-947.

Wright L.P., Rohwer J.M., Ghirardo A., Hammerbacher A., Ortiz-Alcaide M., Raguschke B., Schnitzler J.P., Gershenzon J. & Phillips M.A. (2014) Deoxyxylulose 5-phosphate synthase controls flux through the methylerythritol 4-phosphate pathway in Arabidopsis. *Plant Physiology*, **165**, 1488-1504.

Xiang S., Usunow G., Lange G., Busch M. & Tong L. (2007) Crystal structure of 1-deoxy-D-xylulose 5-phosphate synthase, a crucial enzyme for isoprenoids biosynthesis. *Journal of Biological Chemistry*, **282**, 2676-2682.

Yuan L.Z., Rouviere P.E., Larossa R.A. & Suh W. (2006) Chromosomal promoter replacement of the isoprenoid pathway for enhancing carotenoid production in *E. coli*. *Metabolic Engineering*, **8**, 79-90.

Zhou C., Li Z., Wiberley-Bradford A.E., Weise S.E. & Sharkey T.D. (2013) Isopentenyl diphosphate and dimethylallyl diphosphate/isopentenyl diphosphate ratio measured with

recombinant isopentenyl diphosphate isomerase and isoprene synthase. *Analytical Biochemistry*, **440**, 130-136.

CHAPTER 4

Methylerythritol 4-phosphate (MEP) pathway metabolic regulation

Part of this chapter was adapted from the following manuscript.
[Banerjee, A., and Sharkey, T. D. (2014) Methylerythritol 4-phosphate (MEP) pathway metabolic regulation. *Natural Product Reports* **31**, 1043-1055] - Reproduced by permission of The Royal Society of Chemistry

4.1 SUMMARY

The methylerythritol 4-phosphate (MEP) pathway is the recently discovered source of isoprenoid precursors isopentenyl diphosphate and dimethylallyl diphosphate in most bacteria, some eukaryotic parasites, and the plastids of plant cells. The precursors lead to the formation of various isoprenoids having diverse roles in different biological processes. Some isoprenoids have important commercial uses. Isoprene, which is made in surprising abundance by some trees, plays a significant role in atmospheric chemistry. The genetic regulation of this pathway has been discussed but information about metabolic regulation is just now becoming available. This review covers metabolic regulation of the MEP pathway starting from the inputs of carbon, ATP, and reducing power. A number of different regulatory mechanisms involving intermediate metabolites and/or enzymes are discussed. Some recent data indicate that methylerythritol cyclodiphosphate, the fifth intermediate of this pathway, is a key metabolite. It has been found to play diverse roles in regulation within the pathway as well as coordinating other biological processes by acting as a stress regulator in bacteria and possibly a retrograde signal from plastids to the nucleus in plants. In this review we focus on the role of the MEP pathway in photosynthetic leaves during isoprene emission and more generally the metabolic regulation of the MEP pathway in both plants and bacteria.

(Covering up to February, 2014)

4.2 INTRODUCTION

Isoprenoids are the most abundant secondary metabolites present in all living organisms including both prokaryotes and eukaryotes (Lohr *et al.* 2012; Wanke *et al.* 2001). They are the largest group of natural products having various roles in primary metabolism as well as secondary biological processes (Hemmerlin *et al.* 2003; Hunter 2007; Phillips *et al.* 2008; Sacchettini & Poulter 1997; Wanke *et al.* 2001). In addition to various biological roles, some isoprenoids have commercial applications as pigments, fragrance and flavors, drugs, and polymers (Rodríguez-Concepción 2006).

In terms of total production, the most important isoprenoid is isoprene, the smallest member of isoprenoid family. Isoprene is emitted by many organisms including bacteria, plants, and humans and contributes to a large flux of hydrocarbon entering into the atmosphere. A few plants, mainly certain species of pine trees (e.g., lodgepole, ponderosa) in the western part of North America (Ferronato *et al.* 1998; Gray *et al.* 2011; Harley *et al.* 1998; Lerdau & Gray 2003) also produce the related compound 2-methyl-3-buten-2-ol (methylbutenol or MBO) (Goldan *et al.* 1993). Atmospheric chemistry is strongly affected by these hemiterpenes emitted by vegetation. In this regard, an important target for environmental chemists is to build up an effective model for the prediction of global annual isoprene-emission.

In spite of the functional diversity, all isoprenoids except isoprene are derived from two isomeric five-carbon units called isopentenyl diphosphate (IDP) and dimethylallyl diphosphate (DMADP) (Cordoba *et al.* 2009; Eisenreich *et al.* 1998). These compounds are also known as pyrophosphates but diphosphate is the IUPAC-preferred term. Isoprene itself is made from DMADP (Silver & Fall 1991; Silver & Fall 1995). Both IDP and DMADP are synthesized by the

2-*C*-methyl-D-erythritol 4-phosphate (MEP) pathway. For a long time it was believed that the acetate/mevalonate (MVA) pathway is the only route for the biosynthesis of IDP (Eisenreich *et al.* 1998). However, the alternative MEP pathway for the biosynthesis of both IDP and DMADP was discovered in bacteria (Eisenreich *et al.* 1998; Rohmer *et al.* 1993; Rohmer *et al.* 1996), followed by its discovery in plastids of green algae and higher plants (Arigoni *et al.* 1997; Eisenreich *et al.* 1996; Lichtenthaler *et al.* 1997a; Lichtenthaler *et al.* 1997b; Schwender *et al.* 1996; Schwender *et al.* 1997; Zeidler *et al.* 1997). The MEP pathway is absent in humans, but higher plants have both the MEP and the MVA pathway operative in the chloroplast and cytoplasm respectively (Hemmerlin *et al.* 2003).

The MEP pathway is composed of seven enzymatic steps, which have been described in detail in Chapter 1. Figure 4.1, in this chapter, depicts the schematic of these various steps involved in the MEP pathway. The alternative names of the various enzymes of this pathway are also summarized in Figure 4.1.

The MEP pathway was originally known as non-mevalonate pathway or Rohmer pathway (Rodríguez-Concepción & Boronat 2002; Rohdich *et al.* 2001; Rohmer 1999; Rohmer *et al.* 1996). The discovery of the first step of this pathway involving the formation 1-deoxy-D-xylulose 5-phosphate (DXP) from pyruvate and glyceraldehyde-3-phosphate (GAP) led to the name of the DXP pathway or pyruvate/glyceraldehyde-3-phosphate pathway (Rodríguez-Concepción & Boronat 2002). DXP is, however, found to be a precursor for the biosynthesis of thiamin and pyridoxal (Lois *et al.* 1998; Rodríguez-Concepción & Boronat 2002; Sprenger *et al.* 1997). The second intermediate MEP, on the other hand, contains the characteristic branched C5 skeleton for all isoprenoids and is so far not known to be involved in other biochemical pathways (Rohmer 2003). Thus MEP is considered to be the first committed intermediate of this pathway

and the name of this pathway is widely accepted as MEP pathway (Rodríguez-Concepción & Boronat 2002; Rohmer 2003).

Numerous commercial applications of different isoprenoids and the limited availability from their natural sources make them important targets for biotechnological manipulation (Cordoba *et al.* 2009; DellaPenna & Posgon 2006; Misawa 2011). In this regard, it is critical to understand the regulation of the MEP pathway responsible for the biosynthesis of their building blocks. The genetic regulation of the MEP pathway has been reviewed extensively (Cordoba *et al.* 2009; Rodríguez-Concepción 2006; Vranova *et al.* 2013). A recent review has discussed the mechanistic details of the enzymes involved in this pathway (Zhao *et al.* 2013). A short account of the regulation involved in the metabolomics of the MEP pathway has also been recently discussed (Chang *et al.* 2013). Here I emphasize the discoveries that have been made in the past ten years regarding the regulation of MEP pathway based on enzymatic activity and metabolites involved in the pathway. Insights into the metabolic regulation of the MEP pathway can be beneficial for biomedical and biotechnological purposes. In this review I provide some examples of how improved understanding of the MEP pathway may improve models of global isoprene emission.

4.3 REGULATION OF INPUTS INTO THE PATHWAY

Metabolic regulation of the MEP pathway is dictated by the source of carbon and energetic cofactors. Intensive research has been carried out in the past few years to understand how the carbon flux contributes to the regulation of this pathway. Earlier studies were mainly done by

observing the pattern of labeled isoprene emission after feeding $^{13}CO_2$ or deuterated deoxyxylulose, the isotopic composition of isoprene being an indicator of the carbon source of DMADP and hence the MEP pathway (Affek & Yakir 2003; Delwiche & Sharkey 1993; Karl *et al.* 2002b; Kreuzwieser *et al.* 2002; Kühnemann *et al.* 2002; Loreto *et al.* 1996; Loreto *et al.* 2004; Schnitzler *et al.* 2004). The effect of the availability of carbon, ATP, and reducing power equivalents on the metabolomics of the MEP pathway are summarized here.

4.3.1 Carbon supply

Results from early studies involving the incorporation of ^{13}C-labeled precursors into terpenoids were inconsistent with acetate as the starting compound (Eisenreich *et al.* 2001; Eisenreich *et al.* 1998; Rohmer *et al.* 1993). Later studies showed that the MEP pathway starts with the synthesis of DXP from GAP and pyruvate catalyzed by DXS (Bouvier *et al.* 1998; Kuzuyama *et al.* 2000; Lange *et al.* 1998; Lois *et al.* 1998; Miller *et al.* 1999; Rohmer *et al.* 1996; Sprenger *et al.* 1997). The supply of GAP and pyruvate for the MEP pathway in bacteria can be maintained through primary metabolism and so will not be considered here. The source of GAP and pyruvate for the MEP pathway in chloroplasts of plants is potentially more complex (Figure 4.2).

When $^{13}CO_2$ is fed to photosynthesizing plant leaves, isoprene rapidly becomes labeled confirming the close relationship between isoprene synthesis and the Calvin-Benson cycle (Brilli *et al.* 2007; Delwiche & Sharkey 1993; Ferrieri *et al.* 2005; Karl *et al.* 2002b; Sanadze *et al.* 1972). Sugars transported in the xylem can provide additional carbon for leaf isoprene biosynthesis through MEP pathway (Kreuzwieser *et al.* 2002; Schnitzler *et al.* 2004). Isoprene

does not become completely labeled when $^{13}CO_2$ is fed, but, for reasons not yet known, the intermediates of the Calvin-Benson cycle also do not become fully labeled over short time frames (Atkins & Canvin 1971; Szecowka *et al.* 2013), thus isoprene labeling kinetics may be fully consistent with all of the carbon for isoprene coming from the Calvin-Benson cycle (Delwiche & Sharkey 1993). However, analysis of the fragments of isoprene in mass spectrometry studies have been interpreted to indicate a slightly slower labeling of carbon atoms derived from pyruvate (Karl *et al.* 2002b; Trowbridge *et al.* 2012).

There are several sources of chloroplastic pyruvate for the MEP pathway. A small amount of pyruvate is produced by Rubisco through β-elimination of phosphate from a carbocation intermediate of the Rubisco reaction (Andrews & Kane 1991). The ratio of pyruvate produced by carboxylation of ribulose bisphosphate is 0.7% at 25 °C. One pyruvate leads to the loss of five carbons as isoprene. Therefore, Rubisco production of pyruvate could support carbon loss as isoprene at a rate of 3.5% (0.7% times five carbons in isoprene) of carbon assimilation and as much as 4.3% if photorespiration, which makes the rate of CO_2 assimilation smaller than the rate of carboxylation, is considered. Carbon loss as a result of isoprene emission in excess of 3.5 to 4.3% of photosynthetically fixed carbon would require pyruvate from other carbon sources.

Pyruvate cannot be directly synthesized from 3-phosphoglycerate inside the chloroplast of mesophyll cells mainly because of the absence of the glycolytic enzymes phosphoglyceromutase and enolase (Bagge & Larsson 1986; Prabhakar *et al.* 2009; Stitt & Rees 1979). The activity of these enzymes inside plastids are observed only in the developing embryos in Arabidopsis (Andriotis *et al.* 2010). A feasible route could be the transport of phospho*enol*pyruvate (PEP) produced by glycolysis in the cytosol into the chloroplast involving a phospho*enol*pyruvate/phosphate translocator (PPT) followed by the synthesis of pyruvate from

PEP by pyruvate kinase inside the chloroplast (Fischer *et al.* 1997; Flügge 1999). It is known that the chloroplast of photosynthesizing leaves is dependent on the cytosol for PEP (but not necessarily pyruvate) (Voll *et al.* 2003).

There is evidence for the presence of plastidic pyruvate kinase (PK_p) in different heterotrophic tissues, e.g. leucoplast pyruvate kinase has been purified and characterized from developing castor bean (*Ricinus communis*) endosperm, *Brassica napus* (Rapeseed) suspension cells, and plastidic pyruvate kinase complex has been purified and characterized from the developing seeds of Arabidopsis (Andre *et al.* 2007; Negm *et al.* 1995; Plaxton *et al.* 1990; Plaxton *et al.* 2002). Isoenzymes of pyruvate kinase from green leaves of castor bean and etiolated leaves of pea plants have been separated by ion filtration chromatography and one of the isoenzymes is located in the plastid (Ireland *et al.* 1979). Considering the use of pyruvate in other metabolic pathways inside the chloroplast (e.g. fatty acid biosynthesis), it is highly likely that a plastidic pyruvate kinase exists.

Recently, a plastidial sodium-dependent pyruvate transporter, BASS2, has been discovered (Furumoto *et al.* 2011). It has been observed abundantly in C_4 plant species and in considerable amount in C_3/C_4 intermediate species. The authors showed that an Arabidopsis BASS2 orthologue is mainly observed in developing leaves and is thought to provide pyruvate for the MEP pathway in developing leaves (Furumoto *et al.* 2011). Chloroplastic pyruvate obtained from imported cytosolic PEP is important for the MEP pathway in a fully expanded leaf when the isoprene emission occurs in its full capacity (Sharkey *et al.* 2008; Wiberley *et al.* 2005).

The suppression of isoprene emission and DMADP content under high CO_2 concentration has been hypothesized to be due to the competition for PEP by cytosolic PEP carboxylase over the transport of PEP from cytosol to chloroplast (Rosenstiel *et al.* 2003). However, this

hypothesis has been challenged (Li & Sharkey 2013b; Rasulov *et al.* 2009b). Rasulov *et al.* concluded that the variation of isoprene emission with CO_2 concentration depends on the regulation of the synthesis of DMADP by energetic cofactors instead of the carbon availability. In addition, there is now evidence that CO_2-suppression is eliminated at 30 °C and above (Potosnak *et al.* 2014; Rasulov *et al.* 2010; Sharkey & Monson 2014; Sun *et al.* 2013).

4.3.2 Input of reducing power

Several enzymatic steps of the MEP pathway need reducing power. DXR, the second enzyme of the MEP pathway uses NADPH for reducing power (Proteau 2004). It is likely that NADPH is obtained from the photosynthetic electron transport chain in phototrophic organisms. This helps explain the lack of isoprene emission in the darkness, when NADPH from photosynthesis is not available. A post-illumination isoprene burst is often observed in oak and poplar leaves (Li *et al.* 2011). It has been suggested that this burst results from NADPH supplied by the oxidative branch of the pentose phosphate pathway in darkness (Li & Sharkey 2013a) but other mechanisms are possible. It has also been suggested that the dark isoprene emission from the aspen leaves could arise from the pool of phosphorylated intermediates of the MEP pathway when the required energetics (ATP and NADPH) are available through the chloroplastic glycolysis or chlororespiration (Rasulov *et al.* 2011).

Both 4-hydroxy-3-methylbut-2-enyl diphosphate (HMBDP) synthase (HDS) and HMBDP reductase (HDR), the last two enzymes of the MEP pathway, have [4Fe-4S] clusters and involve double one-electron transfers in their catalytic reaction mechanism (Seemann & Rohmer 2007). It has been observed that in presence of light the HDS/GcpE from Arabidopsis obtain the

required electrons from the photosynthetic electron transport chain through ferredoxin whereas the bacterial HDS enzyme requires flavodoxin/flavodoxin reductase and NADPH as the reducing system (Seemann *et al.* 2006; Seemann *et al.* 2002). It has however, been suggested that an electron shuttle is required for plant HDS in darkness and a ferredoxin/ferredoxin reductase/NADPH system can provide the required electron shuttle in the darkness (Seemann *et al.* 2006). The bacterial HDR enzyme is also found to be dependent on the flavodoxin/flavodoxin reductase/NADPH system for the shuttle of electrons for its reducing activity (Wolff *et al.* 2003).

Reducing power can affect the MEP pathway in a complex fashion. Carbon flow through the pathway can be limited at DXR by low NADPH/NADP ratio as DXR is dependent on NADPH. Recent measurements of metabolites have shown that the ratio of DXP to MEP is high, indicating a potential limitation at DXR (Li & Sharkey 2013a). NADPH can also indirectly restrict the supply of GAP to the MEP pathway during photosynthesis by modifying the ratio of PGA to GAP in the Calvin-Benson cycle.

The consumption of ferredoxin instead of NADPH by the last two iron-sulfur-containing enzymes introduces another reducing-power-mediated regulation of the MEP pathway (Seemann *et al.* 2006; Seemann *et al.* 2002; Seemann & Rohmer 2007). Ferredoxin has significantly more reduced midpoint potential than NADPH (Cammack *et al.* 1977). This means that even though the NADPH/NADP ratio may be very high (Bennett *et al.* 2009), the effective redox potential of the NADP/NADPH redox pair is likely to be well below that of ferredoxin (Huang *et al.* 2012). This allows the ferredoxin supply to be limiting even when NADPH supply is favorable. HDS (Xu *et al.* 2010) and HDR (Xiao *et al.* 2009) require a very negative reducing potential that could be supplied by ferredoxin but not NADPH. Plant enzymes appear to use ferredoxin directly even though some bacteria use an NADPH/flavodoxin system (Seemann *et al.* 2006). The importance

of reducing power is supported by the finding that MEcDP can accumulate to very high concentration (Li & Sharkey 2013a; Mongélard *et al.* 2011; Rivasseau *et al.* 2009). In chloroplasts, it is likely that maximal MEcDP concentrations are limited by the amount of available phosphate. As much as 3 mM phosphate (Li & Sharkey 2013a) and even 20 mM phosphate (Rivasseau *et al.* 2009) in MEcDP has been reported while chloroplasts typically contain just 2 mM free phosphate (Sharkey & Vanderveer 1989).

4.3.3 Input of ATP (CTP)

The conversion of MEP into diphosphocytidylyl methylerythritol (CDPME) followed by its conversion to diphosphocytidylyl methylerythritol 2-phosphate (CDPMEP) by CDPME synthase (CMS) and CDPME kinase (CMK) respectively involves the consumption of CTP and ATP. The MEP pathway uses one CTP and one ATP molecule for the synthesis of each DMADP molecule. However, CTP loses a diphosphate moiety in the course of conversion of MEP to CDP-ME. It is assumed that the regeneration of CTP requires two more ATP molecules. Therefore, the overall cost becomes three molecules of ATP for the synthesis of each DMADP molecule.

The control of the MEP pathway by ATP is evident from the study demonstrating that isoprene emission is best correlated with ATP among all the other metabolites when monitored under a range of environmental factors with the condition of non-limiting carbon availability (Loreto & Sharkey 1993). The dependence of CMS and CMK on ATP can explain the effect of ATP content on the MEP pathway and isoprene emission. ATP can also have an indirect effect on the MEP pathway by affecting the availability of GAP. This is due to the higher affinity of phosphoribulokinase for ATP than PGA kinase (Slabas & Walker 1976). In the presence of a low

level of ATP during darkness, it can preferentially be used by phosphoribulokinase rather than PGA kinase, leading to a high amount of PGA and low availability of GAP. Another study shows that an initial increase in the rate of isoprene emission is observed with the feeding of methyl viologen to oak leaves (Loreto & Sharkey 1990). Methyl viologen leads to the reduction of oxygen to superoxide by diverting the electron flow from photosystem I. The superoxide is further converted to water by the consumption of NADPH. This results in a significant disturbance in the balance of reducing power to ATP availability inside the chloroplast. It was originally interpreted that the initial increase in the rate of isoprene emission in the presence of methyl viologen demonstrates that ATP control is more important than the reducing power control of the carbon flux through the MEP pathway. Recently, it has been shown that methyl viologen can facilitate the transfer of electrons to HDS and HDR (Xiao *et al.* 2009; Xu *et al.* 2010). This would provide an alternative explanation for the initial increase of isoprene emission in presence of methyl viologen.

4.4 REGULATION OF DXS

Several gene expression studies have demonstrated indirect evidence supporting the regulatory role for DXS (Cordoba *et al.* 2009). The first evidence from the metabolic stand-point came from the observation of labeled isoprene emission when leaves were fed with dideuterated deoxyxylulose (DOX-d_2) (Wolfertz *et al.* 2004; Wolfertz *et al.* 2003). Feeding eucalyptus leaves with DOX-d_2 results in the displacement of the endogenous, unlabeled isoprene by labeled isoprene derived from exogenous DOX, keeping the overall rate of isoprene emission almost

constant. This indicates that the concentration of DMADP remains constant inside the chloroplast even during feeding. Maintenance of a constant level of DMADP would require reduced activity of some enzyme upstream of the entry point of exogenous DOX resulting in a tight regulation of the flow of carbon through this pathway. Therefore, it is possible that a negative feedback loop from any metabolite downstream of DXP affects the activity of DXS.

Recently, I found that the recombinant DXS enzyme from *Populus trichocarpa* (*Pt*DXS) is inhibited by IDP and DMADP (Banerjee *et al.* 2013). This can explain the observation of Wolfertz *et al.* (2004; 2003). Feedback inhibition of DXS by IDP and DMADP can control the carbon flow through the MEP pathway and therefore, constitutes a significant regulatory mechanism of the MEP pathway (Figure 4.3). Overall, this inhibitory mechanism allows DMADP and IDP, the last metabolites of the MEP pathway, to limit their pool size by controlling the activity of the very first enzyme of the pathway. Feedback from the last metabolite on the activity of the first enzyme in a pathway is a common regulatory mechanism. Another group has also recently confirmed the feedback regulation of DMADP on poplar DXS and this potentially contributes to the *in vivo* regulation of the MEP pathway (Ghirardo *et al.* 2014).

It was observed that IDP and DMADP compete with thiamin diphosphate (ThDP) for binding with *Pt*DXS (Banerjee *et al.* 2013). This was unexpected, as ThDP is considered to act as a cofactor tightly embedded in the active site of the enzyme. The K_i of IDP and DMADP are in the low micromolar range (60-80 μM) indicating their significant binding ability relative to ThDP under physiological conditions. DXP, the product of DXS, serves as a precursor for thiamin and pyridoxol biosynthesis in *E. coli* (Lois *et al.* 1998; Rodríguez-Concepción &

Boronat 2002; Sprenger *et al.* 1997). Therefore, inhibition of DXS by IDP and DMADP might have some regulatory effects on thiamin biosynthesis in bacteria.

Another recent study has shown that the rate of pyruvate decarboxylation by DXS is accelerated by the presence of GAP (Patel *et al.* 2012). This constitutes a potential feedforward regulation at DXS by its substrate (Figure 4.3). This effect ensures that the initial product of pyruvate and ThDP, lactyl-ThDP, will not be converted to the *C*2α-carbanion or its conjugate acid, hydroxyethyl-ThDP (HEThDP), unless GAP is present so that the reaction can go to completion. Elimination of ThDP from the HEThDP intermediate leads to the formation of acetaldehyde and ThDP. Formation of acetaldehyde is specifically catalyzed by pyruvate decarboxylase (Kluger & Tittmann 2008). Hydroxyethyl-ThDP made by DXS could be the source of a short burst of acetaldehyde observed when a leaf is first put into darkness or subjected to mechanical stress (Brilli *et al.* 2011; Jardine *et al.* 2009; Karl *et al.* 2002a). If declining GAP levels inhibit the use of HEThDP before its production, HEThDP could accumulate. In darkness, the pH of the chloroplast stroma declines making release of acetaldehyde more likely. However, once the GAP level declines enough, production of HEThDP would stop along with the release of acetaldehyde.

4.5 REGULATION OF DXR AND CMS BY PHOSPHORYLATION

It has been reported that DXR from *Francisella tularensis* has a phosphorylation site at Ser-177, which is equivalent to Ser-186 in the *E. coli* DXR enzyme (Jawaid *et al.* 2009). Ser-186 of *E. coli* DXR acts as an important residue for binding of substrate. It is positioned near the

substrate binding site in such a way that it participates in hydrogen bonding with the phosphate moiety of the substrate (Sweeney *et al.* 2005). It also causes some conformational changes upon substrate binding which is important for the enzyme activity. Ser-177 of *Francisella tularensis* DXR has roles in substrate binding and enzyme activity. It has been shown that mutation of Ser-177 by an aspartate or glutamate results in complete abolition of enzyme activity (Jawaid *et al.* 2009). Both aspartate and glutamate act as mimics of phosphoserine and disrupt the required interaction for substrate binding. This causes the enzyme to be inactive. This indicates that the activity of the enzyme is affected by the phosphorylation of this particular serine residue. This serine residue is conserved in the plant DXR. There is no information at present whether this mechanism plays any role in regulating the MEP pathway. This mechanism has not been demonstrated for plant DXR.

Similar studies on CMS from *Francisella tularensis* have found a phosphorylation site at Thr-141, which is equivalent to Thr-140 in the *E. coli* CMS enzyme (Tsang *et al.* 2011). The crystal structure of *E. coli* CMS complexed with CDP-ME has revealed that Thr-140 plays critical role in binding with the substrate. The sidechain hydroxyl and backbone amide groups of Thr-140 participate in the hydrogen bonding with the C3 and C1 hydroxyl oxygen atoms of MEP respectively (Richard *et al.* 2001; Richard *et al.* 2004). It has been suggested by mutagenesis studies that Thr-141 in the *Francisella tularensis* also involves in substrate binding. Mutagenesis of Thr-141 with aspartate or glutamate, both of which mimic phosphothreonine, lead to reduced or abolished activity of the enzyme respectively. As discussed above for DXR, both T141D and T141E can lead to the disruption of important interactions involving substrate binding resulting in the impairment of enzyme activity. This could be another mechanism controlling carbon flux

through the MEP pathway in bacteria but this has not yet been demonstrated. This mechanism has not yet been tested in plants.

There is a need for further investigation of these potential control mechanisms in both bacteria and plants.

4.6 REGULATION OF AND BY MECDP CONCENTRATION

Several recent studies have demonstrated that MEcDP is a key intermediate in the MEP pathway. It has been observed that in leaves in the presence of light, more MEcDP is accumulated than all the other MEP pathway intermediates (Li & Sharkey 2013a). Here I discuss the various types of regulation inside and outside the MEP pathway that are coordinated by this metabolite.

4.6.1 A feedforward effect

MEcDP, the cyclo-diphosphate-containing intermediate of the MEP pathway, is synthesized by MEcDP synthase (MCS) from CDP-MEP. The crystal structure of MCS is known from different organisms (Kemp *et al.* 2005; Kemp *et al.* 2002; Ni *et al.* 2004; Richard *et al.* 2002). These structural studies have shown that a hydrophobic cavity is present along the threefold non-crystallographic symmetry axis of the enzyme. Evidence indicates that the cavity is occupied with different isoprenoids containing a diphosphate moiety like IDP/DMADP, geranyl diphosphate (GDP), and farnesyl diphosphate (FDP) (Kemp *et al.* 2005; Ni *et al.* 2004).

Sequence alignment studies of the MCS enzyme from various organisms indicate that the motif involved in the formation of the cavity and the binding of the ligand are well conserved in the protein family suggesting that the simultaneous conservation of both the motifs might have evolved as a result of biological function (Ni *et al.* 2004). It has been proposed that MCS could be a significant point of feedback regulation by the downstream isoprenoids (Kemp *et al.* 2005; Ni *et al.* 2004).

Recent studies have shown that recombinant MCS enzyme from *E. coli* is stabilized and activated in the presence of IDP, DMADP, GDP, and FDP (Bitok & Freel Meyers 2012). Analysis of the effect of different MEP pathway metabolites on MCS stability and activation by the *in vitro* assays has identified MEP as the most effective modulator for MCS. It has also been shown by *in vitro* studies that the methylerythritol scaffold is essential and sufficient for the observed effect of activation and enhancement of stability of MCS by MEP. The 2-*C*-methylerythritol scaffold is unique to the MEP pathway. The feedforward activation of MCS by MEP (Figure 4.3) constitutes a regulatory mechanism very specific to the MEP pathway.

It has also been observed that FDP inhibits the *E. coli* MCS-MEP complex whereas it activates and stabilizes *E. coli* MCS alone (Bitok & Freel Meyers 2012). It has been speculated that the binding of MEP to MCS might cause some conformational changes of MCS and the inhibitory effect of FDP is selective for the MEP-bound conformation of MCS. The feedback inhibition of MCS-MEP complex by FDP (Figure 4.3) indicates that the downstream isoprenoids control their biosynthesis by modulating the activity of a key enzyme involved in the biosynthesis of their precursor. There is another significance of this feedback inhibition. It sets a limit on the activated MCS-MEP complex in the presence of high levels of downstream

isoprenoids so that the carbon flux through the MEP pathway is controlled. Overall, this observation suggests that MCS plays a key role in the regulation of the MEP pathway.

4.6.2 Regulation of the biosynthesis and metabolism of MEcDP

It has been observed that MEcDP accumulates in bacteria under oxidative stress (Artsatbanov *et al.* 2012; Ostrovsky *et al.* 1998; Ostrovsky *et al.* 1992b). Nitrosative stress (caused by the reactive species nitric oxide, NO) is also found to be responsible for the accumulation of MEcDP, to a lesser extent than oxidative stress, in *Corynebacterium ammoniagenes* (Artsatbanov *et al.* 2012). Recently, spinach leaves were also found to accumulate MEcDP under high light and high temperature and in the presence of heavy metals like Cd (Rivasseau *et al.* 2009). These external factors can cause oxidative stress *in vivo* leading to the accumulation of MEcDP. HDS contains a [4Fe-4S] cluster susceptible to oxidative stress. Studies have found that ROS generated under oxidative stress damages the reconstitution of the [4Fe-4S]-cluster and thus interferes with the turnover of the holo enzyme (Rivasseau *et al.* 2009). It has been suggested that under oxidative stress, the reconstitution of the apo-HDS with the [4Fe-4S]-cluster functions as the rate limiting step of the MEP pathway and thus is a bottleneck in the MEP pathway.

MEcDP has also been found to act as an effective antioxidant (Ostrovsky *et al.* 2003). This property of MEcDP allows the repair of the HDS enzyme to keep it functional by limiting oxidative stress. This protective ability of MEcDP is not sufficient for the reconstitution of the holo-enzyme in the presence of inhibitors like Cd. The accumulation of MEcDP in illuminated leaves may affect the phosphate balance of the chloroplast. Synthesis of high levels of MEcDP could potentially act as a sink for phosphate and disturb the phosphate supply for ATP synthesis.

It has been demonstrated that utilization of phosphate to maintain the synthesis of high level of MEcDP can cause a phosphate deficiency syndrome in chloroplast (Rivasseau *et al.* 2009). It is possible that the maximal MEcDP concentration is restricted by the amount of chloroplastic phosphate.

Another interesting observation in this context is the accumulation of a very high level of MEcDP and blocking of isoprene emission from leaves under nitrogen atmosphere (i.e. CO_2- and O_2-free air) (Li & Sharkey 2013a; Wolfertz *et al.* 2003). Limited availability of carbon through the Calvin-Benson cycle to feed the MEP pathway cannot explain the phenomenon of suppressed isoprene emission from leaves held under nitrogen. This is because replenishing the carbon supply of the MEP pathway by feeding the leaves directly with deoxyxylulose in the presence of nitrogen is not able to restore isoprene emission (Wolfertz *et al.* 2003). Accumulation of a high level of MEcDP under nitrogen atmosphere indicates that the downstream enzymes may not be functional, causing isoprene emission to stop. It is likely that under a nitrogen atmosphere the iron-sulfur complexes of HDS and HDR are disrupted. A nitrogen atmosphere can possibly lead to some signals that cause these enzymes to become inactive. The exact mechanisms by which nitrogen atmosphere disrupts the activity of these two enzymes in leaves are yet to be determined.

4.6.3 Effect of MEcDP accumulation in other biochemical processes

It has been found that MEcDP plays a significant role in various other biochemical pathways unrelated to isoprenoid biosynthesis.

4.6.3.a Bacteria

In bacteria, studies have shown that oxidative stresses caused by benzyl viologen or other redox mediators lead to the accumulation of MEcDP, which has been suggested to play an important role as an antistressor in bacteria (Ostrovsky *et al.* 1998; Ostrovsky *et al.* 1992a; Ostrovsky *et al.* 1992b). It has also been observed that MEcDP prevents DNA from falling apart in the presence of Fenton's reagent (Ostrovskiĭ *et al.* 2003). This is achieved when a complex is formed between the ferrous ions (present in the Fenton's reagent) and MEcDP resulting in their reduced ability to form hydroxyl radicals and hydrogen peroxide (Ostrovskiĭ *et al.* 2003). This suggests that MEcDP could act as an endogenous stabilizing agent for bacterial cells subjected to oxidative stress (Ostrovskiĭ *et al.* 2003).

MEcDP has also been found to modulate chromatin structure by disrupting the chlamydial histone-DNA interaction in the intracellular pathogen *Chlamydia trachomatis* (Grieshaber *et al.* 2004; Grieshaber *et al.* 2006). The chlamydial developmental cycle alternates between the extracellular infectious form called the elementary body (EB) and the intracellular replicative form termed the reticulate body (RB). These two different forms have characteristic chromatin structures. The RB form has condensed nucleoid structure mediated by histone-like DNA binding proteins, Hc1 and Hc2 (Grieshaber *et al.* 2004; Grieshaber *et al.* 2006). Within a few hours of infection, the metabolically inert EB form is transformed into the metabolically active RB form. Dispersion of the chromatin structure is required for the differentiation of the EB form into the RB form. It was suggested that MEcDP disrupts the binding between DNA and histone-like proteins leading to the release of Hc1and Hc2 from the DNA causing the dispersion of the chromatin and initiation of transcription. Thus, MEcDP mediates the decondensation of the chromatin allowing the differentiation of the EB form to the RB form. Another example of the

role of MEcDP in the regulation of the bacterial genome activity includes its resuscitating effect regulating the transition of the non-culturable form of *Mycobacterium smegmatis* into the state of its active growth (Goncharenko *et al.* 2007).

Recent metabolite profiling studies have shown an efflux of MEcDP from genetically engineered *E. coli* cells containing the overexpressed enzymes DXS, IDI, CMS, and MCS (Zhou *et al.* 2012). It has been observed that the efflux of MEcDP is accompanied with the simultaneous reduction of the production of lycopene, a downstream isoprenoid. It was possible to reduce the efflux of MEcDP by the overexpression of HDS, which consumes MEcDP, directing more carbon through the last part of the MEP pathway, resulting in the increased production of lycopene. This indicates that the efflux of MEcDP could act as a limiting step in microbial isoprenoid production. Preliminary studies have indicated the involvement of a fosmidomycin resistance (fsr) efflux pump (Fujisaki *et al.* 1996) for the process of exporting MEcDP out of the cell (Zhou *et al.* 2012). The active efflux of MEcDP from the engineered lycopene-producing *E. coli* cells suggests the possibility of a potential MEP pathway branch point which diverts the carbon source of the MEP pathway to another competing pathway (Zhou *et al.* 2012). This is also supported by the study of restoration of the complete and active MEP pathway by heterologous expression of HDS and HDR into *Listeria innocua* which lacks these enzymes (Begley *et al.* 2008). Bioinformatics analysis has shown that *L. innocua* has lost the genes for HDS and HDR through evolution while the rest of the MEP pathway genes are present (Begley *et al.* 2008). The ability of this organism to have an active MEP pathway with the introduction of the lost enzymes suggests that the rest of the MEP pathway enzymes, which were already present, are functional. Evolution has selectively truncated the MEP pathway in such a way that the existing enzymes could catalyze the biosynthesis of MEcDP, which can further lead

to end products of the MEP pathway in the presence of HDS and HDR. This suggests some important yet unidentified biochemical role for MEcDP (Begley *et al.* 2008).

4.3.6.b Plants

In plants, recent studies have demonstrated that in addition to its role in the bacterial system, MEcDP has a potential role as a signaling molecule in Arabidopsis. Plastidial MEcDP leads to a retrograde signal regulating the expression of nuclear-encoded, stress-responsive genes for plastidial proteins (Figure 4.3) (Xiao *et al.* 2012). Hydroperoxide lyase (HPL) is a stress-inducible plastidial protein in the oxylipin pathway encoded by a nuclear gene. It has been shown that a mutant *ceh1* shows constitutive expression of HPL. *CEH1* encodes for HDS and thus the *ceh1* mutant is defective in the utilization of MEcDP resulting in its accumulation. It has also been reported that abiotic stresses including high light or wounding cause a high level of MEcDP to build up. These abiotic stresses causing accumulation of endogenous MEcDP, as well as exogenous MEcDP, lead to the elevated expression of HPL. This indicates that MEcDP is, directly or indirectly, a retrograde signaling molecule. It has been shown that abscisic acid and methyl jasmonate, stress-responsive hormones of plants, increase the activity of DXS (Yang *et al.* 2012). It is tempting to speculate that these stress-responsive hormones lead to the regulation of HPL by accumulating MEcDP through the increased activity of the upstream enzyme DXS. The mode of action of MEcDP in the retrograde signaling is not fully understood. Considering the involvement of MEcDP in the nucleoid decondensation in chlamydia, it may be that MEcDP modulates nuclear gene expression in plants through the remodeling of the nuclear architecture (Grieshaber *et al.* 2004; Grieshaber *et al.* 2006). This mechanistic model would require the

transport of plastid-localized MEcDP to the nucleus. No information is available for any such transport of MEcDP in plants but the presence of the fsr efflux pump in bacteria for moving MEcDP out of the cells (Zhou *et al.* 2012) raises the possibility of such transporter in plants as well. One such candidate is the Arabidopsis gene At3g47450.

Accumulation of MEcDP can cause transient effects in isoprene emission. Upon darkening a leaf, isoprene emission continues long enough to consume the existing DMADP and IDP but not MEcDP (Li & Sharkey 2013a; Rasulov *et al.* 2009a). After about five minutes in the dark the leaf regains the ability to consume MEcDP but not to make additional MEcDP. This causes a small post-illumination burst of isoprene between 5 and 10 min after darkening the leaf (Figure 4.4). The very high level of MEcDP that builds up in leaves held in a nitrogen atmosphere (Section 4.6.2) is likely responsible for a large overshoot in isoprene emission when O_2 and CO_2 are added back to the air (Figure 4.4).

4.7 REGULATION AT HDS AND HDR

Given the propensity for MEcDP to accumulate in plants and bacteria it is likely that there is significant regulation of HDS. However, less is known about HDS regulation than HDR regulation. It has been shown that nitrosative stress in *Mycobacterium smegmatis* causes the accumulation of HMBDP, the substrate for HDR (Artsatbanov *et al.* 2012). This suggests that NO damages the [4Fe-4S]-cluster of HDR resulting in the dysfunctional enzyme, which leads to the accumulation of HMBDP. The gene of HDR in *E. coli* has been found to be involved in penicillin tolerance through its interaction with RelA responsible for the synthesis of guanosine

3',5'-bispyrophosphate (ppGpp), which acts as a nutritional stress alarmone (Gustafson *et al.* 1993).

It has been shown that a point mutation in *E. coli* HDR ($LytB^{G120D}$) enables it to selectively synthesize DMADP over IDP (Puan *et al.* 2005). This suggests that the structural modification of HDR can potentially regulate the *in vivo* concentration of DMADP and IDP, the end products of the MEP pathway.

It has been seen that engineering an additional HDS gene into *E. coli* without increasing the activity of HDR leads to a reduction in productivity in bacteria engineered to emit isoprene (A.E. Wiberley, E.L. Singsaas, T.D. Sharkey, unpublished) (Chotani *et al.* 2013). Chotani *et al.* (2013) found that HMBDP accumulated in such bacteria and that this was correlated with reduced isoprene production from engineered bacteria. One explanation for this is that HMBDP is toxic to cells.

Purified HDR is shown to require a very negative redox potential, maximal activity was found at -450 mV, much lower than the midpoint potential of NADPH (-320 mV). The presumed electron source for this enzyme gives an activity less than 2% of maximal. Xiao et al. suggest that HDR might be regulated by modulation of the redox potential of its [4Fe-4S] cluster (Xiao *et al.* 2009).

It is likely that both HDS and HDR are highly regulated and this regulation has a strong impact on the carbon flow of the MEP pathway. These are likely to be the steps where light regulation of DMADP in plants occurs, but there is no information on how this occurs. It is also tempting to assume that the metabolites downstream of MEcDP might have some toxic effect in the cell. This might lead the carbon flux of the MEP pathway to be constricted, building up a pool of only MEcDP under the condition of oxidative stresses.

4.8 CONCLUSIONS AND PERSPECTIVES

The MEP pathway is one of the most important biochemical pathways for sustaining life on earth. Understanding the different regulatory mechanisms involved in this pathway is critical for biological, environmental, as well as commercial purposes. Mechanisms of genetic regulation of this pathway have started emerging only in the last decade. I have discussed in this review several different regulatory mechanisms involved in the metabolism of this pathway and these are summarized in Figure 4.3.

Several questions are still to be answered regarding regulatory mechanisms of the MEP pathway, especially in plants. The source of pyruvate for the MEP pathway is not clearly understood. Understanding the source of pyruvate may explain the discrepancy in the labeling of the isoprenoids derived from the MEP pathway. Several studies have indicated that MEcDP has potential roles in MEP pathway regulation. MEcDP may connect metabolism in the MEP pathway with other cellular metabolism, independent of its role in making precursors for isoprenoids. It has been suggested that MEcDP can act as a stress sensor and can accordingly coordinate stress responses. The exact mode of its action in response to the stress signals has yet to be understood.

It has been suggested that the [4Fe-4S]-cluster containing enzymes, HDS and HDR, can also contribute to the regulatory mechanisms of the MEP pathway. The susceptibility of the [4Fe-4S]-clusters to oxidative stress indicates that the *in vivo* redox status can influence the carbon flow of the MEP pathway through these enzymes. In-depth knowledge of the structural and functional integrity of these enzymes under various redox-sensitive conditions would be helpful in understanding their role in the regulation of the MEP pathway.

Understanding of the metabolic regulation of the MEP pathway has emerged in the past decade and currently can be considered as being at its nascent stage. Studies so far have demonstrated that several enzymes and metabolites could have various regulatory roles in this pathway. However, not much is known regarding the primary points of regulation and how the overall regulation of the pathway is finely tuned by both the primary and secondary points of regulation. Future studies in the field should be aimed at a complete understanding of the metabolic regulation of the MEP pathway. This would be useful in biomedical and biotechnological uses of the MEP pathway and would also help in finding a mechanistic basis for modeling isoprene emission.

4.9 ACKNOWLEDGEMENTS

This material is based in part on work supported by the National Science Foundation under Grant No. 0950574. Any opinions, findings, and conclusions or recommendations expressed in this material are those of the author(s) and do not necessarily reflect the views of the National Science Foundation. The authors have no conflicts of interest to declare. I thank Professor Caren Freel Meyers, Dr. Sean Weise, and Chris Harvey for comments on the manuscript.

APPENDIX

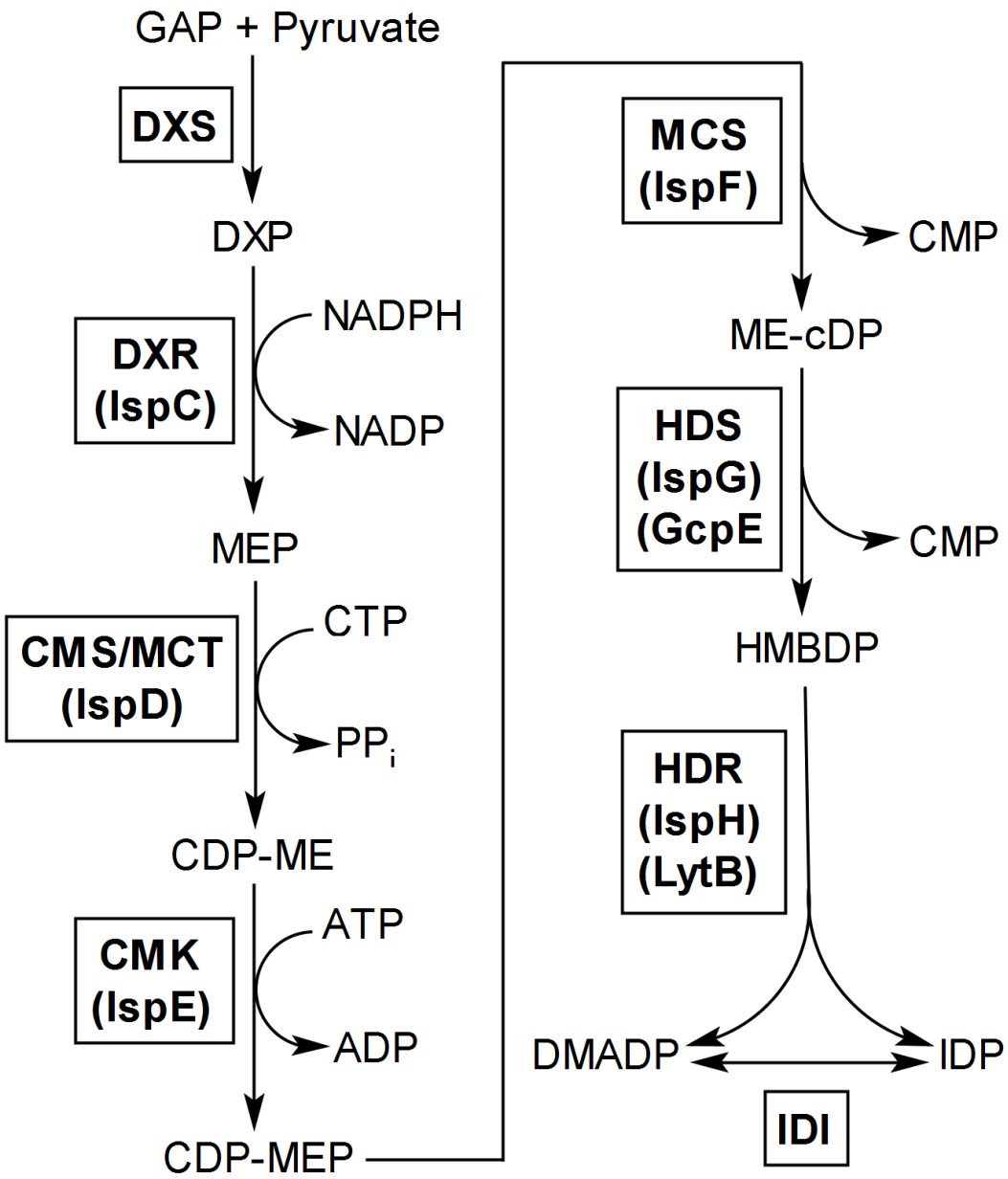

FIGURE 4.1 The metabolites and the enzymes involved in the MEP pathway. *DXS*: 1-deoxy-D-xylulose 5-phosphate (*DXP*) synthase; *DXR*: 1-deoxy-D-xylulose 5-phosphate reductoisomerase; *MEP*: 2-*C*-methyl-D-erythritol 4-phosphate; *CMS*/*MCT*: 4-diphosphocytidyl-2-*C*-methylerythritol synthase/2-*C*-methyl-D-erythritol 4-phosphate cytidylyltransferase; *CMK*: 4-(cytidine 5'-diphospho)-2-*C*-methyl-D-erythritol (*CDP-ME*) kinase; *CDP-MEP*: 4-(cytidine 5'-diphospho)-2-*C*-methyl-D-erythritol 2-phosphate; *MCS*: 2-*C*-methyl-D-erythritol 2,4-cyclodiphosphate (*MEcDP*) synthase; *HDS*: 4-hydroxy-3-methylbut-2-enyl diphosphate (*HMBDP*) synthase; *HDR*: 4-hydroxy-3-methylbut-2-enyl diphosphate reductase; *IDI*: isopentenyl diphosphate (*IDP*) isomerase; *DMADP*: dimethylallyl diphosphate.

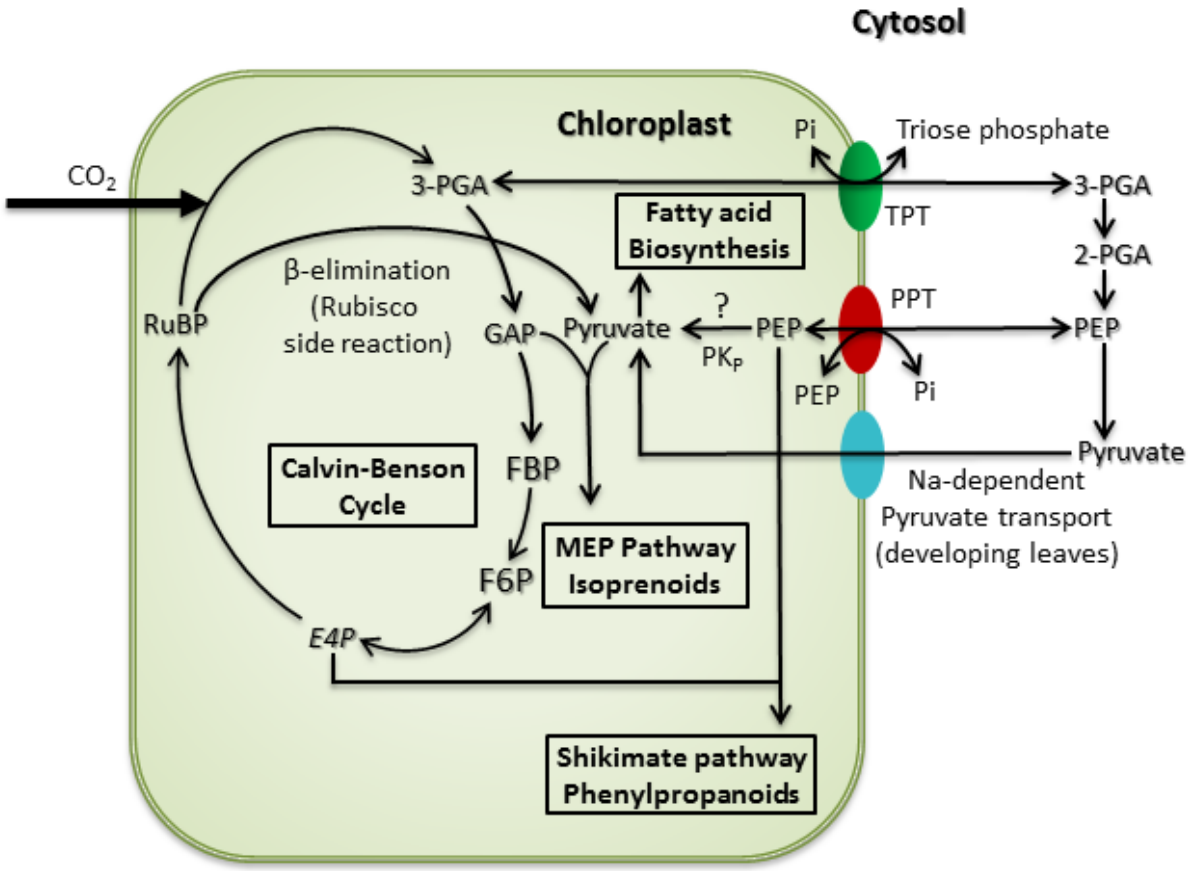

FIGURE 4.2 Possible sources of pyruvate required for feeding into the MEP pathway. Abbreviations RuBP = ribulose 1,5-bisphosphate, 3-PGA = 3-phosphoglyceric acid, FBP = fructose 1,6-bisphosphate, F6P = fructose 6-phosphate, E4P = erythrose 4-phosphate, PEP = phosphoenolpyruvate, GAP = glyceraldehyde 3-phosphate, 2-PGA = 2-phosphoglyceric acid, TPT = triose phosphate/phosphate transporter, PPT = phosph*oenol*pyruvate/phosphate translocator, Pi = inorganic phosphate, PK_p = pyruvate kinase (plastidic).

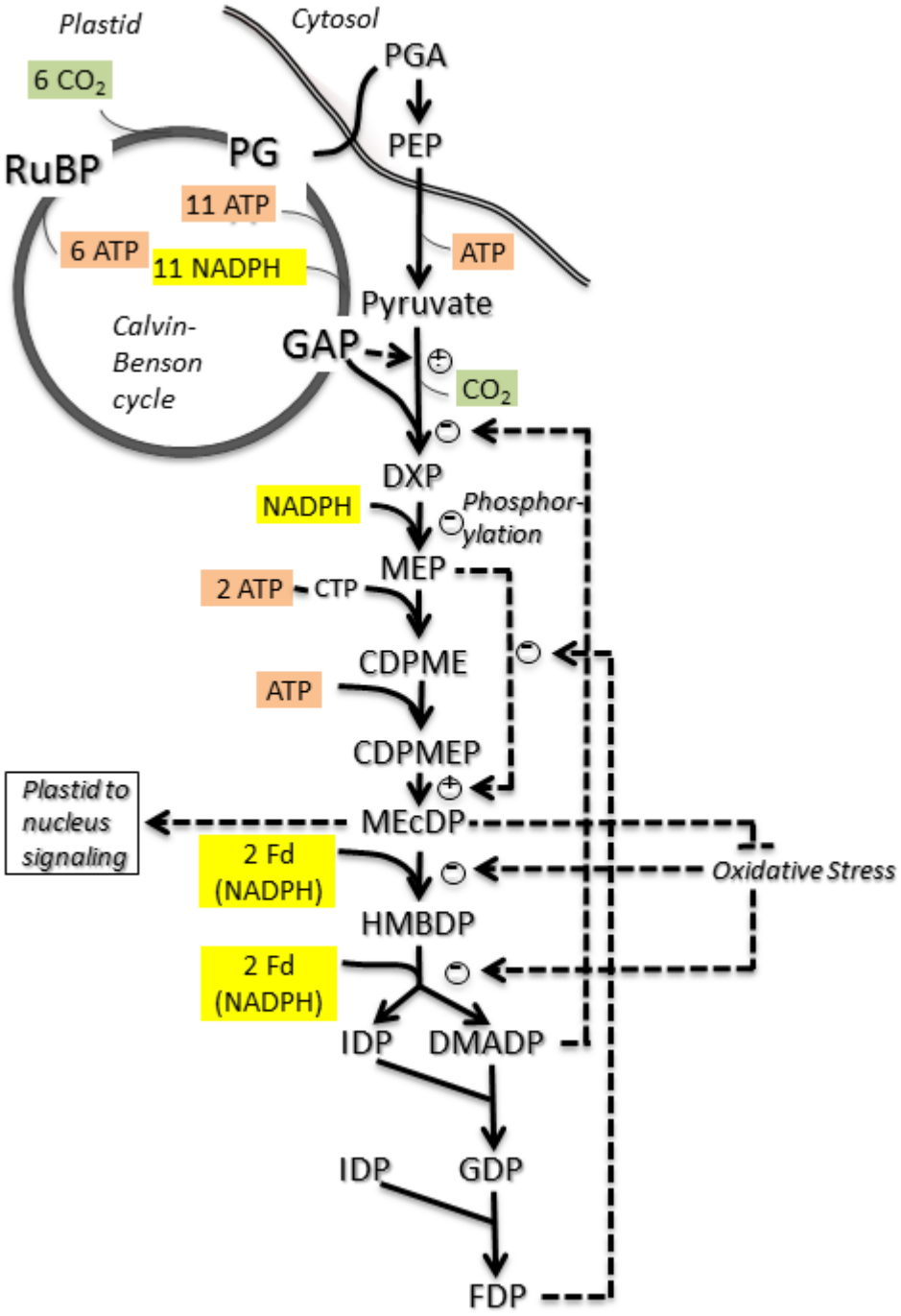

FIGURE 4.3 MEP pathway and related metabolism showing the major metabolic regulatory points discussed. Abbreviations GDP = geranyl diphosphate, FDP = farnesyl diphosphate, Fd = ferredoxin.

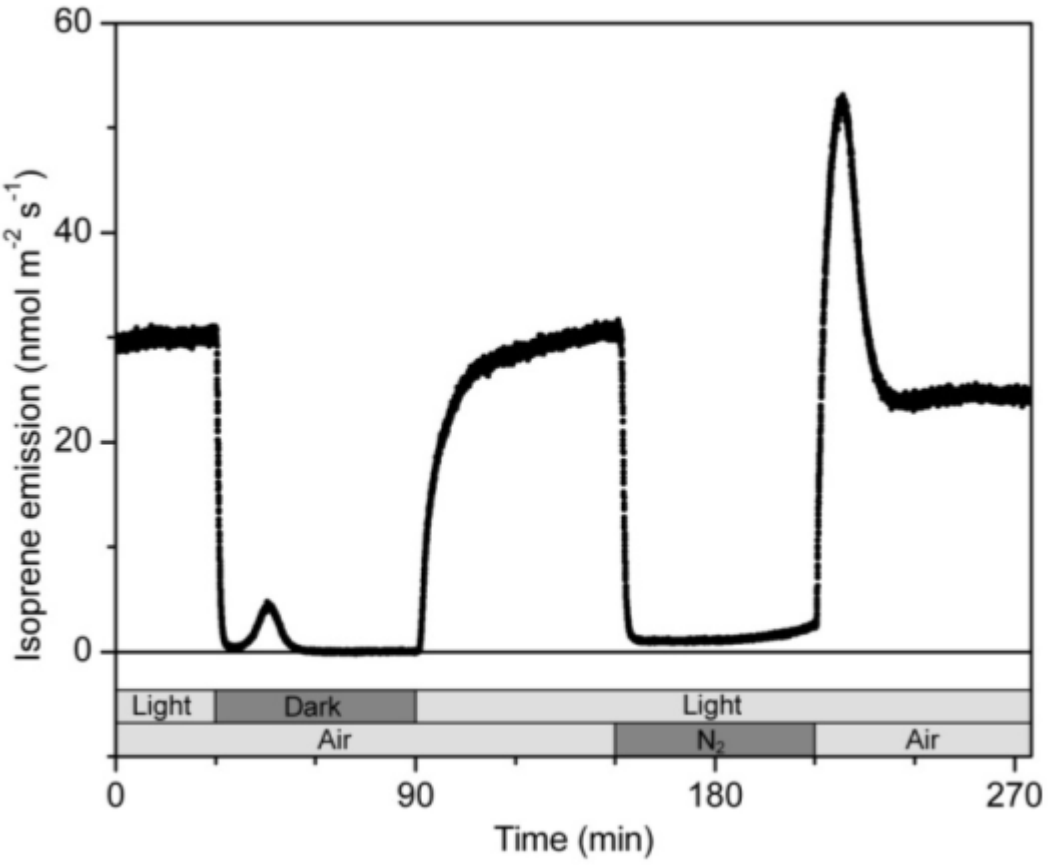

FIGURE 4.4 Effects of MEcDP on isoprene emission after darkness or nitrogen atmosphere. Following darkness MEcDP causes a small second burst of isoprene while a nitrogen atmosphere stops isoprene emission without a burst. Upon adding oxygen and CO_2 isoprene emission overshoots but establishes a steady state slightly lower than before imposing a nitrogen atmosphere. This may result from a very high MEcDP level in the leaf. From Li and Sharkey, 2013 (Li & Sharkey 2013a) (Copyright John Wiley & Sons Ltd).

LITERATURE CITED

LITERATURE CITED

Affek H.P. & Yakir D. (2003) Natural abundance carbon isotope composition of isoprene reflects incomplete coupling between isoprene synthesis and photosynthetic carbon flow. *Plant Physiology*, **131**, 1727-1736.

Andre C., Froehlich J.E., Moll M.R. & Benning C. (2007) A heteromeric plastidic pyruvate kinase complex involved in seed oil biosynthesis in *Arabidopsis*. *The Plant Cell*, **19**, 2006-2022.

Andrews T.J. & Kane H.J. (1991) Pyruvate is a by-product of catalysis by ribulosebisphosphate carboxylase/oxygenase. *Journal of Biological Chemistry*, **266**, 9447-9452.

Andriotis V.M.E., Kruger N.J., Pike M.J. & Smith A.M. (2010) Plastidial glycolysis in developing Arabidopsis embryos. *New Phytologist*, **185**, 649-662.

Arigoni D., Sagner S., Latzel C., Eisenreich W., Bacher A. & Zenk M.H. (1997) Terpenoid biosynthesis from 1-deoxy-D-xylulose in higher plants by intramolecular skeletal rearrangement. *Proceedings of the National Academy of Sciences of the United States of America*, **94**, 10600-10605.

Artsatbanov V.Y., Vostroknutova G.N., Shleeva M.O., Goncharenko A.V., Zinin A.I., Ostrovsky D.N. & Kapreliants A.S. (2012) Influence of oxidative and nitrosative stress on accumulation of diphosphate intermediates of the non-mevalonate pathway of isoprenoid biosynthesis in corynebacteria and mycobacteria. *Biochemistry (Moscow)*, **77**, 362-371.

Atkins C.A. & Canvin D.T. (1971) Photosynthesis and CO_2 evolution by leaf discs: gas exchange, extraction, and ion-exchange fractionation of ^{14}C-labeled photosynthetic products. *Canadian Journal of Botany*, **49**, 1225-1234.

Bagge P. & Larsson C. (1986) Biosynthesis of aromatic amino acids by highly purified spinach chloroplasts – Compartmentation and regulation of the reactions. *Physiologia Plantarum*, **68**, 641-647.

Banerjee A., Wu Y., Banerjee R., Li Y., Yan H. & Sharkey T.D. (2013) Feedback inhibition of deoxy-D-xylulose-5-phosphate synthase regulates the methylerythritol 4-phosphate pathway. *Journal of Biological Chemistry*, **288**, 16926-16936.

Begley M., Bron P.A., Heuston S., Casey P.G., Englert N., Wiesner J., Jomaa H., Gahan C.G.M. & Hill C. (2008) Analysis of the isoprenoid biosynthesis pathways in *Listeria monocytogenes* reveals a role for the alternative 2-*C*-methyl-D-erythritol 4-phosphate pathway in murine infection. *Infection and Immunity*, **76**, 5392-5401.

Bennett B.D., Kimball E.H., Gao M., Osterhout R., Dien S.J.V. & Rabinowitz J.D. (2009) Absolute metabolite concentrations and implied enzyme active site occupancy in *Escherichia coli*. *Nature Chemical Biology*, **5**, 593-599.

Bitok J.K. & Freel Meyers C. (2012) 2*C*-Methyl-D-erythritol 4-phosphate enhances and sustains cyclodiphosphate synthase IspF activity. *ACS Chemical Biology*, **7**, 1702-1710.

Bouvier F., d'Harlingue A., Suire C., A. Backhaus R.A. & Camara B. (1998) Dedicated roles of plastid transketolases during the early onset of isoprenoid biogenesis in pepper fruits. *Plant Physiology*, **117**, 1423-1431.

Brilli F., Barta C., Fortunati A., Lerdau M., Loreto F. & Centritto M. (2007) Response of isoprene emission and carbon metabolism to drought in white poplar (*Populus alba*) saplings. *New Phytologist*, **175**, 244-254.

Brilli F., Ruuskanen T.M., Schnitzhofer R., Müller M., Breitenlechner M., Bittner V., Wohlfahrt G., Loreto F. & Hansel A. (2011) Detection of plant volatiles after leaf wounding and darkening by proton transfer reaction "time-of-flight" mass spectrometry (PTR-TOF). *PLoS ONE*, **6**, e20419.

Cammack R., Rao K.K., Bargeron C.P., Hutson K.G., Andrew P.W. & Rogers L.J. (1977) Midpoint redox potentials of plant and algal ferredoxins. *Biochemical Journal*, **168**, 205-209.

Chang W., Song H., Liu H. & Liu P. (2013) Current development in isoprenoid precursor biosynthesis and regulation. *Current Opinion in Chemical Biology*, **17**, 571-579.

Chotani G.K., Mcauliffe J.C., Miller M.C., Muir R.E., Vavlline D.V. & Weyler W. (2013) Isoprene production using the DXP and MVA pathway. In: *US 8507235 B2*, pp. 1-486.

Cordoba E., Salmi M. & León P. (2009) Unravelling the regulatory mechanisms that modulate the MEP pathway in higher plants. *Journal of Experimental Botany*, **60**, 2933-2943.

DellaPenna D. & Posgon B.J. (2006) Vitamin synthesis in plants: tocopherols and carotenoids. *Annual Review of Plant Biology*, **57**, 711-738.

Delwiche C.F. & Sharkey T.D. (1993) Rapid appearance of ^{13}C in biogenic isoprene when $^{13}CO_2$ is fed to intact leaves. *Plant, Cell and Environment*, **16**, 587-591.

Eisenreich W., Menhard B., Hylands P.J. & Zenk M.H. (1996) Studies on the biosynthesis of taxol: the taxane carbon skeleton is not of mevalonoid origin. *Proceedings of the National Academy of Sciences of the United States of America*, **93**, 6431-6436.

Eisenreich W., Rohdich F. & Bacher A. (2001) Deoxyxylulose phosphate pathway to terpenoids. *Trends in plant science*, **6**, 78-84.

Eisenreich W., Schwarz M., Cartayrade A., Arigoni D., Zenk M.H. & Bacher A. (1998) The deoxyxylulose phosphate pathway of terpenoid biosynthesis in plants and microorganisms. *Chemistry & Biology*, **5**, R221-R233.

Ferrieri R.A., Gray D.W., Babst B.A., Schueller M.J., Schlyer D.J., Thorpe M.R., Orians C.M. & Lerdau M. (2005) Use of carbon-11 in *Populus* shows that exogenous jasmonic acid increases biosynthesis of isoprene from recently fixed carbon. *Plant, Cell and Environment*, **28**, 591-602.

Ferronato C., Orlando J.J. & Tyndall G.S. (1998) Rate and mechanism of the reactions of OH and Cl with 2-methyl-3-buten-2-ol. *Journal of Geophysical Research: Atmospheres*, **103**, 25579-25586.

Fischer K., Kammerer B., Gutensohn M., Arbinger B., Weber A., Häusler R.E. & Flügge U.I. (1997) A new class of plastidic phosphate translocators: a putative link between primary and secondary metabolism by the phosphoenolpyruvate/phosphate antiporter. *The Plant Cell*, **9**, 453-462.

Flügge U.-I. (1999) Phosphate translocators in plastids. *Annual Review of Plant Physiology and Plant Molecular Biology*, **50**, 27-45.

Fujisaki S., Ohnuma S., Horiuchi T., Takahashi I., Tsukui S., Nishimura Y., Nishino T., Kitabatake M. & Inokuchi H. (1996) Cloning of a gene from *Escherichia coli* that confers resistance to fosmidomycin as a consequence of amplification. *Gene*, **175**, 83-87.

Furumoto T., Yamaguchi T., Ohshima-Ichie Y., Nakamura M., Tsuchida-Iwata Y., Shimamura M., Ohnishi J., Hata S., Gowik U., Westhoff P., Brautigam A., Weber A.P.M. & Izui K. (2011) A plastidial sodium-dependent pyruvate transporter. *Nature*, **476**, 472-475.

Ghirardo A., Wright L.P., Bi Z., Rosenkranz M., Pulido P., Rodríguez-Concepción M., Niinemets Ü., Brüggemann N., Gershenzon J. & Schnitzler J.-P. (2014) Metabolic flux analysis of plastidic isoprenoid biosynthesis in poplar leaves emitting and non-emitting isoprene. *Plant Physiology*, **165**, 37-51.

Goldan P.D., Kuster W.C., Fehsenfeld F.C. & Montzka S.A. (1993) The observation of a C_5 alcohol emission in a North American pine forest. *Geophysical Research Letters*, **20**, 1039-1042.

Goncharenko A.V., Ershov Y.V., Salina E.G., Wiesner J., Vostroknutova G.N., Sandanov A.A., Kaprelyants A.S. & Ostrovsky D.N. (2007) The role of 2-*C*-

methylerythritol-2,4-cyclopyrophosphate in the resuscitation of the "nonculturable" forms of *Mycobacterium smegmatis*. *Microbiology*, **76**, 147-152.

Gray D.W., Breneman S.R., Topper L.A. & Sharkey T.D. (2011) Biochemical characterization and homology modeling of methylbutenol synthase and implications for understanding hemiterpene synthase evolution in plants. *Journal of Biological Chemistry*, **286**, 20582-20590.

Grieshaber N.A., Fischer E.R., Mead D.J., Dooley C.A. & Hackstadt T. (2004) Chlamydial histone–DNA interactions are disrupted by a metabolite in the methylerythritol phosphate pathway of isoprenoid biosynthesis. *Proceedings of the National Academy of Sciences of the United States of America*, **101**, 7451-7456.

Grieshaber N.A., Sager J.B., Dooley C.A., Hayes S.F. & Hackstadt T. (2006) Regulation of the *Chlamydia trachomatis* histone H1-like protein Hc2 is IspE dependent and IhtA independent. *Journal of Bacteriology*, **188**, 5289-5292.

Gustafson C.E., Kaul S. & Ishiguro E.E. (1993) Identification of the *Escherichia coli lytB* gene, which is involved in penicillin tolerance and control of the stringent response. *Journal of Bacteriology*, **175**, 1203-1205.

Harley P., Fridd-Stroud V., Greenberg J., Guenther A. & Vasconcellos P. (1998) Emission of 2-methyl-3-buten-2-ol by pines: A potentially large natural source of reactive carbon to the atmosphere. *Journal of Geophysical Research: Atmospheres*, **103**, 25479-25486.

Hemmerlin A., Hoeffler J.-F., Meyer O., Tritsch D., Kagan I.A., Grosdemange-Billiard C., Rohmer M. & Bach T.J. (2003) Cross-talk between the cytosolic mevalonate and the plastidial methylerythritol phosphate pathways in tobacco bright yellow-2 cells. *Journal of Biological Chemistry*, **278**, 26666-26676.

Huang H., Wang S., Moll J. & Thauer R.K. (2012) Electron bifurcation involved in the energy metabolism of the acetogenic bacterium *Moorella thermoacetica* growing on glucose or H_2 plus CO_2. *Journal of Bacteriology*, **194**, 3689-3699.

Hunter W.N. (2007) The non-mevalonate pathway of isoprenoid precursor biosynthesis. *Journal of Biological Chemistry*, **282**, 21573-21577.

Ireland R.J., Deluca V. & Dennis D.T. (1979) Isoenzymes of pyruvate kinase in etioplasts and chloroplasts. *Plant Physiology*, **63**, 903-907.

Jardine K., Karl T., Lerdau M., Harley P., Guenther A. & Mak J.E. (2009) Carbon isotope analysis of acetaldehyde emitted from leaves following mechanical stress and anoxia. *Plant Biology*, **11**, 591-597.

Jawaid S., Seidle H., Zhou W., Abdirahman H., Abadeer M., Hix J.H., Hoek M.L.v. & Couch R.D. (2009) Kinetic characterization and phosphoregulation of the *Francisella tularensis* 1-deoxy-D-xylulose 5-phosphate reductoisomerase (MEP synthase). *PLoS ONE*, **4**, e8288.

Karl T., Curtis A.J., Rosenstiel T.N., Monson R.K. & Fall R. (2002a) Transient releases of acetaldehyde from tree leaves–products of a pyruvate overflow mechanism? *Plant, Cell and Environment*, **25**, 1121-1131.

Karl T., Fall R., Rosenstiel T.N., Prazeller P., Larsen B., Seufert G. & Lindinger W. (2002b) On-line analysis of the $^{13}CO_2$ labeling of leaf isoprene suggests multiple subcellular origins of isoprene precursors. *Planta*, **215**, 894-905.

Kemp L.E., Alphey M.S., Bond C.S., Ferguson M.A.J., Hecht S., Bacher A., Eisenreich W., Felix R. & Hunter W.N. (2005) The identification of isoprenoids that bind in the intersubunit cavity of *Escherichia coli* 2*C*-methyl-D-erythritol-2,4-cyclodiphosphate synthase by complementary biophysical methods. *Acta Crystallographica Section D: Biological Crystallography*, **61**, 45-52.

Kemp L.E., Bond C.S. & Hunter W.N. (2002) Structure of 2*C*-methyl-D-erythritol 2, 4-cyclodiphosphate synthase: an essential enzyme for isoprenoid biosynthesis and target for antimicrobial drug development. *Proceedings of the National Academy of Sciences of the United States of America*, **99**, 6591-6596.

Kluger R. & Tittmann K. (2008) Thiamin diphosphate catalysis: enzymic and nonenzymic covalent intermediates. *Chemical Reviews*, **108**, 1797-1833.

Kreuzwieser J., Graus M., Wisthaler A., Hansel A., Rennenberg H. & Schnitzler J.-P. (2002) Xylem-transported glucose as an additional carbon source for leaf isoprene formation in *Quercus robur*. *New Phytologist*, **156**, 171-178.

Kühnemann F., Wolfertz M., Arnold S., Lagemann M., Popp A., Schüler G., Jux A. & Boland W. (2002) Simultaneous online detection of isoprene and isoprene-d_2 using infrared photoacoustic spectroscopy. *Applied Physics B*, **75**, 397-403.

Kuzuyama T., Takagi M., Takahashi S. & Seto H. (2000) Cloning and characterization of 1-deoxy-D-xylulose 5-phosphate synthase from *Streptomyces* sp. strain CL190, which uses both the mevalonate and nonmevalonate pathways for isopentenyl diphosphate biosynthesis. *Journal of Bacteriology*, **182**, 891-897.

Lange B.M., Wildung M.R., Mccaskill D. & Croteau R. (1998) A family of transketolases that directs isoprenoid biosynthesis via a mevalonate-independent pathway. *Proceedings of the National Academy of Sciences of the United States of America*, **95**, 2100-2104.

Lerdau M. & Gray D. (2003) Ecology and evolution of light-dependent and light-independent phytogenic volatile organic carbon. *New Phytologist*, **157**, 199-211.

Li Z., Ratliff E.A. & Sharkey T.D. (2011) Effect of temperature on postillumination isoprene emission in oak and poplar. *Plant Physiology* **155**, 1037-1046.

Li Z. & Sharkey T.D. (2013a) Metabolic profiling of the methylerythritol phosphate pathway reveals the source of post-illumination isoprene burst from leaves. *Plant, Cell and Environment*, **36**, 429-437.

Li Z. & Sharkey T.D. (2013b) Molecular and pathway controls on biogenic volatile organic compound emissions. In: *Biology, Controls and Models of Tree Volatile Organic Compoud Emissions* (eds Ü. Niinemets & R.K. Monson), pp. 119-151. Springer, Dordrecht.

Lichtenthaler H.K., Rohmer M. & Schwender J. (1997a) Two independent biochemical pathways for isopentenyl diphosphate and isoprenoid biosynthesis in higher plants. *Physiologia Plantarum*, **101**, 643-652.

Lichtenthaler H.K., Schwender J., Disch A. & Rohmer M. (1997b) Biosynthesis of isoprenoids in higher plant chloroplasts proceeds via a mevalonate-independent pathway. *FEBS letters*, **400**, 271-274.

Lohr M., Schwender J. & Polle J.E.W. (2012) Isoprenoid biosynthesis in eukaryotic phototrophs: A spotlight on algae. *Plant Science*, **185–186**, 9-22.

Lois L.M., Campos N., Putra S.R., Danielsen K., Rohmer M. & Boronat A. (1998) Cloning and characterization of a gene from *Escherichia coli* encoding a transketolase-like enzyme that catalyzes the synthesis of D-1-deoxyxylulose 5-phosphate, a common precursor for isoprenoid, thiamin, and pyridoxol biosynthesis. *Proceedings of the National Academy of Sciences of the United States of America*, **95**, 2105-2110.

Loreto F., Ciccioli P., Cecinato A., Brancaleoni E., Frattoni M., Fabozzi C. & Tricoli D. (1996) Evidence of the photosynthetic origin of monoterpenes emitted by *Quercus ilex* L. leaves by ^{13}C labeling. *Plant Physiology* **110**, 1317-1322.

Loreto F., Pinelli P., Brancaleoni E. & Ciccioli P. (2004) ^{13}C labeling reveals chloroplastic and extrachloroplastic pools of dimethylallyl pyrophosphate and their contribution to isoprene formation. *Plant Physiology*, **135**, 1903-1907.

Loreto F. & Sharkey T.D. (1990) A gas-exchange study of photosynthesis and isoprene emission in *Quercus rubra* L. *Planta*, **182**, 523-531.

Loreto F. & Sharkey T.D. (1993) On the relationship between isoprene emission and photosynthetic metabolites under different environmental conditions. *Planta*, **189**, 420-424.

Miller B., Heuser T. & Zimmer W. (1999) A *Synechococcus leopoliensis* SAUG 1402-1 operon harboring the 1-deoxyxylulose 5-phosphate synthase gene and two additional open reading frames is functionally involved in the dimethylallyl diphosphate synthesis. *FEBS Letters*, **460**, 485-490.

Misawa N. (2011) Pathway engineering for functional isoprenoids. *Current Opinion in Biotechnology*, **22**, 627-633.

Mongélard G., Seemann M., Boisson A.-M., Rohmer M., Bligny R. & Rivasseau C. (2011) Measurement of carbon flux through the MEP pathway for isoprenoid synthesis by ^{31}P-NMR spectroscopy after specific inhibition of 2-*C*-methyl-D-erythritol 2,4-cyclodiphosphate reductase. Effect of light and temperature. *Plant, Cell and Environment*, **34**, 1241-1247.

Negm F.B., Cornel F.A. & Plaxton W.C. (1995) Suborganellar localization and molecular characterization of nonproteolytic degraded leukoplast pyruvate kinase from developing castor oil seeds. *Plant Physiology*, **109**, 1461-1469.

Ni S., Robinson H., Marsing G.C., Bussiered D.E. & Kennedy M.A. (2004) Structure of 2*C*-methyl-D-erythritol-2,4-cyclodiphosphate synthase from *Shewanella oneidensis* at 1.6Å : identification of farnesyl pyrophosphate trapped in a hydrophobic cavity. *Acta Crystallographica Section D: Biological Crystallography*, **60**, 1949-1957.

Ostrovskiĭ D.N., Demina G.P., Deriabina I., Goncharenko A.V., Eberl M., Shumaev K.B. & Shashkov A.S. (2003) Properties of 2-*C*-methyl-D-erythritol 2,4-cyclopyrophosphate--an intermediate in the non-mevalonate isoprenoid biosynthesis. *Prikladnaia Biokhimiia I Mikrobiologiia*, **39**, 565-570.

Ostrovsky D., Diomina G., Lysak E., Matveeva E., Ogrel O. & Trutko S. (1998) Effect of oxidative stress on the biosynthesis of 2-*C*-methyl-D-erythritol-2,4-cyclopyrophosphate and isoprenoids by several bacterial strains. *Archives of Microbiology*, **171**, 69-72.

Ostrovsky D., Kharatian E., Malarova I., Shipanova I., Sibeldina L., Shashkov A. & Tantsirev G. (1992a) Synthesis of a new organic pyrophosphate in large quantities is induced in some bacteria by oxidative stress. *Biofactors*, **4**, 261-264.

Ostrovsky D., Shipanova I., Sibeldina L., Shashkov A., Kharatian E., Malyarova I. & Tantsyrev G. (1992b) A new cyclopyrophosphate as a bacterial antistressor? *FEBS Letters*, **298**, 159-161.

Ostrovsky D.N., Dyomina G.R., Deryabina Y.I., Goncharenko A.V., Eberl M., Shumaev K.B. & Shashkov A.S. (2003) Properties of 2-*C*-methyl-D-erythritol 2,4-cyclopyrophosphate, an intermediate in nonmevalonate isoprenoid biosynthesis. *Applied Biochemistry and Microbiology*, **39**, 497-502.

Patel H., Nemeria N.S., Brammer L.A., Freel Meyers C.L. & Jordan F. (2012) Observation of thiamin-bound intermediates and microscopic rate constants for their interconversion on 1-deoxy-D-xylulose 5-phosphate synthase: 600-fold rate acceleration of pyruvate decarboxylation by D-glyceraldehyde-3-phosphate. *Journal of the American Chemical Society*, **134**, 18374-18379.

Phillips M.A., León P., Boronat A. & Rodríguez-Concepción M. (2008) The plastidial MEP pathway: unified nomenclature and resources. *Trends in Plant Science*, **13**, 619-623.

Plaxton W.C., Dennis D.T. & Knowles V.L. (1990) Purification of leucoplast pyruvate kinase from developing castor bean endosperm. *Plant Physiology*, **94**, 1528-1534.

Plaxton W.C., Smith C.R. & Knowles V.L. (2002) Molecular and regulatory properties of leucoplast pyruvate kinase from *Brassica napus* (rapeseed) suspension cells. *Archives of Biochemistry and Biophysics*, **400**, 54-62.

Potosnak M.J., LeStourgeon L. & Nunez O. (2014) Increasing leaf temperature reduces the suppression of isoprene emission by elevated CO_2 concentration. *Science of The Total Environment*, **481**, 352-359.

Prabhakar V., Löttgert T., Gigolashvili T., Bell K., Flügge U.-I. & Häusler R.E. (2009) Molecular and functional characterization of the plastid-localized phosphoenolpyruvate enolase (ENO1) from *Arabidopsis thaliana*. *FEBS Letters*, **583**, 983-991.

Proteau P.J. (2004) 1-Deoxy-D-xylulose 5-phosphate reductoisomerase: an overview. *Bioorganic Chemistry*, **32**, 483-493.

Puan K.-J., Wang H., Dairi T., Kuzuyama T. & Morita C.T. (2005) *fldA* is an essential gene required in the 2-*C*-methyl-D-erythritol 4-phosphate pathway for isoprenoid biosynthesis. *FEBS Letters*, **579**, 3802-3806.

Rasulov B., Copolovici L., Laisk A. & Niinemets Ü. (2009a) Postillumination isoprene emission: in vivo measurements of dimethylallyldiphosphate pool size and isoprene synthase kinetics in aspen leaves. *Plant Physiology*, **149**, 1609-1618.

Rasulov B., Huve K., Bichele I., Laisk A. & Niinemets Ü. (2010) Temperature response of isoprene emission in vivo reflects a combined effect of substrate limitations and isoprene synthase activity: a kinetic analysis. *Plant Physiology*, **154**, 1558-1570.

Rasulov B., Huve K., Laisk A. & Niinemets Ü. (2011) Induction of a longer term component of isoprene release in darkened aspen leaves: origin and regulation under different environmental conditions. *Plant Physiology*, **156**, 816-831.

Rasulov B., Huve K., Valbe M., Laisk A. & Niinemets Ü. (2009b) Evidence that light, carbon dioxide, and oxygen dependencies of leaf isoprene emission are driven by energy status in hybrid aspen. *Plant Physiology*, **151**, 448-460.

Richard S.B., Bowman M.E., Kwiatkowski W., Kang I., Chow C., Lillo A.M., Cane D.E. & Noel J.P. (2001) Structure of 4-diphosphocytidyl-2-*C*-methylerythritol synthetase involved in mevalonate-independent isoprenoid biosynthesis. *Nature Structural Biology*, **8**, 641-648.

Richard S.B., Ferrer J.L., Bowman M.E., Lillo A.M., Tetzlaff C.N., Cane D.E. & Noel J.P. (2002) Structure and mechanism of 2-*C*-methyl-D-erythritol 2,4-cyclodiphosphate synthase an enzyme in the mevalonate-independent isoprenoid biosynthetic pathway. *Journal of Biological Chemistry*, **277**, 8667-8672.

Richard S.B., Lillo A.M., Tetzlaff C.N., Bowman M.E., Noel J.P. & Cane D.E. (2004) Kinetic analysis of *Escherichia coli* 2-*C*-methyl-D-erythritol-4-phosphate cytidyltransferase, wild type and mutants, reveals roles of active site amino acids. *Biochemistry*, **43**, 12189-12197.

Rivasseau C., Seemann M., Boisson A.-M., Streb P., Gout E., Douce R., Rohmer M. & Bligny R. (2009) Accumulation of 2-*C*-methyl-D-erythritol 2,4-cyclodiphosphate in illuminated plant leaves at supraoptimal temperatures reveals a bottleneck of the prokaryotic methylerythritol 4-phosphate pathway of isoprenoid biosynthesis. *Plant, Cell and Environment*, **32**, 82-92.

Rodríguez-Concepción M. (2006) Early steps in isoprenoid biosynthesis: multilevel regulation of the supply of common precursors in plant cells. *Phytochemistry Reviews*, **5**, 1-15.

Rodríguez-Concepción M. & Boronat A. (2002) Elucidation of the methylerythritol phosphate pathway for isoprenoid biosynthesis in bacteria and plastids. A metabolic milestone achieved through genomics. *Plant Physiology*, **130**, 1079-1089.

Rohdich F., Kis K., Bacher A. & Eisenreich W. (2001) The non-mevalonate pathway of isoprenoids: genes, enzymes and intermediates. *Current Opinion in Chemical Biology*, **5**, 535-540.

Rohmer M. (1999) The discovery of a mevalonate-independent pathway for isoprenoid biosynthesis in bacteria, algae and higher plants. *Natural Product Reports*, **16**, 565-574.

Rohmer M. (2003) Mevalonate-independent methylerythritol phosphate pathway for isoprenoid biosynthesis. Elucidation and distribution. *Pure and Applied Chemistry*, **75**, 375-388.

Rohmer M., Knani M., Simonin P., Sutter B. & Sahm H. (1993) Isoprenoid biosynthesis in bacteria: a novel pathway for the early steps leading to isopentenyl diphosphate. *Biochemical Journal*, **295**, 517-524.

Rohmer M., Seemann M., Horbach S., Bringer-Meyer S. & Sahm H. (1996) Glyceraldehyde 3-phosphate and pyruvate as precursors of isoprenic units in an alternative non-mevalonate pathway for terpenoid biosynthesis. *Journal of the American Chemical Society*, **118**, 2564-2566.

Rosenstiel T.N., Potosnak M.J., Griffin K.L., Fall R. & Monson R.K. (2003) Increased CO_2 uncouples growth from isoprene emission in an agriforest ecosystem. *Nature*, **421**, 256-259.

Sacchettini J.C. & Poulter C.D. (1997) Creating isoprenoid diversity. *Science*, **277**, 1788-1789.

Sanadze G.A., Dzhaiani G.I. & Tevzadze I.M. (1972) Incorporation into the isoprene molecule of carbon from $^{13}CO_2$ assimilated during photosynthesis. *Soviet Plant Physiology*, **19**, 17-20.

Schnitzler J.-P., Grau M., Kreuzwieser J., Heizmann U., Rennenberg H., Wisthaler A. & Hansel A. (2004) Contribution of different carbon sources to isoprene biosynthesis in poplar leaves. *Plant Physiology*, **135**, 152-160.

Schwender J., Seemann M., Lichtenthaler H.K. & Rohmer M. (1996) Biosynthesis of isoprenoids (carotenoids, sterols, prenyl side-chains of chlorophylls and plastoquinone) via a novel pyruvate/glyceraldehyde 3-phosphate non-mevalonate pathway in the green alga *Scenedesmus obliquus*. *Biochemical Journal*, **316**, 73-80.

Schwender J., Zeidler J., Gröner R., Müller C., Focke M., Braun S. & Lichtenthaler H.K. (1997) Incorporation of 1-deoxy-D-xylulose into isoprene and phytol by higher plants and algae. *FEBS letters*, **414**, 129-134.

Seemann M., Bui B.T.S., Wolff M., Miginiac-Maslow M. & Rohmer M. (2006) Isoprenoid biosynthesis in plant chloroplasts via the MEP pathway: Direct thylakoid/ferredoxin-dependent photoreduction of GcpE/IspG. *FEBS letters*, **580**, 1547-1552.

Seemann M., Bui B.T.S., Wolff M., Tritsch D., Campos N., Boronat A., Marquet A. & Rohmer M. (2002) Isoprenoid biosynthesis through the methylerythritol phosphate

pathway: the (*E*)-4-hydroxy-3-methylbut-2-enyl diphosphate synthase (GcpE) is a [4Fe-4S] protein. *Angewandte Chemie International Edition* **41**, 4337-4339.

Seemann M. & Rohmer M. (2007) Isoprenoid biosynthesis via the methylerythritol phosphate pathway: GcpE and LytB, two novel iron–sulphur proteins. *Comptes Rendus Chimie*, **10**, 748-755.

Sharkey T.D. & Monson R.K. (2014) The future of isoprene emission from leaves, canopies and landscapes. *Plant, Cell and Environment*, **37**, 1727–1740.

Sharkey T.D. & Vanderveer P.J. (1989) Stromal phosphate concentration is low during feedback limited photosynthesis. *Plant Physiology*, **91**, 679-684.

Sharkey T.D., Wiberley A.E. & Donohue A.R. (2008) Isoprene emission from plants: why and how. *Annals of Botany*, **101**, 5-18.

Silver G.M. & Fall R. (1991) Enzymatic synthesis of isoprene from dimethylallyl diphosphate in aspen leaf extracts. *Plant Physiology*, **97**, 1588-1591.

Silver G.M. & Fall R. (1995) Characterization of aspen isoprene synthase, an enzyme responsible for leaf isoprene emission to the atmosphere. *Journal of Biological Chemistry*, **270**, 13010-13016.

Slabas A.R. & Walker D.A. (1976) Transient inhibition by ribose 5-phosphate of photosynthetic O_2 evolution in a reconstituted chloroplast system. *Biochimica et Biophysica Acta*, **430**, 154-164.

Sprenger G.A., Schörken U., Wiegert T., Grolle S., Graaf A.A.D., Taylor S.V., Begley T.P., Bringer-Meyer S. & Sahm H. (1997) Identification of a thiamin-dependent synthase in *Escherichia coli* required for the formation of the 1-deoxy-D-xylulose 5-phosphate precursor to isoprenoids, thiamin, and pyridoxol. *Proceedings of the National Academy of Sciences of the United States of America*, **94**, 12857-12862.

Stitt M. & Rees T.A. (1979) Capacities of pea chloroplasts to catalyse the oxidative pentose phosphate pathway and glycolysis. *Phytochemistry*, **18**, 1905-1911.

Sun Z., Huve K., Vislap V. & Niinemets Ü. (2013) Elevated [CO_2] magnifies isoprene emissions under heat and improves thermal resistance in hybrid aspen. *Journal of Experimental Botany*, **64**, 5509-5523.

Sweeney A.M., Lange R., Fernandes R.P.M., Schulz H., Dale G.E., Douangamath A., Proteau P.J. & Oefner C. (2005) The crystal structure of *E.coli* 1-deoxy-D-xylulose-5-phosphate reductoisomerase in a ternary complex with the antimalarial compound fosmidomycin and NADPH reveals a tight-binding closed enzyme conformation. *Journal of Molecular Biology*, **345**, 115-127.

Szecowka M., Heise R., Tohge T., Nunes-Nesi A., Vosloh D., Huege J., Feil R., Lunn J., Nikoloski Z., Stitt M., Fernie A.R. & Arrivault S. (2013) Metabolic fluxes in an illuminated *Arabidopsis* rosette. *The Plant Cell*, **25**, 694-714.

Trowbridge A.M., Asensio D., Eller A.S.D., Way D.A., Wilkinson M.J., Schnitzler J.-P., Jackson R.B. & Monson R.K. (2012) Contribution of various carbon sources toward isoprene biosynthesis in poplar leaves mediated by altered atmospheric CO_2 concentrations. *PLoS ONE*, **7**, e32387.

Tsang A., Seidle H., Jawaid S., Zhou W., Smith C. & Couch R.D. (2011) *Francisella tularensis* 2-*C*-methyl-D-erythritol 4-phosphate cytidylyltransferase: kinetic characterization and phosphoregulation. *PLoS One*, **6**, e20884.

Voll L., Häusler R.E., Hecker R., Weber A., Weissenböck G., Fiene G., Waffenschmidt S. & Flügge U.-I. (2003) The phenotype of the *Arabidopsis cue1* mutant is not simply caused by a general restriction of the shikimate pathway. *The Plant Journal*, **36**, 301-317.

Vranova E., Coman D. & Gruissem W. (2013) Network analysis of the MVA and MEP pathways for isoprenoid synthesis. *Annual Review of Plant Biology*, **64**, 665-700.

Wanke M., Skorupinska-Tudek K. & Swiezewska E. (2001) Isoprenoid biosynthesis via 1-deoxy-D-xylulose 5-phosphate/2-*C*-methyl-D-erythritol 4-phosphate (DOXP/MEP) pathway. *Acta Biochimica Polonica*, **48**, 663-672.

Wiberley A.E., Linskey A.R., Falbel T.G. & Sharkey T.D. (2005) Development of the capacity for isoprene emission in kudzu. *Plant, Cell and Environment*, **28**, 898-905.

Wolfertz M., Sharkey T.D., Boland W. & Kühnemann F. (2004) Rapid regulation of the methylerythritol 4-phosphate pathway during isoprene synthesis. *Plant Physiology*, **135**, 1939-1945.

Wolfertz M., Sharkey T.D., Boland W., Kühnemann F., Yeh S. & Weise S.E. (2003) Biochemical regulation of isoprene emission. *Plant, Cell and Environment*, **26**, 1357-1364.

Wolff M., Seemann M., Bui B.T.S., Frapart Y., Tritsch D., Estrabot A.G., Rodríguez-Concepción M., Boronat A., Marquet A. & Rohmer M. (2003) Isoprenoid biosynthesis via the methylerythritol phosphate pathway: the (*E*)-4-hydroxy-3-methylbut-2-enyl diphosphate reductase (LytB/IspH) from *Escherichia coli* is a [4Fe-4S] protein. *FEBS Letters* **541** 115-120.

Xiao Y., Chu L., Sanakis Y. & Liu P. (2009) Revisiting the IspH catalytic system in the deoxyxylulose phosphate pathway: achieving high activity. *Journal of the American Chemical Society*, **131**, 9931-9933.

Xiao Y., Savchenko T., Baidoo E.E.K., Chehab W.E., Hayden D.M., Tolstikov V., Corwin J.A., Kliebenstein D.J., Keasling J.D. & Dehesh K. (2012) Retrograde signaling by the plastidial metabolite MEcPP regulates expression of nuclear stress-response genes. *Cell* **149**, 1525-1535.

Xu W., Lees N.S., Adedeji D., Wiesner J., Jomaa H., Hoffman B.M. & Duin E.C. (2010) Paramagnetic intermediates of (*E*)-4-hydroxy-3-methylbut-2-enyl diphosphate synthase (GcpE/IspG) under steady-state and pre-steady-state conditions. *Journal of the American Chemical Society*, **132**, 14509-14520.

Yang D., Ma P., Liang X., Wei Z., Liang Z., Liu Y. & Liu F. (2012) PEG and ABA trigger methyl jasmonate accumulation to induce the MEP pathway and increase tanshinone production in *Salvia miltiorrhiza* hairy roots. *Physiologia Plantarum*, **146**, 173-183.

Zeidler J.G., Lichtenthaler H.K., May H.U. & Lichtenthaler F.W. (1997) Is isoprene emitted by plants synthesized via the novel isopentenyl pyrophosphate pathway? *Zeitschrift für Naturforschung*, **52c**, 15-23.

Zhao L., Chang W., Xiao Y., Liu H. & Liu P. (2013) Methylerythritol phosphate pathway of isoprenoid biosynthesis. *Annual Review of Biochemistry*, **82**, 497-530.

Zhou K., Zou R., Stephanopoulos G. & Too H.-P. (2012) Metabolite profiling identified methylerythritol cyclodiphosphate efflux as a limiting step in microbial isoprenoid production. *PLoS One*, **7**, e47513.

CHAPTER 5

Concluding remarks

5.1 INTRODUCTION

This thesis mainly encompasses the study of the metabolic regulation of the 2-*C*-methyl-D-erythritol 4-phosphate (MEP) pathway. It is an important biochemical pathway leading to the biosynthesis of the precursors of isoprenoids, which are ubiquitous natural products present in all living organisms (Wanke *et al.* 2001). This pathway was discovered in the early 1990s and as a comparatively new pathway, not much was known about the regulatory mechanisms involved in this pathway (Rohmer *et al.* 1993). Many isoprenoids have important commercial applications and they are important targets for biotechnological applications. Regulatory mechanisms of this pathway are also important to environmental chemists as they are interested in building up a suitable mechanistic model for the prediction of global isoprene emission considering its adverse effects on the atmospheric chemistry. So, there are growing interests to study the regulatory mechanisms of this pathway.

Understanding the metabolic regulation of the MEP pathway was an important goal in the field when I first started my graduate studies. Earlier observations of genetic regulation demonstrated the regulatory role of 1-deoxy-D-xylulose-5-phosphate synthase (DXS), the first enzyme of the MEP pathway (Enfissi *et al.* 2005; Estévez *et al.* 2001; Gong *et al.* 2006; Lois *et al.* 2000; Morris *et al.* 2006; Wiberley *et al.* 2009). In early 2000's, Wolfertz and coworkers suggested from their feeding experiment that a metabolic feedback regulation of DXS is likely to be operative in the MEP pathway (Wolfertz *et al.* 2004; Wolfertz *et al.* 2003). This previous work directed me to focus my graduate research on exploration of the role of DXS in the metabolic regulation of the MEP pathway.

5.2 REVIEW OF WORK

5.2.1 Feedback regulation of PtDXS

In this work, my aim was to study the role of DXS in the metabolic regulation of the MEP pathway by studying the kinetics of DXS in the presence of different metabolites of this pathway. A common assay used to study the activity of DXS involved a coupled spectrophotometric assay. However, this assay was not useful in studying the kinetic behavior of DXS in presence of different MEP pathway metabolites. Therefore, I developed an independent assay for DXS based on liquid chromatography-tandem mass spectrometry (LC-MS/MS). This assay directly measured the amount of 1-deoxy-D-xylulose 5-phosphate (DXP) produced in the catalytic reaction of DXS. Subsequently, I used this assay to study the effect of different MEP pathway metabolites on *Populus trichocarpa* DXS (*Pt*DXS) activity.

Among the different metabolites of the MEP pathway, it was observed that isopentenyl diphosphate (IDP) and dimethylallyl diphosphate (DMADP), the two end products of this pathway, significantly inhibit *Pt*DXS activity (Banerjee *et al.* 2013). The detailed mechanistic study of this inhibition showed that both IDP and DMADP compete with thiamin diphosphate (ThDP) for binding at the active site of the enzyme (Banerjee *et al.* 2013). The computational modeling study, which was done in collaboration with Dr. Honggao Yan (Biochemistry and Molecular Biology, Michigan State University), also predicted that both ThDP and IDP/DMADP use similar interactions for binding at the active site of the enzyme and thus supported these experimental results (Banerjee *et al.* 2013). This work demonstrated that feedback inhibition of *Pt*DXS by IDP and DMADP plays a significant role in controlling the carbon flux through the

MEP pathway and therefore, contributes to the metabolic regulation of this pathway. Soon after, Ghirardo and coworkers (2014) also demonstrated that feedback regulation of poplar DXS *in vivo* by plastidic DMADP constitutes a significant regulatory mechanism of this pathway.

5.2.2 Improvement of PtDXS by site-directed mutagenesis

The aim of this work was to improve the activity of *Pt*DXS by reducing the affinity of this enzyme for IDP/DMADP over ThDP. Two residues, Ala-147 and Ala-352, were chosen to be modified as they were critical for binding the carbon chain of IDP and DMADP with the enzyme. Site-directed mutagenesis was used to mutate these residues to Gly to generate A147G*Pt*DXS, A352G*Pt*DXS, and the double mutant A147G/A352G*Pt*DXS. It was observed that these mutations affect the binding of both ThDP and IDP/DMADP. However one of the mutants, A147G*Pt*DXS, exhibited reduced binding affinity for the inhibitors compared to that of the WT*Pt*DXS. A147G*Pt*DXS was also found to have a higher K_m for ThDP as well as higher k_{cat} than those of the WT enzyme. Overall, A147G*Pt*DXS was found to be a better enzyme considering it is faster with a lower K_i for the inhibitors. Therefore, A147G*Pt*DXS would be important for biotechnological applications if higher level of ThDP could be maintained.

5.3 FUTURE PERSPECTIVE

Understanding of the metabolic regulation of the MEP pathway has started to emerge very recently. Evidence suggests that there might be other regulatory points in this pathway in addition to DXS. It has been demonstrated that the cyclic intermediate, methylerythritol 2,4-

cyclodiphosphate (MEcDP), accumulated the most among all the different metabolites of this pathway under nitrogen atmosphere and in darkness (Li & Sharkey 2013). Additionally, MEcDP has been found to be involved in retrograde signaling from the plastid to some stress-responsive, nuclear-encoded genes (Xiao *et al.* 2012). It is yet to be understood how MEcDP functions as a signaling molecule and whether it has any further role in the regulation of this pathway. It has also been predicted that the iron-sulfur-cluster-containing enzymes, 4-hydroxy-3-methylbut-2-enyl diphosphate (HMBDP) synthase (HDS) and HMBDP reductase (HDR), could be additional regulatory points of this pathway (Banerjee & Sharkey 2014; Rivasseau *et al.* 2009). But their exact role in the regulation has to be established.

Engineering *Pt*DXS by site-directed mutagenesis showed that A147G*Pt*DXS behaves as a better enzyme *in vitro* than the WT*Pt*DXS. It would be interesting to test if the incorporation of this mutant protein in an engineered organism leads to the increased production of isoprenoid precursors *in vivo*. In the course of studying the feedback inhibition of DXS, it was observed that the inhibitors IDP/DMADP compete with ThDP for binding at the active site of the enzyme. Considering the structural similarities of ThDP with IDP/DMADP, it was tempting to predict that other ThDP-dependent enzymes would also be inhibited by IDP and DMADP. I have tested the effect of IDP and DMADP on two different ThDP-dependent enzymes (described in the Chapter 6) and found that these enzymes are inhibited by IDP/DMADP to different extents. At this point, the physiological relevance of this is not clear. In order to obtain a more conclusive explanation of the physiological relevance of this phenomenon, more ThDP-dependent enzymes would have to be tested in the future.

LITERATURE CITED

LITERATURE CITED

Banerjee A. & Sharkey T.D. (2014) Methylerythritol 4-phosphate (MEP) pathway metabolic regulation. *Natural Product Reports*, **31**, 1043-1055.

Banerjee A., Wu Y., Banerjee R., Li Y., Yan H. & Sharkey T.D. (2013) Feedback inhibition of deoxy-D-xylulose-5-phosphate synthase regulates the methylerythritol 4-phosphate pathway. *Journal of Biological Chemistry*, **288**, 16926-16936.

Enfissi E.M.A., Fraser P.D., Lois L.M., Boronat A., Schuch W. & Bramley P.M. (2005) Metabolic engineering of the mevalonate and non-mevalonate isopentenyl diphosphate-forming pathways for the production of health-promoting isoprenoids in tomato. *Plant Biotechnology Journal*, **3**, 17-27.

Estévez J.M., Cantero A., Reindl A., Reichler S. & León P. (2001) 1-Deoxy-D-xylulose-5-phosphate synthase, a limiting enzyme for plastidic isoprenoid biosynthesis in plants. *Journal of Biological Chemistry*, **276**, 22901-22909.

Ghirardo A., Wright L.P., Bi Z., Rosenkranz M., Pulido P., Rodríguez-Concepción M., Niinemets Ü., Brüggemann N., Gershenzon J. & Schnitzler J.-P. (2014) Metabolic flux analysis of plastidic isoprenoid biosynthesis in poplar leaves emitting and non-emitting isoprene. *Plant Physiology*, **165**, 37-51.

Gong Y.F., Liao Z.H., Guo B.H., Sun X.F. & Tang K.X. (2006) Molecular cloning and expression profile analysis of *Ginkgo biloba DXS* gene encoding 1-deoxy-D-xylulose 5-phosphate synthase, the first committed enzyme of the 2-*C*-methyl-D-erythritol 4-phosphate pathway. *Planta Medica*, **72**, 329-335.

Li Z. & Sharkey T.D. (2013) Metabolic profiling of the methylerythritol phosphate pathway reveals the source of post-illumination isoprene burst from leaves. *Plant, Cell and Environment*, **36**, 429-437.

Lois L.M., Rodríguez-Concepción M., Gallego F., Campos N. & Boronat A. (2000) Carotenoid biosynthesis during tomato fruit development: regulatory role of 1-deoxy-D-xylulose 5-phosphate synthase. *Plant Journal*, **22**, 503-513.

Morris W.L., Ducreux L.J.M., Hedden P., Millam S. & Taylor M.A. (2006) Overexpression of a bacterial 1-deoxy-D-xylulose 5-phosphate synthase gene in potato tubers perturbs the isoprenoid metabolic network: implications for the control of the tuber life cycle. *Journal of Experimental Botany*, **57**, 3007-3018.

Rivasseau C., Seemann M., Boisson A.-M., Streb P., Gout E., Douce R., Rohmer M. & Bligny R. (2009) Accumulation of 2-*C*-methyl-D-erythritol 2,4-cyclodiphosphate in illuminated plant leaves at supraoptimal temperatures reveals a bottleneck of the prokaryotic

methylerythritol 4-phosphate pathway of isoprenoid biosynthesis. *Plant, Cell and Environment*, **32**, 82-92.

Rohmer M., Knani M., Simonin P., Sutter B. & Sahm H. (1993) Isoprenoid biosynthesis in bacteria: a novel pathway for the early steps leading to isopentenyl diphosphate. *Biochemical Journal*, **295**, 517-524.

Wanke M., Skorupinska-Tudek K. & Swiezewska E. (2001) Isoprenoid biosynthesis via 1-deoxy-D-xylulose 5-phosphate/2-*C*-methyl-D-erythritol 4-phosphate (DOXP/MEP) pathway. *Acta Biochimica Polonica*, **48**, 663-672.

Wiberley A.E., Donohue A.R., Westphal M.M. & Sharkey T.D. (2009) Regulation of isoprene emission from poplar leaves throughout a day. *Plant, Cell and Environment*, **32**, 939-947.

Wolfertz M., Sharkey T.D., Boland W. & Kühnemann F. (2004) Rapid regulation of the methylerythritol 4-phosphate pathway during isoprene synthesis. *Plant Physiology*, **135**, 1939-1945.

Wolfertz M., Sharkey T.D., Boland W., Kühnemann F., Yeh S. & Weise S.E. (2003) Biochemical regulation of isoprene emission. *Plant, Cell and Environment*, **26**, 1357-1364.

Xiao Y., Savchenko T., Baidoo E.E.K., Chehab W.E., Hayden D.M., Tolstikov V., Corwin J.A., Kliebenstein D.J., Keasling J.D. & Dehesh K. (2012) Retrograde signaling by the plastidial metabolite MEcPP regulates expression of nuclear stress-response genes. *Cell* **149**, 1525-1535.

CHAPTER 6

Additional studies: General effect of IDP and DMADP on ThDP-dependent enzymes

6.1 INTRODUCTION

Thiamin diphosphate (ThDP, previously known as thiamin pyrophosphate, TPP) is a widely known cofactor used by various enzymes for their catalytic activity. This cofactor can be biosynthesized by various microorganisms, fungi, and plants, whereas most other eukaryotes cannot (Chatterjee *et al.* 2007). ThDP is the diphosphorylated derivative of thiamin, which is an essential nutrient (vitamin B_1) for animals. They are dependent on their dietary uptake for the requirement of thiamin as they do not synthesize it (Bunik *et al.* 2013; Rapala-Kozik 2011). The essential role of this molecule in most organisms, and its involvement in several central points of anabolic and catabolic metabolisms such as the pentose-phosphate pathway and the TCA cycle, suggest an early evolutionary emergence of this molecule (Frank *et al.* 2007). The thiamin molecule is composed of two heterocycle moieties; a substituted pyrimidine (4-amino-2-methyl-5-hydroxymethylpyrimidyl) ring and a substituted thiazole [4-methyl-5-(2-hydroxymethyl)-thiazolium] ring. These rings are linked by a methylene bridge (Figure 6.1) (Bunik *et al.* 2013; Rapala-Kozik 2011). In addition to free thiamin, a variety of phosphorylated and adenylated derivatives, such as thiamin monophosphate (ThMP), ThDP, thiamin triphosphate (ThTP), adenosine thiamin triphosphate (AThTP), and adenosine thiamin diphosphate (AThDP) are known (Bunik *et al.* 2013; Rapala-Kozik 2011). Among the different derivatives of thiamin, ThDP has been found to have the most widely recognized biological role (Bunik *et al.* 2013). ThDP constitutes the major part of the total *in vivo* pool of thiamin and mostly acts as a cofactor for a variety of enzymes involved in the central metabolisms (Table 6.1) (Bunik *et al.* 2013).

ThDP-dependent enzymes occur in numerous biosynthetic pathways and catalyze a wide spectrum of chemical reactions (Müller *et al.* 2009). They exhibit the potential of both the

cleavage and formation of the C–C bonds (Müller *et al.* 2009; Sprenger & Pohl 1999). Some of the reactions catalyzed by ThDP-dependent enzymes include the nonoxidative and oxidative decarboxylation of α-keto acids, carboligation, synthesis of α-hydroxy ketones, and the transfer of activated aldehyde to a variety of acceptors (Müller *et al.* 2009; Sprenger & Pohl 1999). Some ThDP-dependent enzymes can also catalyze C–N, C–O, and C–S bond formation reactions (Müller *et al.* 2009). All of these reactions are broadly categorized into decarboxylating and transferase type of reactions (Frank *et al.* 2007). In spite of catalyzing a wide variety of reactions, all ThDP-dependent enzymes share a common ThDP-bound 'active aldehyde' intermediate formed either by decarboxylation (e.g., of pyruvate through the action of pyruvate decarboxylase, PDC) or by transfer from a suitable donor compound (from xylulose-5-phosphate by transketolase, TK) (Sprenger & Pohl 1999). In addition, some of the enzymes can catalyze the formation of chiral α-hydroxyketones through an acyloin-type condensation reactions (Sprenger & Pohl 1999).

Structurally, weak amino acid sequence similarity (usually less than 20% identity) is observed between various ThDP-dependent enzymes, which are grouped according to the reactions catalyzed by them (Frank *et al.* 2007). However, these enzymes exhibit remarkable similarity in their tertiary folds despite their low amino acid sequence similarity (Frank *et al.* 2007). The structural motif, G-D-G-$(X)_{25\text{-}30}$-N, has been identified as the putative ThDP binding site of these enzymes (Hawkins *et al.* 1989; Lindqvist *et al.* 1992). The cofactor is bound at the active site of these enzymes primarily through its diphosphate group, which coordinates a divalent cation (usually Mg^{2+}) (Frank *et al.* 2007).

In my earlier work, I found that 1-deoxy-D-xylulose-5-phosphate synthase (DXS), the first enzyme of the 2-*C*-methyl-D-erythrytol 4-phosphate (MEP) pathway, is inhibited by the two

isoprenoid precursors, isopentenyl diphosphate (IDP) and dimethylallyl diphosphate (DMADP) (Banerjee *et al.* 2013). DXS is a ThDP-dependent transketolase-type enzyme and it has been reported to have sequence similarity with other ThDP-dependent enzymes like transketolase, pyruvate decarboxylase, and pyruvate dehydrogenase E1 subunit (Bouvier *et al.* 1998; Hahn *et al.* 2001; Lange *et al.* 1998; Lois *et al.* 1998; Mandel *et al.* 1996; Querol *et al.* 2001; Sprenger *et al.* 1997; Xiang *et al.* 2007). Feedback inhibition of *Populus trichocarpa* DXS (*Pt*DXS) by IDP and DMADP, the end products of the MEP pathway, has been demonstrated to play a key role in the metabolic regulation of this pathway (Banerjee *et al.* 2013; Ghirardo *et al.* 2014). The detailed mechanistic study of this inhibition revealed that the inhibitors compete with ThDP for binding at the active site of the enzyme. As a cofactor of DXS, ThDP used to be considered to be a tightly-binding entity of the enzyme. This kind of competitive inhibition against ThDP has not been reported earlier. Interestingly, both IDP and DMADP possess structural similarity with ThDP (Figure 6.2). This led me to examine if IDP/DMADP-mediated inhibition is a general phenomenon for any ThDP-dependent enzymes. In this study, I tested the effect of IDP and DMADP on two ThDP-dependent enzymes, namely pyruvate decarboxylase (PDC) and transketolase (TK).

6.2 EXPERIMENTAL METHODS

6.2.1 Materials

Alcohol dehydrogenase (ADH) from *S. cerevisiae*, required for the coupled assay of *Zymomonas mobilis* PDC *(Zm*PDC), was purchased from Sigma (catalog number: A7011). Commercially available transketolase from *E. coli* (Sigma Aldrich, catalog number: 68138) was used for transketolase assay. Xylulose 5-phosphate (Xu 5-P), one of the substrates of transketolase, was not commercially available. A mixture of D-ribulose 5-phosphate (Ru 5-P) and D-ribulose-5-phosphate 3-epimerase was used to produce Xu 5-P *in situ* in the coupled assay mixture for transketolase. D-Ribulose-5-phosphate 3-epimerase from baker's yeast (*S. cerevisiae*) (catalog number: R-3251) and D-ribulose 5-phosphate sodium salt (catalog number: R9875) were also bought from Sigma-Aldrich. The other reagents for transketolase assay, D-ribose 5-phosphate (R 5-P), disodium salt (catalog number: R-7750), α-glycerophosphate dehydrogenase (GPDH) from rabbit muscle (catalog number: G6751), and triosephosphate isomerase (TPI) from rabbit muscle (catalog number: T6258) were also purchased from Sigma Aldrich.

6.2.2 Overexpression and purification of ZmPDC

*Zm*PDC was cloned into the pET28 vector with a His-tag in the laboratory of Dr. Tim Whitehead (Chemical Engineering & Materials Science, Michigan State University). He generously provided the plasmid construct for my experiments. The plasmid construct of *Zm*PDC was over-expressed in *E. coli* strain BL21(DE3). 500 mL of LB medium containing 25

μg/mL kanamycin was used for protein expression. Cells were grown at 37 ºC until the OD_{600} reached ~0.6. The culture was then cooled with ice to room temperature and induced with 0.5 mM (final concentration) isopropyl β-D-1-thiogalactopyranoside (IPTG). The cells were then incubated at RT for overnight. Next, the *E. coli* cells were harvested by centrifugation and the cell pellets were resuspended in cold lysis buffer (4 mL lysis buffer/g of pellet; 50 mM sodium phosphate, 300 mM NaCl, pH 8.0) containing lysozyme (10 μL/mL of lysis buffer; from Qiagen Qproteome Bacterial Protein Prep Kit, catalog number 37900), Benzonase® Nuclease (1 μL/mL of lysis buffer; from Qiagen Qproteome Bacterial Protein Prep Kit, catalog number 37900), and EDTA-free protease inhibitor cocktail (Sigma, catalog number S8830; final concentration of ~1X the concentration recommended by the manufacturer). The cells were lysed on ice by sonication (Sonifier 250, VWR Scientific). The sonicator was set at 50% duty cycle and the sonication was done for 3 min with pulses of 15 s ON and 15 s OFF at an output control of 1 followed by 2 min with pulses of 15 s ON and 15 s OFF at an output control of 1.5. The lysed cell suspension was centrifuged at ~27,000 g for 30 min at 4 ºC and the supernatant was collected as crude lysate. Ni-NTA resin (Qiagen) was added to the crude lysate (1 mL resin used for every 4 mL dialyzed protein solution) with gentle stirring for 1 h at 4 ºC. The mixture was then loaded to a column and the flow-through was collected. The column was then washed with wash buffer (50 mM sodium phosphate, 300 mM NaCl, 10 mM imidazole, pH 8.0) until OD_{280} of the effluent reached less than 0.05. The protein was then eluted with elution buffer containing elution buffer (50 mM sodium phosphate, 300 mM NaCl, 250 mM imidazole, pH 8.0) containing EDTA-free protease inhibitor cocktail (Sigma, catalog number S8830; final concentration of ~0.5X the concentration recommended by the manufacturer). SDS-PAGE was carried out to identify the fractions containing the most protein. The Ni-NTA column purification was

performed in the cold room at 4 ºC. Fractions containing the maximum amount of the protein were combined together and glycerol was added to a final concentration of 15%. The protein solution was then dispensed into microtubes, frozen in liquid nitrogen, and stored at -80 ºC.

6.2.3 Coupled spectrophotometric assay for ZmPDC

The activity of *Zm*PDC was studied using a coupled spectrophotometric assay. The assay was performed in 96-well plates using a SpectraMax M2 microplate reader (Molecular Devices, Sunnyvale, CA). The assay mixture contained 200 mM Tris-HCl buffer at pH 6.0, 1 mM $MgCl_2$, ThDP, 200 µM NADH, 0.6 U/mL *S. cerevisiae* ADH, and 10 µM *Zm*PDC in a total volume of 200 µL. The reaction was initiated with pyruvate at a final concentration of 10 mM. The concentration of ThDP used to study its K_m was 0-1 mM. The consumption of NADH was monitored spectrophotoetrically at 340 nm. The K_m was evaluated by nonlinear least squares fitting of the data to the Michaelis-Menten equation using the program Origin (http://www.originlab.com/). For the inhibition study, the assay was done as indicated before in the presence of ~30 µM ThDP (~*Km* for ThDP) and 0-1mM IDP or DMADP. In this inhibition assays, the master mix (without pyruvate) was prepared by adding IDP/DMADP first followed by ThDP after 5 min. The reaction was initiated with 10 mM of pyruvate. The non-linear fitting of the IC_{50} curves was done using the program Origin (http://www.originlab.com/) and the determination of K_i of each of the enzymes for both IDP and DMADP were done as reported earlier (Banerjee *et al.* 2013).

6.2.4 Coupled spectrophotometric assay for transketolase (TK)

The activity of TK was also studied using a coupled spectrophotometric assay. The assay was performed in cuvette using a Sigma ZFP 22 dual wavelength filter photometer (Sigma Instrumente, Berlin, Germany). The assay mixture contained 200 mM Tris-HCl buffer at pH 7.70, 1 mM $MgCl_2$, 100 μM NADH, 0.5 U/mL D-Ribulose-5-phosphate 3-epimerase from baker's yeast (*S. cerevisiae*), 1 U/mL rabbit muscle TPI, 1 U/mL rabbit muscle GPDH, and 0.01 U/mL TK from *E. coli* in a total volume of 1 mL. The reaction was initiated with a mixture of R 5-P (final concentration of 0.5 mM) and Ru 5-P (final concentration of 0.5 mM). The concentration of ThDP used to study its K_m was 0-1 mM. The consumption of NADH was monitored spectrophotometrically at 340 nm. The K_m was evaluated by nonlinear least squares fitting of the data to the Michaelis-Menten equation using the program Origin (http://www.originlab.com/). For the inhibition study, the assay was done as indicated before in the presence of ~45 μM ThDP (~K_m for ThDP) and 0-1mM IDP. The reaction was initiated with a mixture of 0.5 mM of R 5-P and 0.5 mM of Ru 5-P. The non-linear fitting of the IC_{50} curves was done using the program Origin (http://www.originlab.com/) and the determination of K_i of each of the enzymes for both IDP and DMADP were done as reported earlier (Banerjee *et al.* 2013).

6.3 RESULTS

6.3.1 Effect of IDP and DMADP on ZmPDC

A coupled spectrophotometric assay was used to study the enzymatic activity of *Zm*PDC, which decarboxylases pyruvate to form acetaldehyde. In this assay, the activity of *Zm*PDC is coupled with alcohol dehydrogenase (ADH), which converts acetaldehyde into ethanol by using NADH. The consumption of NADH can be monitored spectrophotometrically at 340 nm. In presence of excess ADH, the rate of the coupled assay gives a good estimation of the activity of *Zm*PDC. By using this assay, the K_m of *Zm*PDC for ThDP was determined to be 30.5 ± 2.7 μM.

The effect of both IDP and DMADP on *Zm*PDC was tested in presence of ~K_m concentration of ThDP. Both of these metabolites were found to inhibit *Zm*PDC (Figure 6.3). The IC_{50} value of IDP and DMADP for inhibiting *Zm*PDC was calculated to be 123 ± 26 μM and 94 ± 30 μM respectively. The mechanism of this inhibition has not been tested in detail. Assuming competitive inhibition of *Zm*PDC by IDP and DMADP against ThDP (as was observed for DXS), the K_i values are calculated as 50 ± 14 μM for IDP and 47 ± 15 μM for DMADP.

6.3.2 Effect of IDP on E. coli TK

TK catalyzes the formation of glyceraldehyde 3-phosphate (GAP) and sedoheptulose 7-phosphate from xylulose 5-phsphate (Xu 5-P) and ribose 5-phosphate (R 5-P). A coupled spectrophotometric assay was used to study the enzymatic activity of TK. GAP produced in the enzymatic reaction of TK is converted to glycerol 3-phosphate by the coupled reactions of

triosephosphate isomerase (TPI) and glycerophosphate dehydrogenase (GPDH) in presence of NADH (De La Haba *et al.* 1955; Heinrich *et al.* 1971). The consumption of NADH was followed spectrophotometrically at 340 nm. In presence of excess TPI and GPDH, TK activity was measured by the rate of consumption of NADH. In this coupled assay, Xu 5-P was generated *in situ* by the enzymatic reaction of ribulose-5-phosphate 3-epimeras on ribulose 5-phosphate (Ru 5-P) (Ashwell & Hickman 1957). By using this assay, the K_m of TK for ThDP was determined to be 44.3 ± 8.0 μM.

The effect of IDP on TK was tested in presence of ~K_m concentration of ThDP. IDP was found to inhibit TK (Figure 6.4). The IC_{50} value of IDP for inhibiting TK was calculated to be 519 ± 17 μM. The mechanism of this inhibition has not been tested in detail. Assuming competitive inhibition of TK by IDP against ThDP (as it was observed for DXS, another ThDP-dependent enzyme), the K_i value for IDP is calculated to be 259 ± 8 μM.

6.4 DISCUSSION

My previous work showed that *Pt*DXS, a ThDP-dependent enzyme, is inhibited by both IDP and DMADP and these metabolites compete with ThDP for binding at the active site of the enzyme (Banerjee *et al.* 2013). The structural similarity of IDP and DMADP with ThDP as well as the similarity in the catalytic activity of DXS with other ThDP-dependent enzymes led me to examine if this inhibitory effect of IDP/DMADP is a general phenomenon on any ThDP-dependent enzymes. In this study, I tested the effect of these metabolites on *Zm*PDC and *E. coli* TK.

It was observed that inhibition of *Zm*PDC by both IDP and DMADP is effective, but *E. coli* TK inhibition by IDP is not very strong. The K_i values of both IDP and DMADP for *Zm*PDC were comparable to those of K_i values for *Pt*DXS (K_i^{IDP} = 65 ± 4 μM and K_i^{DMADP} = 81 ± 10 μM) (Banerjee *et al.* 2013). On the other hand, the K_i value of IDP for *E. coli* TK is much lower than that for *Pt*DXS. These results indicate that the inhibition by IDP and DMADP may be a general effect on any ThDP-dependent enzymes, but the degree of inhibition might be different for different enzymes. The inhibition of PDC and TK by IDP and DMADP may not have any regulatory potential or any other important physiological relevance given that the enzymes tested here are not metabolically related to IDP or DMADP. The inhibition by IDP and DMADP becomes physiologically relevant only for their own biosynthesis when feedback inhibition of DXS by IDP and DMADP constitutes a significant regulatory mechanism of the MEP pathway.

6.5 CONCLUSION

The aim of this study was to determine whether the inhibitory effect of IDP and DMADP is a general phenomenon on any ThDP-dependent enzymes. The study on *Zm*PDC showed that the inhibitory effect of these metabolites on this enzyme is comparable to that of *Pt*DXS. However, the initial experiments on *E. coli* TK showed that the inhibitory effect of these metabolites is much weaker for TK as compared to *Pt*DXS. From these preliminary studies, it can be concluded that IDP and DMADP could inhibit any ThDP-dependent enzymes, but the degree of inhibition could vary. More ThDP-dependent enzymes need to be studied to determine if this inhibition of ThDP-dependent enzymes by IDP and DMADP could have any evolutionary significance.

6.6 ACKNOWLEDGEMENTS

I would like to thank Laura E. Cheaney, an undergraduate student in my laboratory, who performed the experiments described in this section. I would also like to thank Dr. Tim Whitehead (Chemical Engineering & Materials Science, Michigan State University) for providing me the plasmid construct for *Zm*PDC.

APPENDIX

TABLE 6.1 Various ThDP-dependent enzymes and their catalyzed reactions. (Adapted from (Bunik *et al.* 2013)

Occurrence	Enzyme	Common Abbre-viation	Metabolic pathway and/or catalyzed reaction
Mammals and other kingdoms	Pyruvate dehydrogenase (component E1p of pyruvate dehydrogenase complex)	PDH	Pyruvate entry into the TCA cycle, oxidative decarboxylation of pyruvate
	2-Oxoglutarate dehydrogenase (component E1o of 2-oxoglutarate dehydrogenase)	OGDH	TCA cycle, oxidative decarboxylation of 2-oxoglutarate
	Branched chain 2-oxoacid dehydrogenase (component E1b of branched chain 2-oxoacid dehydrogenase complex)	BCOADH	Branched chain amino acid catabolism, oxidative decarboxylation of the branched chain 2-oxo acids
	Transketolase (glycolaldehyde transferase)	TK	Pentose phosphate pathway
	2-Hydroxyphytanoyl-CoA lyase (2-hydroxyacyl-CoA lyase)	HACL	Peroxisomal alpha-oxidation of 2-methyl-branchd fatty acids
Non-mammalian sources	Pyruvate oxidase (phosphate-dependent pyruvate oxidase)	POX	Oxidative decarboxylation of pyruvate to acetyl phosphate
	Pyruvate ferredoxin oxidoreductase (pyruvate synthase, pyruvate oxidoreductase)	PFOR	Reductive TCA cycle, ferredoxin-dependent synthesis of pyruvate
	2-Oxoglutarate ferredoxin oxidoreductase (2-oxoglutarate synthase)	–	Reductive TCA cycle, ferredoxin-dependent synthesis of 2-oxoglutarate
	2-Oxoisovalerate ferredoxin oxidoreductase	–	Ferredoxin-dependent metabolism of branched chain amino acids
	Indolepyruvate ferredoxin oxidoreductase (indole pyruvate or phenylpyruvate oxidase)	–	Ferredoxin-dependent metabolism of aromatic amino acids
	Oxalate oxidoreductase	–	Oxidation of oxalate coupled to production of reduced ferredoxin
	Dihydroxyacetone synthase (formaldehyde transketolase)	DHAS	Assimilation of methanol, transfer of glycoaldehyde from the xylulose 5-phosphate to the

TABLE 6.1 (cont'd)

Occurrence	Enzyme	Common Abbre-viation	Metabolic pathway and/or catalyzed reaction
Non-mammalian sources			formaldehyde to form dihydroxyacetone and glyceraldehyde-3-phosphate
	Acetohydroxyacid synthase (acetolactate synthase)	AHAS	Biosynthesis of branched chain amino acids, condensation of two pyruvate molecules forming 2-acetolactate and CO_2
	1-Deoxy-D-xylulose 5-phosphate synthase	DXS	Non-mevalonate isoprenoid biosynthesis in plants and bacteria
	2-Succinyl-5-enolpyruvyl-6-hydroxy-3-cyclohexene-1-carboxylic-acid synthase	MenD	Biosynthesis of menaquinone (vitamin K_2), converts isochorismate and 2-oxoglutarate to 2-succinyl-6-hydroxy-2,4-cyclohexadiene-1-carboxylate, pyruvate, and CO_2
	N^2-(2-carboxyethyl)arginine synthase	–	Clavulanic acid biosynthesis, converts glyceraldehyde-3-phosphate and arginine to N2-(2-carboxyethyl)-arginine and phosphate
	Cyclohexane-1,2-dione hydrolase	–	Anaerobic degradation of alicyclic alcohols, conversion of cyclohexane-1,2-dione to 6-oxohexanoate and adipate
	Pyruvate decarboxylase	PDC	Alcoholic fermentation, decarboxylation of pyruvate to acetaldehyde
	Benzoylformate decarboxylase	BFD	Decarboxylation of benzoylformate to benzaldehyde
	Oxayl-CoA decarboxylase	OXC	Catabolism to oxalate, decarboxylation of oxayl-CoA to formyl-CoA
	Phenylpyruvate decarboxylase	–	Catabolism to phenylalanine via the Ehrlich pathway, decarboxylation of phenylpyruvate to phenylacetaldehyde

TABLE 6.1 (cont'd)

Occurrence	Enzyme	Common Abbre-viation	Metabolic pathway and/or catalyzed reaction
Non-mammalian sources	Glyoxylate carboligase (tartronate semialdehyde synthase)	–	Decarboxylation of glyoxylate and ligation to a second molecule of glyoxylate to form tartronate semialdehyde
	2-oxoglutarate decarboxylase	–	Restoration of the TCA cycle in organisms lacking OGDHC, decarboxylation of 2-oxoglutarate to succinyl semialdehyde
	Indolepyruvate decarboxylase	–	Catabolism of tryptophan, decarboxylation of indole-3-pyruvate to indole-3-acetaldehyde
	Sulfopyruvate decarboxylase	–	Coenzyme M biosynthesis, decarboxylation of 3-sulfopyruvate to 2-sulfoacetaldehyde
	3-Phosphonopyruvate decarboxylase	–	Biosynthesis of 2-aminoethylphosphonate, decarboxylation of phosphonopyruvate to phosphonoacetaldehyde
	Phosphoketolase (D-xylulose-5-phosphate phosphoketolase)	PHK	Carbohydrate catabolism, pentose fermentation, xyxlose-5-phosphate cleavage into acetyl phosphate and glyceraldehyde-3-phosphate
	Benzaldehyde lyase (benzoin aldolase)	BAL	Reversible conversion of (*R*)-benzoin (2-hydroxy-1,2-diphenylethanone) into two molecules of benzaldehyde

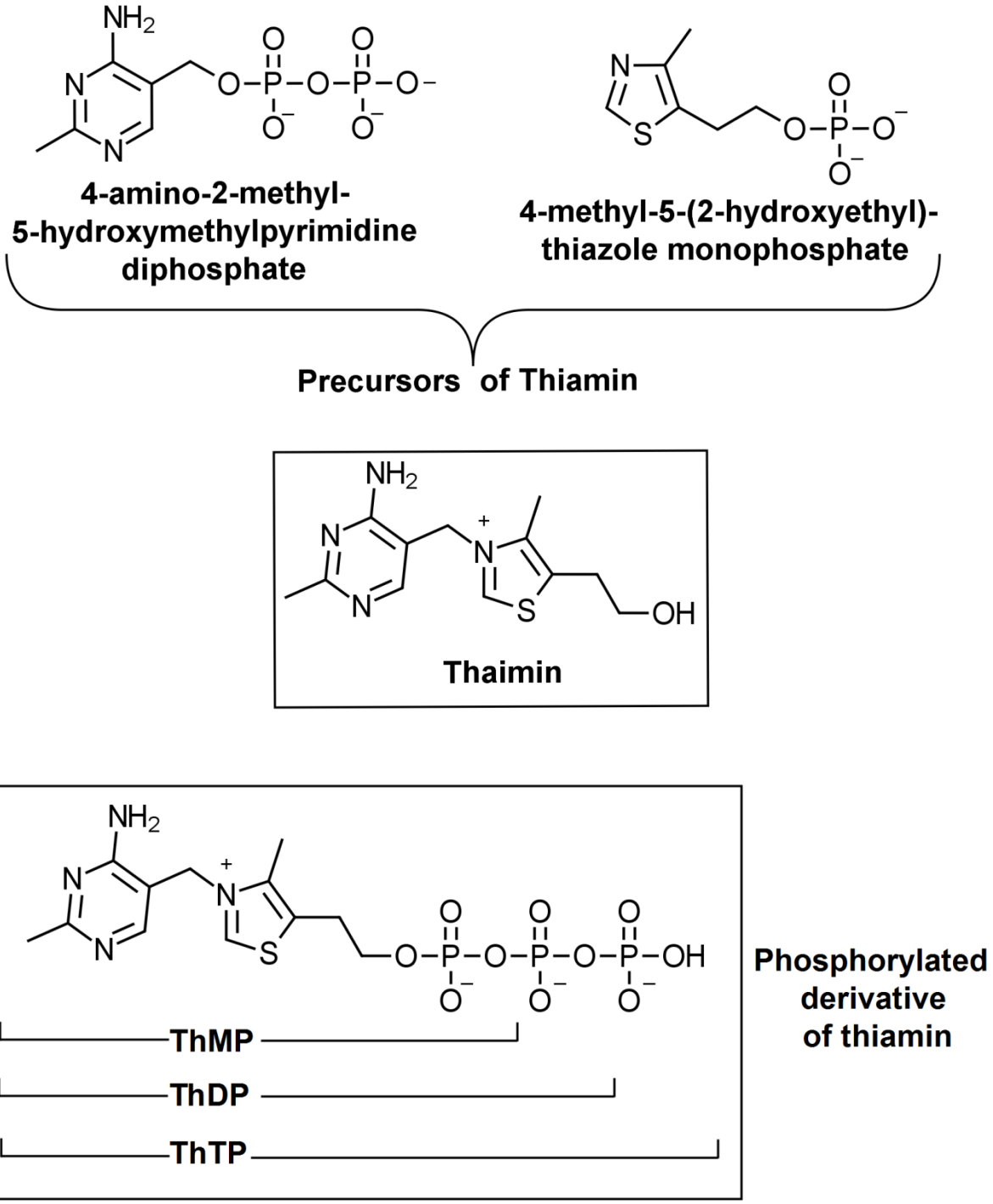

FIGURE 6.1 Thiamin, its biosynthetic precursors and various derivatives. ThMP: thiamin monophosphate; ThDP: thiamin diphosphate, ThTP: thiamin triphosphate, AThTP: adenosine thiamin triphosphate, AThDP: adenosine thiamin diphosphate.

FIGURE 6.1 (cont'd)

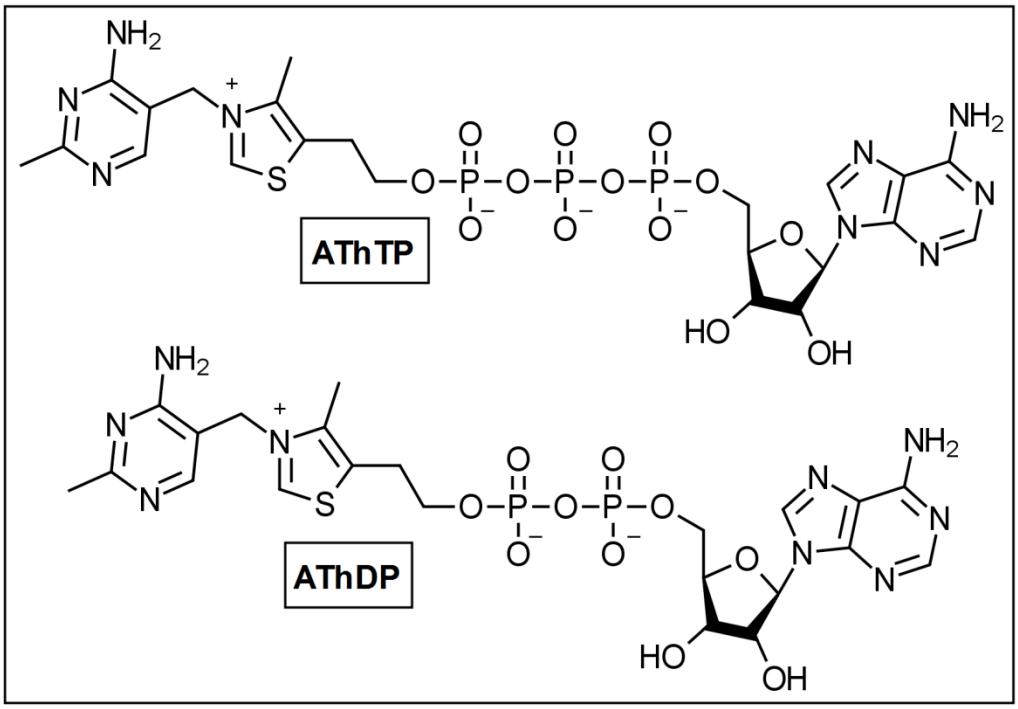

Adenylated derivative of thiamin

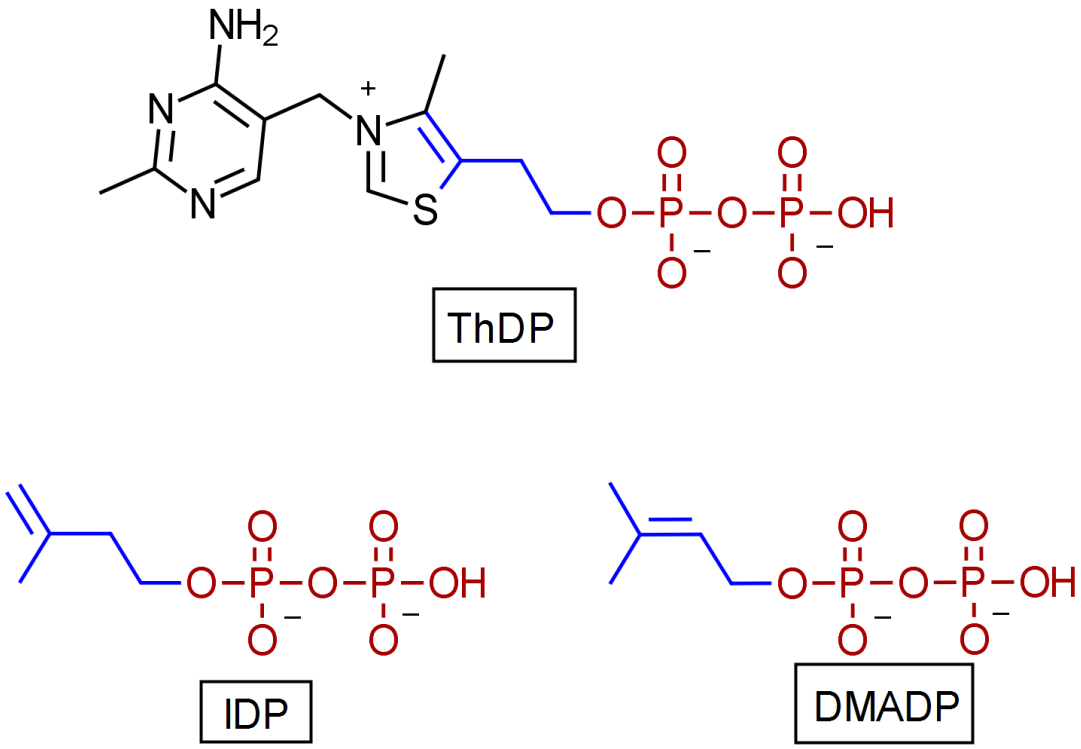

FIGURE 6.2 Structural similarity between ThDP and IDP/DMADP. ThDP: thiamin diphosphate; IDP: isopentenyl diphosphate; DMADP: dimethylallyl diphosphate.

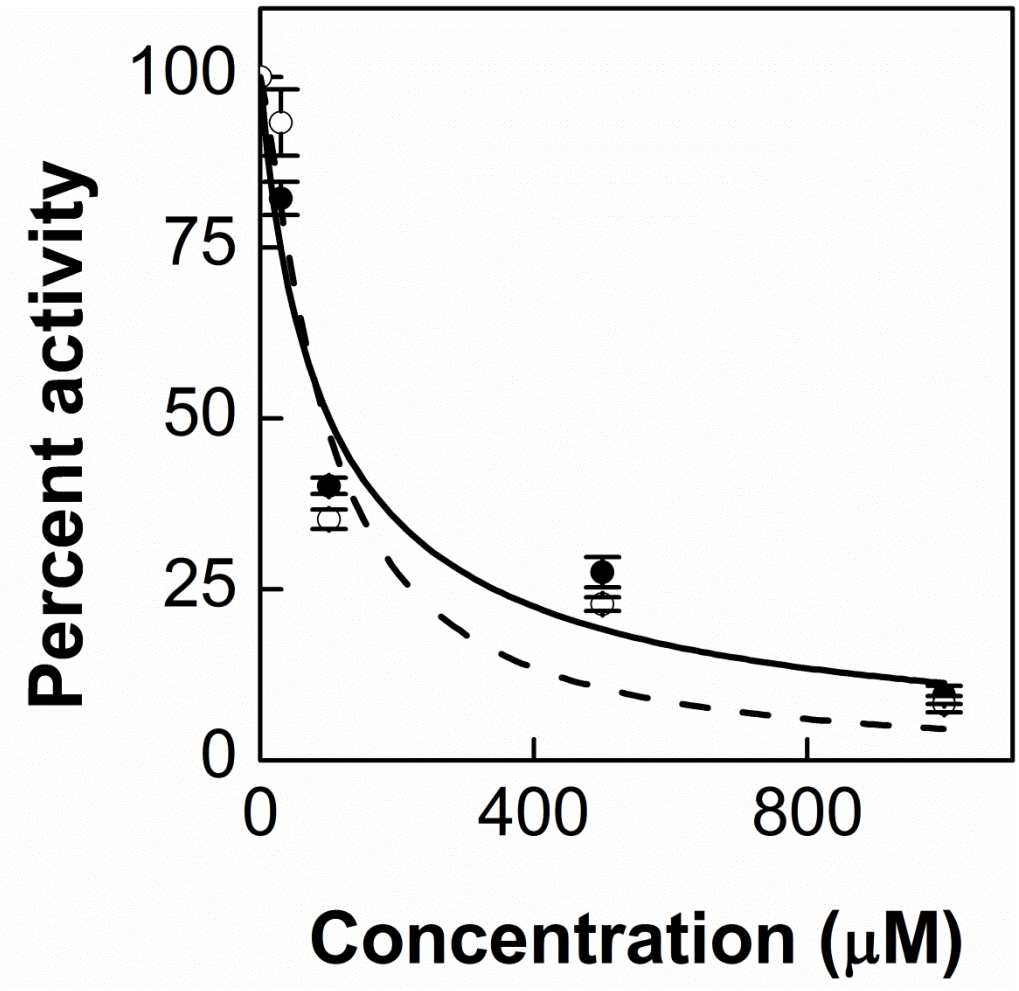

FIGURE 6.3 IC_{50} curve of DMADP and IDP for *Zm*PDC in presence of K_m concentration of ThDP. Each data point represents mean ± SE, n = 4. The IC_{50} curves were obtained from the non-linear curve fitting of the experimental data points using Origin. The solid and empty circles represent the experimental data points for IDP and DMADP respectively and the solid and dotted lines represent the fitted IC_{50} curve for IDP and DMADP respectively. The K_i values of IDP and DMADP were calculated to be ~50 μM and ~47 μM respectively.

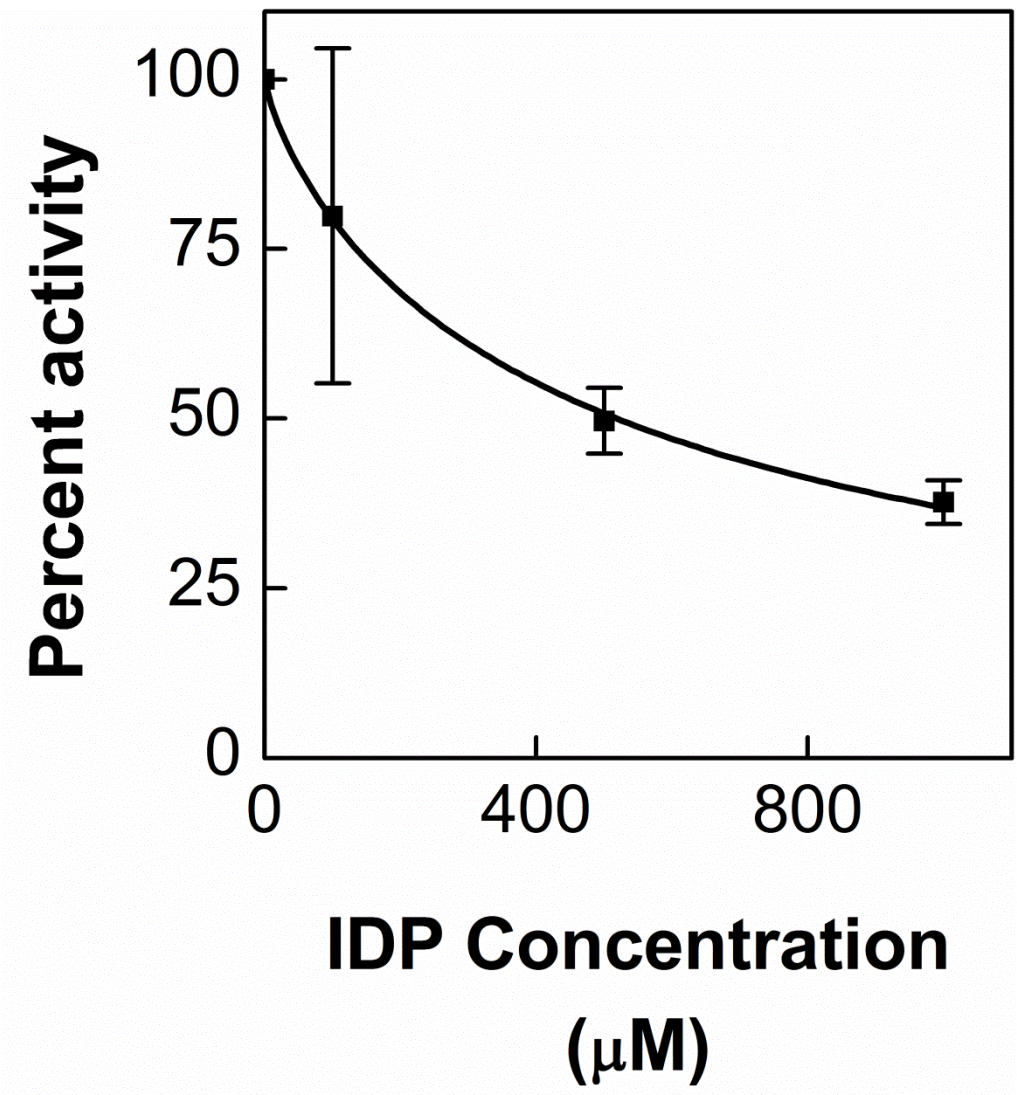

FIGURE 6.4 IC_{50} curve of IDP for TK in presence of K_m concentration of ThDP. Each data point represents mean ± SE, n = 2. The IC_{50} curves were obtained from the non-linear curve fitting of the experimental data points using Origin. The K_i values of IDP was calculated to be ~259 μM.

LITERATURE CITED

LITERATURE CITED

Ashwell G. & Hickman J. (1957) Enzymatic formation of xylulose 5-phosphate from ribose 5-phosphate in spleen. *Journal of Biological Chemistry*, **226**, 65-76.

Banerjee A., Wu Y., Banerjee R., Li Y., Yan H. & Sharkey T.D. (2013) Feedback inhibition of deoxy-D-xylulose-5-phosphate synthase regulates the methylerythritol 4-phosphate pathway. *Journal of Biological Chemistry*, **288**, 16926-16936.

Bouvier F., d'Harlingue A., Suire C., A. Backhaus R.A. & Camara B. (1998) Dedicated roles of plastid transketolases during the early onset of isoprenoid biogenesis in pepper fruits. *Plant Physiology*, **117**, 1423-1431.

Bunik V.I., Tylicki A. & Lukashev N.V. (2013) Thiamin diphosphate-dependent enzymes: from enzymology to metabolic regulation, drug design and disease models. *FEBS Journal*, **280**, 6412-6442.

Chatterjee A., Jurgenson C.T., Schroeder F.C., Ealick S.E. & Begley T.P. (2007) Biosynthesis of thiamin thiazole in eukaryotes: Conversion of NAD to an advanced intermediate. *Journal of the American Chemical Society*, **129**, 2914-2922.

De La Haba G., Leder I.G. & Racker E. (1955) Crystalline transketolase from bakers' yeast: isolation and properties. *Journal of Biological Chemistry*, **214**, 409-426.

Frank R.A., Leeper F.J. & Luisi B.F. (2007) Structure, mechanism and catalytic duality of thiamine-dependent enzymes. *Cellular and Molecular Life Sciences*, **64**, 892-905.

Ghirardo A., Wright L.P., Bi Z., Rosenkranz M., Pulido P., Rodríguez-Concepción M., Niinemets Ü., Brüggemann N., Gershenzon J. & Schnitzler J.-P. (2014) Metabolic flux analysis of plastidic isoprenoid biosynthesis in poplar leaves emitting and non-emitting isoprene. *Plant Physiology*, **165**, 37-51.

Hahn E.M., Eubanks L.M., Testa C.A., Blagg B.S.J., Baker J.A. & Poulter C.D. (2001) 1-Deoxy-D-xylulose 5-phosphate synthase, the gene product of open reading frame (ORF) 2816 and ORF 2895 in *Rhodobacter capsulatus*. *Journal of Bacteriology*, **183**, 1-11.

Hawkins C.F., Borges A. & Perham R.N. (1989) A common structural motif in thiamin pyrophosphate-binding enzymes. *FEBS Letters*, **255**, 77-82.

Heinrich C.P., Noack K. & Wiss O. (1971) A circular dichroism study of transketolase from baker's yeast. *Biochemical and Biophysical Research Communications*, **44**, 275-279.

Lange B.M., Wildung M.R., Mccaskill D. & Croteau R. (1998) A family of transketolases that directs isoprenoid biosynthesis via a mevalonate-independent pathway. *Proceedings of the National Academy of Sciences of the United States of America*, **95**, 2100-2104.

Lindqvist Y., Schneider G., Ermler U. & Sundstrom M. (1992) Three-dimensional structure of transketolase, a thiamine diphosphate dependent enzyme, at 2.5 Å resolution. *The EMBO Journal*, **11**, 2373-2379.

Lois L.M., Campos N., Putra S.R., Danielsen K., Rohmer M. & Boronat A. (1998) Cloning and characterization of a gene from *Escherichia coli* encoding a transketolase-like enzyme that catalyzes the synthesis of D-1-deoxyxylulose 5-phosphate, a common precursor for isoprenoid, thiamin, and pyridoxol biosynthesis. *Proceedings of the National Academy of Sciences of the United States of America*, **95**, 2105-2110.

Mandel M.A., Feldmann K.A., Herrera-Estrella L., Rocha-Sosa M. & León P. (1996) *CLA1*, a novel gene required for chloroplast development, is highly conserved in evolution. *Plant Journal*, **9**, 649-658.

Müller M., Gocke D. & Pohl M. (2009) Thiamin diphosphate in biological chemistry: exploitation of diverse thiamin diphosphate-dependent enzymes for asymmetric chemoenzymatic synthesis. *FEBS Journal*, **276**, 2894-2904.

Querol J., Rodríguez-Concepción M., Boronat A. & Imperial S. (2001) Essential role of residue H49 for activity of *Escherichia coli* 1-deoxy-D-xylulose 5-phosphate synthase, the enzyme catalyzing the first step of the 2-*C*-methyl-D-erythritol 4-phosphate pathway for isoprenoid Synthesis. *Biochemical and Biophysical Research Communications*, **289**, 155-160.

Rapala-Kozik M. (2011) Vitamin B1 (thiamine): A cofactor for enzymes involved in the main metabolic pathways and an environmental stress protectant. *Advances in Botanical Research*, **58**, 37-91.

Sprenger G.A. & Pohl M. (1999) Synthetic potential of thiamin diphosphate-dependent enzymes. *Journal of Molecular Catalysis B: Enzymatic*, **6**, 145-159.

Sprenger G.A., Schörken U., Wiegert T., Grolle S., Graaf A.A.D., Taylor S.V., Begley T.P., Bringer-Meyer S. & Sahm H. (1997) Identification of a thiamin-dependent synthase in *Escherichia coli* required for the formation of the 1-deoxy-D-xylulose 5-phosphate precursor to isoprenoids, thiamin, and pyridoxol. *Proceedings of the National Academy of Sciences of the United States of America*, **94**, 12857-12862.

Xiang S., Usunow G., Lange G., Busch M. & Tong L. (2007) Crystal structure of 1-deoxy-D-xylulose 5-phosphate synthase, a crucial enzyme for isoprenoids biosynthesis. *Journal of Biological Chemistry*, **282**, 2676-2682.